國立臺灣大學醫學院暨工學院醫學工程學研究所

碩士論文

Graduate Institute of Biomedical Engineering

College of Medicine and Engineering

National Taiwan University

Master Thesis

中草藥應用於關節軟骨組織工程之研究

The Effects of Chinese Herbal Medicine on

Chondrocytes for Cartilage Tissue Engineering

林文央

Lin, Wen-Yang

指導教授：林峯輝 博士

Advisor: Lin Feng-Huei, Ph.D.

中華民國 96 年 7 月

July, 2007

ABSTRACT

The skeleton is composed of cartilage and bone which provide the functions such as support, protection, and movement in daily life. Articular cartilage tissue is composed of chondrocytes and extracellular matrix, where the chondrocytes only make up less than 10% of the total volume of cartilage. In healthy cartilage, the matrix is composed of collagens, especially type II collagen, proteoglycans, and noncollagenous proteins, and is filled with water because of the hydrophilic property of the framework.

Cartilage possesses limited ability to achieve spontaneous repair due to its dense extracellular matrix and lacking of blood vessels, lymphatics and innervation. When lesions occur in articular cartilage, there is no bleeding and thus no mechanism for the replacement of lost or damaged tissue. Neighboring chondrocytes may respond by local proliferation; however, because they are sequestered in the dense matrix, they do not migrate into the damaged region to fill the void. If injury extends through the chondral layer to the subchondral bone and underlying vasculature, a repair response can hence occur, but the newly formed cartilage will be gradually populated with type I collagen and degenerate to a fibrocartilaginous scar tissue after 6–8 months.

Circumstances that impair chondrocytes function hence disrupt the balance of synthesis and catabolism and lead to the development of osteoarthritis. In the progression, osteoarthritis eventually impairs the function of a whole joint, including the cartilage, the subchondral bone, the synovium and the periarticular connective and muscular tissues. The current treatment options are fairly limited which include only symptomatic treatment of limited efficacy with analgesics, non-steroidal anti-inflammatory agents or intra-articular administration of steroids or hyaluronic acid, and if the joint destruction can not be halted, the ultimate measure is joint

replacement.

Tissue engineering has been a feasible way to regenerate cartilage in vitro, which combines cells, scaffolds, and signals to mimic the original environment of tissues *in vitro*. In addition, there are some Chinese herbal medicines have been used to treat the degeneration of the cartilage for thousands of years, but the precise mechanism of their potent chondrogenesis effects have not been fully elucidated. Therefore, in this study, we investigated the involved mechanism of two single chemical compounds: aucubin and betulin which were separately extracted from *Plantago asiatic* and *Ampelopsis brevipedunculata* (Maxim.) Trautv. by focusing on their proliferation and antioxidant activity.

The experiment was divided into two parts. One was two-dimensional chondrocytes culture; the other was three-dimensional scaffold culture. After treating two-dimensional chondrocytes or three-dimensional seeded chondrocytes with optimal concentration of single chemical compounds, the proliferation and matrix productivity of them were evaluated by real-time reverse-transcriptase polymerase chain reaction, ELISA assays, and immuno-histochemical staining. The important role in scavenging free radicals by those extracted chemical compounds was detected by the chemiluminescence method.

The results showed that, in two-dimensional chondrocytes culture, both aucubin and betulin could effectively promote the mRNA expression of ECM and inhibit the mRNA expression related with ECM degradation at appropriate concentration, and the ability of $O_2^{\bullet-}$ scavenging made aucubin and betulin as protectants of chondrocytes, which would stimulate chondrocyte proliferation and maintain the basic chondrocyte activities. In three-dimensional scaffold culture environment, betulin can significantly stimulate chondrocyte proliferation and maintain the basic chondrocyte activities until four-week cultivation, which suggested that in the future application

the in vitro three-dimensional cultivation of chondrocyte-scaffold hybrids should be maintained more than four weeks, and of course the addition of 0.32μg/ml of betulin into the cultured environment possessed positive effects toward chondrocytes and the whole cartilage-mimic tissue.

Keywords: Chinese herbal medicine, Cartilage, Tissue Engineering, Real-time RT-PCR, ROS, Aucubin, Betulin

中文摘要

人類的骨骼是由硬骨和軟骨構成的器官，具有支持、保護和運動的功能。軟骨是由僅佔總體積百分之五的軟骨細胞和其所分泌的大量細胞外基質組成，在健康的軟骨內，其細胞外基質主要為第二型膠原蛋白和多醣類，由於它們攜帶大量的負電性，使水分子及正電離子易受吸引而聚集到軟骨中，因而使軟骨在受到壓力時，能具有吸收震動力而達緩衝的效果。

然而受到破壞的軟骨其自我修復的能力很有限，除了因為軟骨中沒有血管或神經的分布，使得受傷的部位沒有血流侵入而攜帶發炎因子，因而無法啟動修復機制；另外在軟骨中的軟骨細胞數量本來就很有限，即使受傷部位鄰近的細胞可以進行細胞分裂，但卻因數量過少且加上黏滯的細胞基質阻礙了細胞的遷移；而當受傷侵入軟骨下方的硬骨時，受到破壞的硬骨內的血流便有機會侵入軟骨而啟動修復，但此時新生成的軟骨組織，只具有分泌第一型膠原蛋白細胞外基質的能力，而這種第一型膠原蛋白的機械特性和強度與原本第二型膠原蛋白相差甚大，最終也將被逐漸降解而喪失軟骨的功能。

於是受到創傷而無法自我修復的軟骨會漸漸影響到整個關節，轉變為退化性骨關節炎。目前臨床上的藥物療法皆著重在止痛而無法有根治之效，最常用的藥物有普拿疼、第二型環氧腖抑制劑、非類固醇類抗發炎藥物、關節內注射透明質酸、關節內注射類固醇，然而這些只治標不治本的療法，最終只能藉由置換人工替代膝關節來取代壞損的關節。

利用組織工程在體外培養軟骨組織近年來已成為修補受損關節軟骨的途徑之一，組織工程利用組織工程的三要素:細胞、生物材料骨架及訊號的刺激，模擬組織在體內的狀態，以期在體外復育仿生組織。此研究從具有促進軟骨再生之

iv

效的傳統中草藥複方中，萃取出主要來自於車前子及山葡萄兩種藥材中的兩種主要有效單一化學成分，並以適當濃度添加到二維及三維支架的軟骨組織培養系統中，而後利用同步定量聚合酵素鏈鎖反應、細胞總 DNA、細胞外基質葡萄胺聚醣濃度、及免疫螢光染色確定細胞增殖情形；並利用化學發光技術配合適當的探針，偵測軟骨細胞中自由基的產生量及其抗氧化的能力。

實驗結果發現，二維單層軟骨細胞的培養中，利用適當濃度的車前子或山葡萄有效單一化學成分之添加，軟骨細胞能夠增加其細胞外基質相關的基因表現，並能抑制與細胞外基質降解相關之蛋白質的基因表現；也由二維系統初步發現，由山葡萄萃取之有效單一化學成分相較於由車前子萃取之有效單一化學成分，更具活性氧之清除能力，因而使得軟骨細胞的整體活性在山葡萄萃取物之添加組更為提升。在三維軟骨組織工程的培養中，經過兩週以上培養的軟骨細胞明顯地增加細胞活性及複製能力，其細胞外基質相關的基因表現也明顯的上昇，而與細胞外基質降解相關的基因被受到抑制；值得注意的是，經過四週以上培養的軟骨細胞，其細胞整體活性相較於一週及兩週更為佳，或許建議在未來之臨床應用也宜取經過四週培養之軟骨組織工程物為較佳。

關鍵詞：中草藥、軟骨、組織工程、定量聚合酵素鏈鎖反應、自由基、抗氧化

TABLE OF CONTENTS

INDEX OF FIGURES

INDEX OF TABLES

LIST OF ABBREVIATIONS

ASCs	Adult Stem Cells
AUC	Area Under Curve
BMPs	Bone Morphogenetic Proteins
CAT	Catalase
CL	Chemiluminescences
C4S	Chondroitin-4-Sulfate
C6S	Chondroitin-6-Sulfate
cDNA	Complementary DNA
COX2	Cyclooxygenase 2
DNA	Deoxyribonucleic Acid
DAB	3, 3'-Diaminobenzidine Tetrahydrochloride
DMMB	1,9-Dimethyl-Methylene Blue
MTT	3-[4,5-Dimethylthiazol-2-Yl]-2,5-Diphenyltetrazolium Bromide
DMEM	Dulbecco/Vogt Modified Eagle's Minimal Essential Medium
ETC	Electron Transport Chain
EGF	Epidermal Growth Factor
EDC	1-Ethyl-3-(3-Dimethylaminopropyl) Carbodiimide
EDTA	Ethylenediamine Tetraacetic Acid
ECM	Extracellular Matrix
FGFs	Fibroblast Growth Factors
GI	Gastrointestinal
GPx	Glutathione Peroxidase
GAPDH	Glyceraldehyde 3-Phosphate Dehydrogenase
GAGs	Glycosaminoglycans
H&E	Hematoxylin & Eosin
HCl	Hydrogen Chloride
H_2O_2	Hydrogen Peroxide
$^{\bullet}OH$	Hydroxyl Radical
OCl^-	Hypochlorite Ion
iNOS	Inducible NOS
IGF	Insulin-like Growth Factor
IL-1β	Interleukin-1β
ICE	Interleukin-converting Enzyme
LDH	Lactate Dehydrogenase
MMP-2	Matrix Metalloproteinase-2
MMP-9	Matrix Metalloproteinase-9
MMPs	Matrix Metalloproteinases

MT-MMPs	Membrane-type Matrix Metalloproteinases
MSCs	Mesenchymal Stem Cells
NBF	Neutral Buffered Formalin
NAD^+	Nicotinamide Adenine Dinucleotide
NADP	Nicotinamide Adenine Dinucleotide Phosphate
NADPH	Nicotinamide Dinucleotide Phosphate
$^{\bullet}NO$	Nitric Oxide
NOS	NO Synthase
NSAID	Non-steroidal Anti-inflammatory Drug
NF-κB	Nuclear Factor-KB
O.D.	Optical Density
OA	Osteoarthritis
PRDX	Peroxiredoxins
PBS	Phosphate-buffered Saline
PMT	Photo Multiplier Tube
ROS	Reactive Oxygen Species
PCR	Real-time Polymerase Chain Reaction
RT-PCR	Reverse Transcription Polymerase Chain Reaction
RNase	Ribonuclease
RNA	Ribonucleic Acid
SEM	Scanning Electron Microscopy
Sox-5	Sex-determining Region Y-Box-5
Sox-6	Sex-determining Region Y-Box-6
Sox-9	Sex-determining Region Y-Box-9
SMADs	Small Mother Against Decapentaplegic
sGAG	Sulphate-glycosaminoglycans
$O_2^{\bullet-}$	Superoxide Anion
SOD	Superoxide Dismutase
INT	Tetrazolium Salt
C_T	Threshold Cycle
TIMP-1	Tissue Inhibitor Of Metalloproteinase-1
TIMPs	Tissue Inhibitors of Metalloproteinases
TGF-β	Transforming Growth Factor-B
TNF-α	Tumor Necrosis Factor-A
COL1	Type I Collagen
COL2	Type II Collagen
UV	Ultraviolet
WST-1	Water Soluble Tetrazolium Salt

CHAPTER 1

INTRODUCTION

1-1 Cartilage Biology

1-1.1 Definition and Composition of Cartilage

Cartilage is an avascular, aneural and alymphatic connective tissue which belongs to the skeleton organ and covers the end of each bone of any joint (Figure 1) [1, 2]. This white-colored tissue has an elastic consistency to absorb mechanical shock and provides an extremely smooth bearing surface to facilitate daily motion between the bones [3], thereby preventing biomechanical damage caused by severe loading and protecting the underlying bones from mechanical stresses of normal joint use [4].
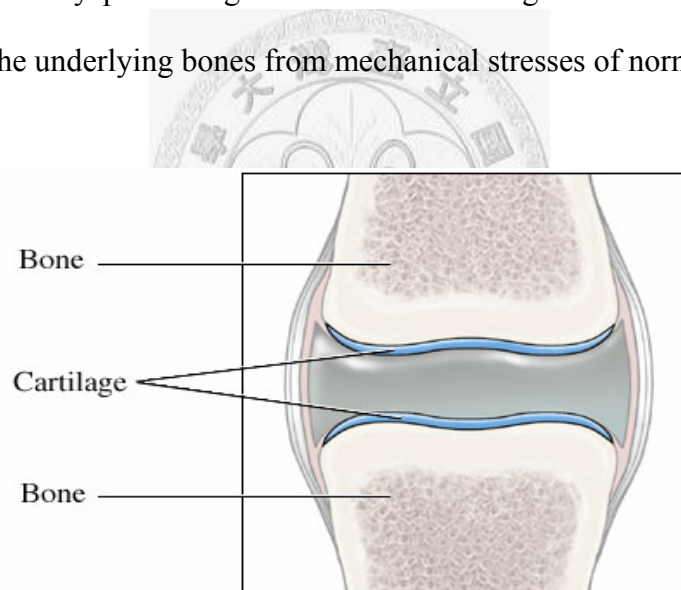
Figure 1 Cartilage covers each end of the bones of any joint [5].

In general, cartilage is composed of chondrocytes and extracellular matrix (ECM) [5]. The phenotypic cells, chondrocytes, are small cells with one oval-shaped nucleus and one to two nucleoli which only make up less than 10% of the total volume of cartilage and do not contribute to the mechanical properties of cartilage [6]. Chondrocytes attach themselves to the framework of ECM which they synthesize, but

do not form contacts with each other [7]. Because chondrocytes are derived from the same cell lineage as fibroblasts, chondrocytes are similar to fibroblasts [8].

The matrix is composed of a framework of macromolecules and is filled with water (Figure 2) [9]. The structural macromolecules are collagens, proteoglycans, and noncollagenous proteins which make up 30% to 40% of the wet weight of cartilage matrix [10]. Collagens form a tight collagen fiber network which contains highly hydrophilic gel of aggregated proteoglycans and other noncollagenous proteins in it and hence provide the tensile strength for cartilage [11]. And because of the hydrophilic property of this framework, the entrapped water and ions make up the remaining 60% to 70% of the wet weight of cartilage matrix [12]. In the cartilage tissue dry weight, collagens account for 50% to 60%, proteoglycans contribute 30% to 35%, and noncollagenous proteins are about 15% to 20% [13]. From the identification of electron microscopy, type II collagen consists 90% to 95% of total cartilage collagen, and the remaining percentage are lesser amounts of collagen types VI, IX, X and XI [14]. Type IX and type XI collagen have been reported to possess important roles in organizing and stabilizing the network of type II collagen [15].
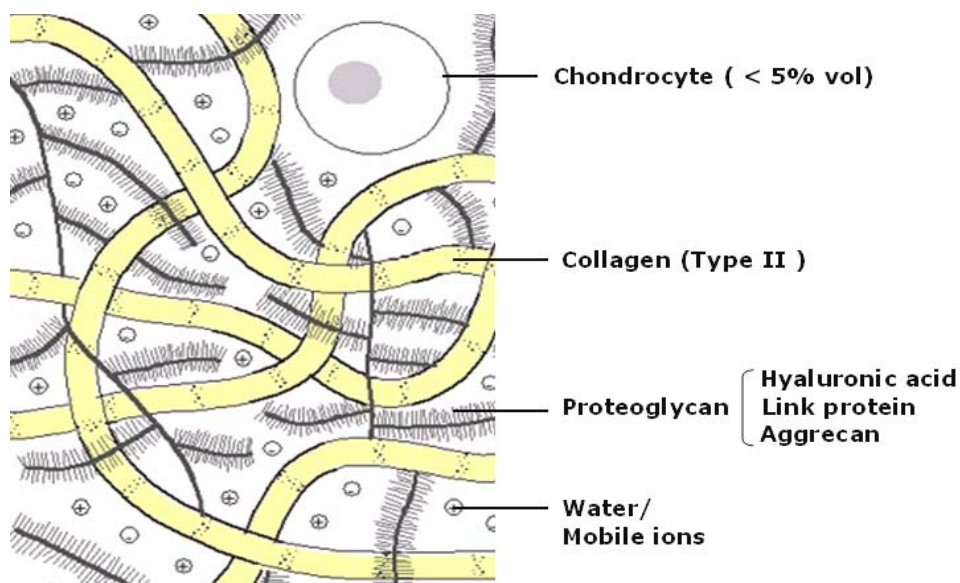
Figure 2 Cartilage is composed of chondrocytes and extracellular matrix.

Proteoglycans are composed of a protein core filament and one or more long glycosaminoglycan chains [16], which are unbranched polysaccharide chains of repeating disaccharides (Figure 3) [16, 17]. In each repeating disaccharide of glycosaminoglycan, one or more negative charges exist and hence attract positively charged ions or water molecules [18, 19]. Glycosaminoglycans that connect to proteoglycan core proteins include chondroitin sulfate, keratin sulfate, and dermatan sulfate [20]. When proteoglycans aggregate through the noncovalent interactions between hyaluronan filaments and link proteins, the resulting proteoglycan aggregate stabilizes these large macromolecules within the matrix (Figure 3) [21].
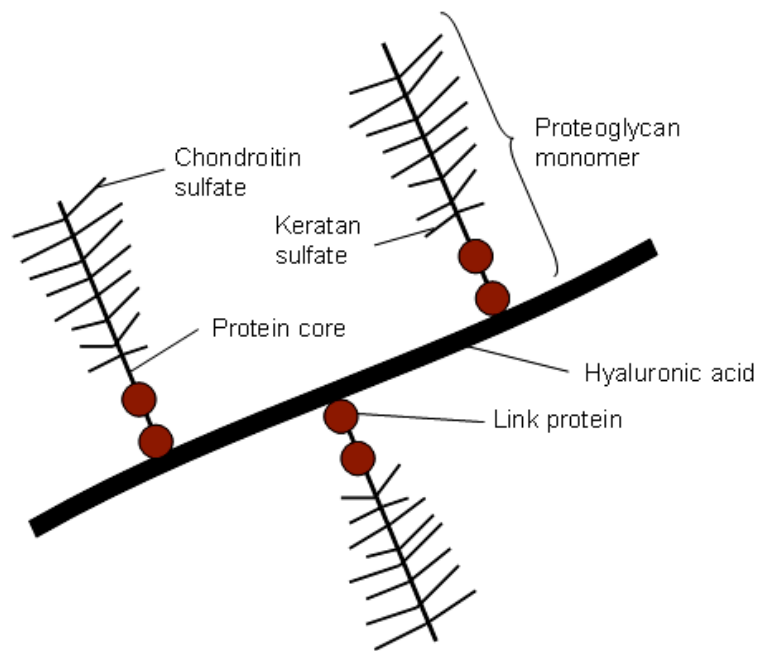
Figure 3 Diagram of proteoglycan aggregate.

The noncollagenous proteins in cartilage have not been extensively studied but seem to have some effects in organizing the matrix and maintaining the relationships between chondrocytes and the macromolecules of the matrix [11].

1-1.2 Types of Cartilage

There are three basic types of cartilage: articular cartilage, fibrous cartilage, and elastic cartilage [22]. Articular cartilage, also called hyaline cartilage, is the most common type among the three types of cartilage. It exists in articular surfaces of the joints, trachea tube rings, larynx, rib, costae, and the tip of the nose [23]. Perichondrium covers articular cartilage and provides nutrients to chondrocytes through the blood vessels in it [24]. Chondrocytes are entrapped in the lacunae structure [25]. The matrix of articular cartilage is smooth and basophilic, and the framework of macromolecules is mainly type II collagen [14].

Fibrous cartilage never occurs alone and exists in locations where high stress occurs such as the intervertebral disks, in front of the pelvic girdle between the pubic bones, and the glenoid cavity in the shoulder joint [26, 27]. It closely adheres to either articular cartilage or dense connective tissue. In fibrous cartilage, perichondrium is often absent. The chondrocytes are less in number and often widely separated, but are still enfolded in lacunae. The matrix of fibrous cartilage is mainly type I collagen [28, 29].

Elastic cartilage exists in the places where the maintenance of specific shapes is important, such as auricular, epiglottis, and the walls of the eustachian tube [30]. Chondrocytes in elastic cartilage are more tightly arranged than in articular cartilage. And because the percentage of the matrix in elastic cartilage is higher than in articular cartilage, elastic cartilage can be easily deformed and spring back into the original shape. The major component of matrix macromolecules is elastin [31].

1-1.3 Homeostasis of Cartilage

Although there is only one type of cell in cartilage, like other tissues, cartilage still needs to keep its homeostasis [32]. Therefore, chondrocytes continually synthesize, combine and degrade ECM proteins to maintain the biochemical composition among cells, and in some manner are influenced and regulated by the mechanical and biochemical signs of ECM which they secrets [33]. This concept, in which chondrocytes maintain the balance and turnover between ECM and themselves, has been called dynamic reciprocity [34].

Under normal physiological condition, the proteins relates to ECM express continuously at constant level. Type II collagen is the most abundant protein in cartilage and constitute the basic framework of ECM. In addition to type II collagen, the fibril network of healthy cartilage also contains type IX and type XI collagen, and there are still small amounts of other types of collagen such as type III, VI, XII, and XIV collagen found in cartilage[35]. Type II and type VI collagens are demonstrated to possess the RGD sequences, which suggest the role in facilitating cell attachment [36]. However, when normal articular cartilage is somehow worn away, the wound healing process of cartilage prefers to deposit type I collagen rather than type II collagen in the newly formed ECM, which makes the articular cartilage become fibrous cartilage [37]. Contrary to type I and type II collagen which are synthesized by chondrocytes, type X collagen is synthesized by hypertrophic chondrocytes which play an important role in endochondral ossification [38]. Hypertrophic chondrocytes direct the mineralization of their surrounding ECM, lead adjacent perichondrial cells to become osteoblasts, and finally undergo apoptotic cell death [39].

The balance in the expression of matrix metalloproteinases (MMPs) and their inhibitors, tissue inhibitors of metalloproteinases (TIMPs), is another important factor for cartilage homeostasis [40]. Matrix metalloproteinases are a family of

zinc-dependent endopeptidases that possess the ability to degrade and remodel ECM [41]. There are 22 human MMPs and can be roughly divided into several groups: collagenase such as MMP-1, MMP-8, and MMP-13, gelatinase such as MMP-2 and MMP-9, and membrane-type MMPs (MT-MMPs) such as MMP-14, 15, 16, 17, 24, and 25 [41, 42]. TIMPs inhibit MMPs in a noncovalent and reversible manner and can also positively regulate MMPs [41]. There are four types of TIMPs have been identified: TIMP-1, 2, 3, and 4, and each TIMP differs in its ability to inhibit or module different MMPs (Table 1) [41, 43]. TIMP-1 inhibits MMP-1 and MMP-3, while TIMP-2 and TIMP-3 inhibit MT1-MMP.

MMP-2, also known as gelatinase-A, is widely expressed in many noninflamed healthy connective tissues [44]. It is activated at the cell surface level to remodel the ECM and the basement membrane substrates such as laminin and fibronectin and hence modulate the migration and adhesion of cells. The activition of MMP-2 is tightly regulated by the expression of MT1-MMP (MMP-14) and TIMP-2 [45].
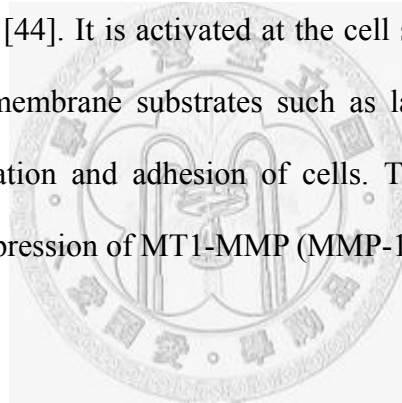
Table 1 Inhibition profile of TIMPs. ($+$) means the MMP is inhibited by the TIMP (Modified from the reference [41]).

Type of MMP	TIMP-1	TIMP-2	TIMP-3	TIMP-4
MMP-1	$+$	$+$	$+$	$+$
MMP-2	$+$	$+$	$+$	$+$
MMP-3	$+$	$+$	$+$	$+$
MMP-7	$+$	$+$	$+$	$+$
MMP-8	$+$	$+$		
MMP-9	$+$	$+$	$+$	$+$
MMP-10	$+$	$+$		
MMP-11	$+$			
MMP-12	$+$			
MMP-13	$+$	$+$	$+$	
MMP-14		$+$	$+$	
MMP-15		$+$	$+$	
MMP-16	$+$	$+$		
MMP-17				
MMP-19				
MMP-20				
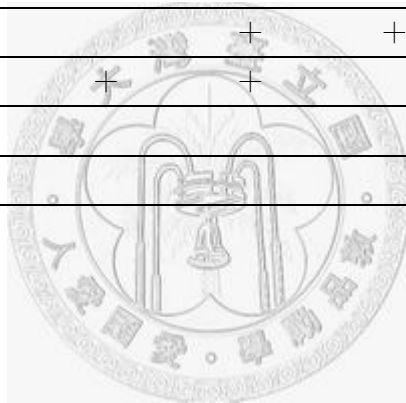
1-2 Natural Limitations of Cartilage

1-2.1 Low Oxygen Tension on Cartilage Metabolism

Articular cartilage is a tissue without vascular invasion, so its nutrition and oxygen are mainly supplied by diffusion from the synovial fluid [46, 47]. Therefore, O_2 tension in cartilage *in vivo* is only about 1% to 8% which is dramatically lower than in normal tissues where O_2 tension is about 21% [48], and chondrocytes are hence adapted to working as anaerobic working cells [49]. The low O_2 consumption in cartilage is because of the Crabtree effect, where the increased glucose concentrations inhibit the cellular respiration and limit the O_2 consumption [50].

The natural low O_2 tension in cartilage not only influences the homeostasis of ECM components but also stabilizes the phenotype of chondrocytes [51-56]. Under hypoxia environment, chondrocytes increase the synthesis of type II collagen and glycosaminoglycans and decrease the synthesis of type I collagen [51-54]. Moreover, MMP-9 mRNA is decreased by interleukin-1β (IL-1β), a catabolic cytokine, in low O_2 tension environment [57].

1-2.2 Limited Cartilage Repair Response

Because the cartilage naturally lacks of the vascularity, it is in the very limited capacity of self-repair [4]. In most tissues, injury is associated with a rupture of blood vessels, an influx of cells and bioactive peptides from the blood, and the formation of a hematoma [58]. Undifferentiated mesenchymal progenitor cells migrate into the lesion, differentiate into the local cellular phenotype and synthesize repair tissue. When lesions occur that are limited to the articular cartilage in adults, there is no bleeding and thus no mechanism for the replacement of lost or damaged tissue [59].

Neighboring chondrocytes may respond by local proliferation; however, because they are sequestered in the dense matrix, they do not migrate into the damaged region to fill the void. As such, focal lesions that are limited to the chondral layer usually remain for life. These can often expand with time and use, and lead to the more generalized cartilage loss associated with osteoarthritis (OA) [59, 60].

A repair response can occur when injury extends through the chondral layer to the subchondral bone and underlying vasculature. Local bleeding and fibrin clot formation causes an infiltration of bone marrow-derived cells which synthesize space-filling repair tissue. This may initially heal to resemble hyaline cartilage after 6–8 months, but in the longer term becomes increasingly populated with type I collagen, degenerating to a fibrocartilaginous scar tissue that does not have the appropriate physical and mechanical properties, and ultimately fails [61, 62].

1-3 Cartilage Pathology

Osteoarthritis (OA) is the most common disease of joints which affects millions of people all over the world [63]. It can occur in any joint but is most common in joints of the knee, shoulder, hand, spine, hip, and foot [4]. The development of OA starts in the cartilage degeneration, where the balance of anabolism and catabolism in cartilage is progressively disrupted by suppression in anabolic genes expression or increase in catabolic genes expression [4, 46, 64]. In this progression, OA eventually impairs the function of a whole joint, including the cartilage, the subchondral bone, the synovium and the periarticular connective and muscular tissues.

As we noted, cartilage continually maintains its homeostasis. Circumstances that impair chondrocytes function can disrupt the balance of synthesis and catabolism in favor of cartilage degradation, which over time can lead to OA [59].

The development of osteoarthritis begins at the degenerative processes in cartilage. Interleukin-converting enzyme (ICE) converts IL-1β to its active form and, therefore, activated IL-1β induces the expression of matrix proteases, which degrade the matrix components (Figure 4). The homeostasis in cartilage starts to be destroyed which contributes to the risk for cartilage degeneration by decreasing the ability of chondrocytes to maintain and repair the articular cartilage tissue [65]. The mitotic and synthetic activity of chondrocytes decline with advancing donor age [66]. In addition, human chondrocytes become less responsive to anabolic mechanical stimuli with ageing and exhibit an age-related decline in response to growth factors such as the anabolic cytokine insulin-like growth factor-I [66]. These findings provide evidence supporting the concept that chondrocytes senescence may be involved in the progression of cartilage degeneration.
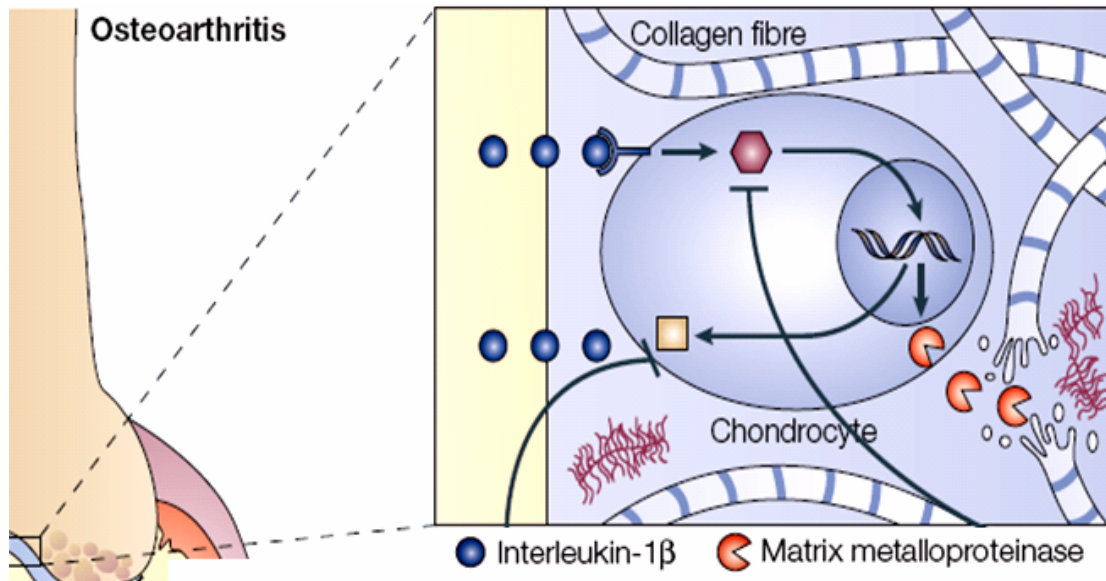
Figure 4 Degenerative processes in osteoarthritis cartilage [4].

Metalloproteinases and ROS are the two main actors of matrix component degradation. They have been found to be overproduced in OA cartilage and synovium. ROS may directly oxidize nucleic acids, transcriptional factors, membrane phospholipids, intracellular and extracellular components leading to impaired biological activity, cell death and matrix components breakdown [67-69]. From the different in vitro and animal studies, Y. Henrotin et al. concluded that in pathological circumstances, ROS contribute to cartilage degradation by directly degrading matrix components, by sustaining the activity of catabolic cytokines and by reducing cartilage repair capacities. Altogether, these observations support the concept of antioxidant therapy in rheumatic diseases and it might also decrease the progression of OA [70].

In severe osteoarthritis, the pathological changes result in radiological changes, such as loss of joint space, subchondral bone sclerosis and presence of osteophytes (bony spurs mostly located at the joint margins) (Figure 5) [4, 60]. These changes can result in joint symptoms such as pain, stiffness and loss of function. The symptoms

11

vary with time and between joint sites and individuals. The main risk factors for OA are age, obesity and any form of joint trauma. In some families, OA seems to be inherited [60].

a Normal **b Osteoarthritis**

Muscle

Tendons/ ligaments

Cartilage
Meniscus
Synovium
Synovial fluid

Capsule

Bone

Weakened and frayed tendons/ ligaments, muscles

Episodically inflamed synovium
Reduced viscosity of synovial fluid
Fibrillated/destroyed cartilage
Bony outgrowths (osteophytes)
Bone sclerosis
Frayed, cracked meniscus
Thickened capsule
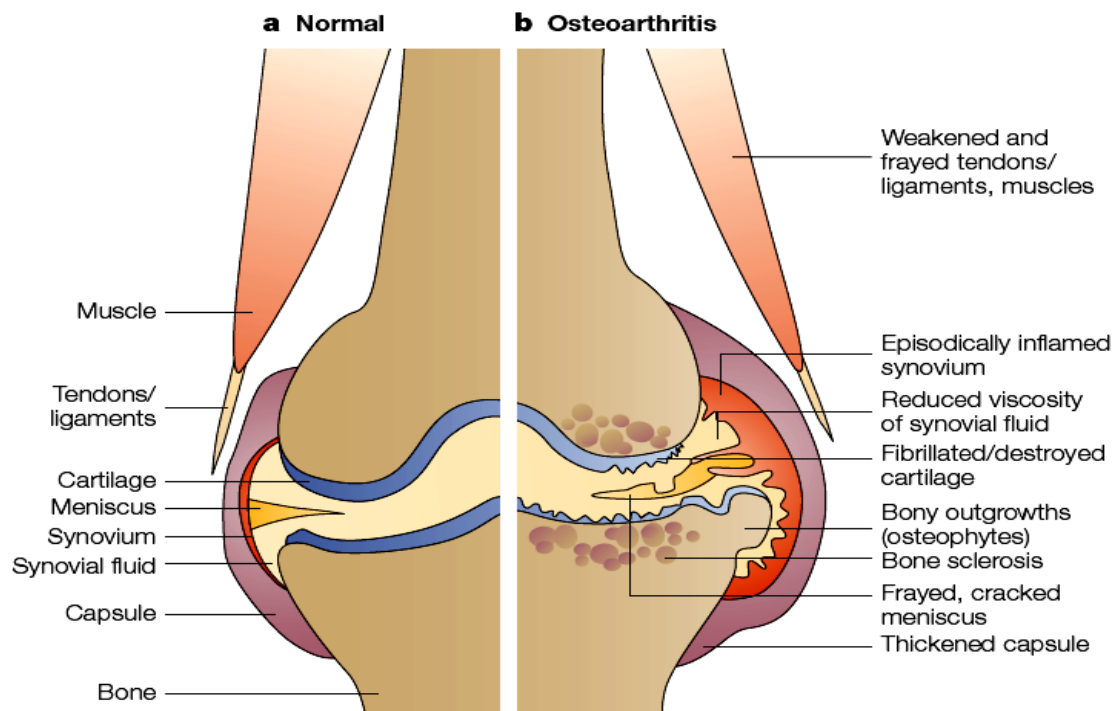
Figure 5 Articular structures that are affected in osteoarthritis. **a,** Normal cartilage is without any fissures, no signs of synovial inflammation. **b,** Early focal degenerate lesion and 'fibrillated' cartilage, as well as remodelling of bone, is observed in osteoarthritis. This can lead to bony outgrowth and subchondral sclerosis [4].

1-4 Current Strategies for Cartilage Treatment

1-4.1 Inadequate Pharmacological Options

The specialized architecture and limited repair capacity of articular cartilage coupled with the high physical demands on this tissue make it exceedingly difficult to treat medically. The current treatment options as issued in the guidelines from the American College of Rheumatology are fairly limited (Figure 6) [71, 72]. In addition to non-pharmaceutical measures such as weight loss and physical exercise they include only symptomatic treatment of limited efficacy with analgesics, non-steroidal anti-inflammatory agents or intra-articular administration of steroids or hyaluronic acid. Because no drugs exist that prevent or halt osteoarthritis joint destruction, the ultimate measure is joint replacement.
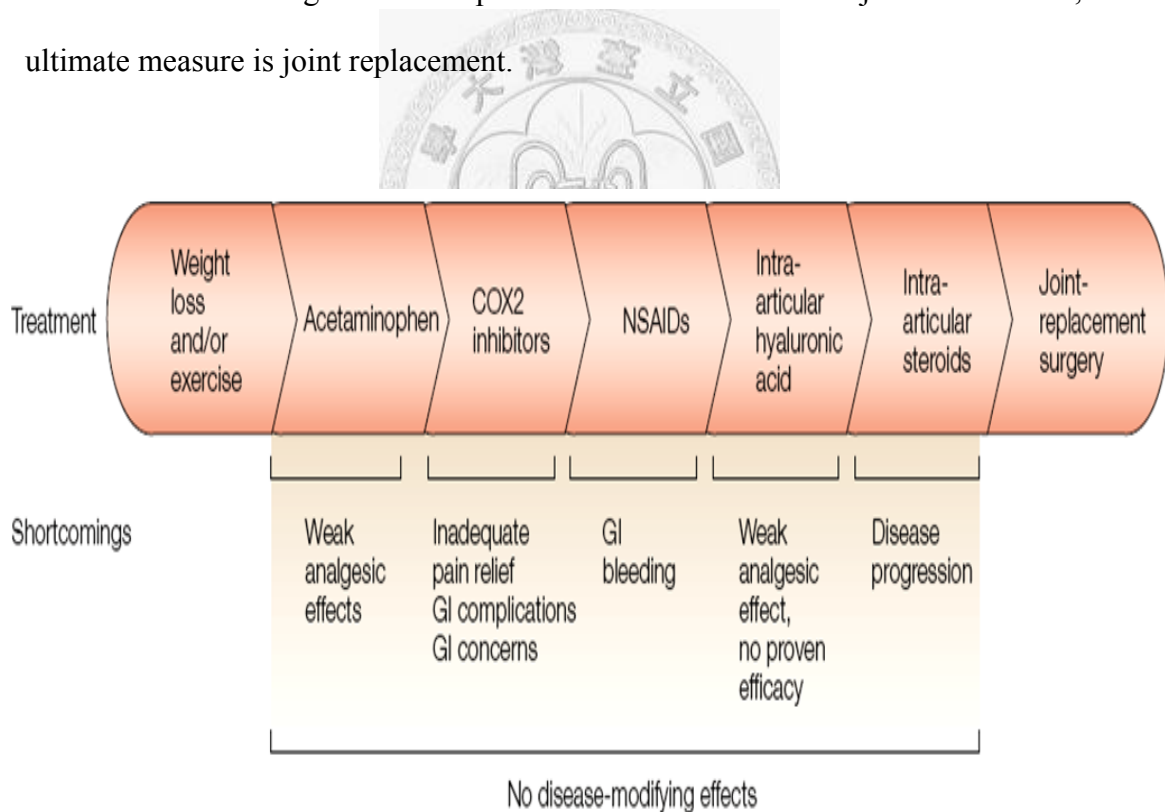
Figure 6 Current osteoarthritis treatment options. Abbreviations: GI, gastrointestinal; COX2, cyclooxygenase 2; NSAID, non-steroidal anti-inflammatory drug [4].

Chronic pain in osteoarthritis patients causes primarily on the activation of sensory neurons that innervate the affected joint. With the exception of cartilage, all joint tissues, including subchondral bone and synovium, are densely supplied by small-diameter nociceptive neurons (Figure 7) [4, 71]. Tissues, including subchondral bone and synovium, are densely supplied by small-diameter nociceptive neurons.

Potential targets for osteoarthritis is to interfere the nociception and possible pathways. Inhibiting the production of the inflammatory cytokine IL-1β or blocking its receptors or interrupting its subsequent intracellular signalling through nuclear factor-κB (NF-κB) and the blockade of bradykinin receptors are more recent approaches to developing symptom-modifying drugs with greater efficacy than non-steroidal anti-inflammatory drugs (NSAIDs) that inhibit the formation of the pain mediator prostaglandin E2 (Figure 7) [4].
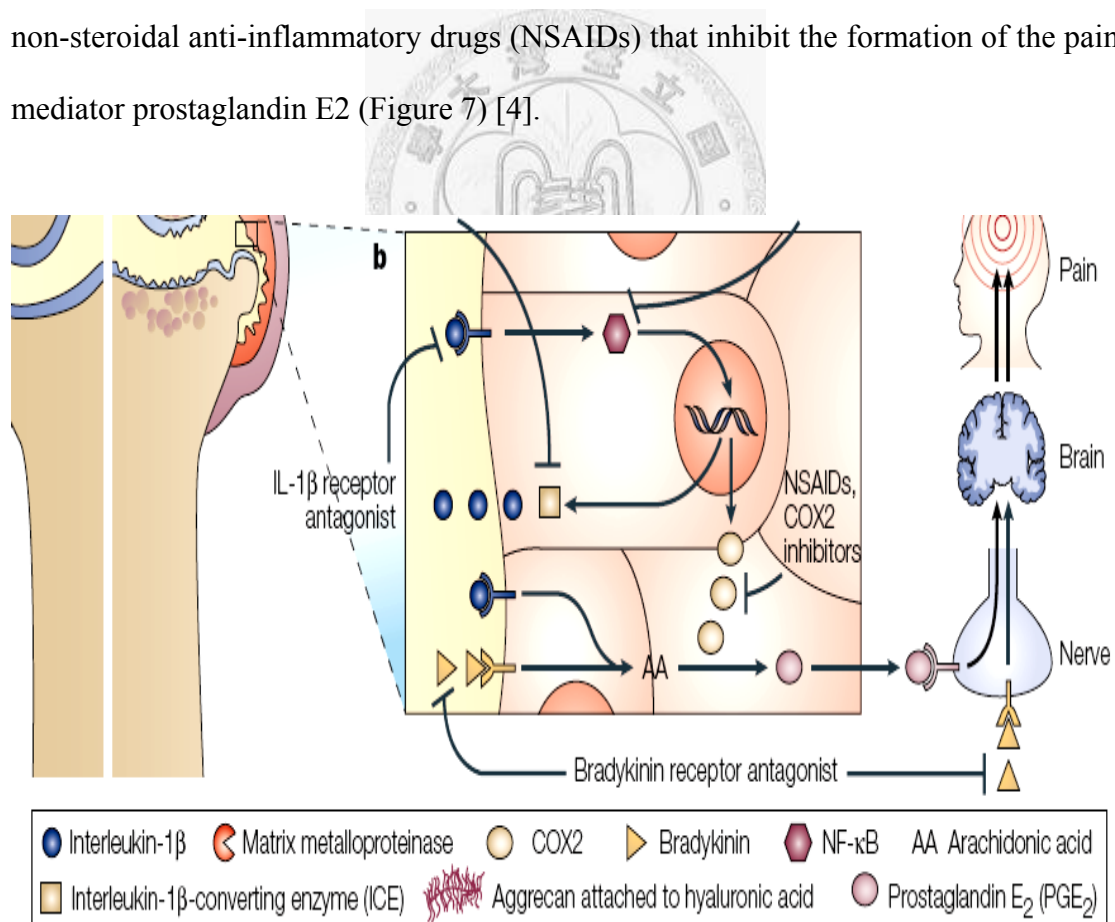
Figure 7 Targets for the development of disease- and symptom-modifying drugs for osteoarthritis. Nociception and possible ways are targets to be interfered by pain relief drugs [4].

1-4.2 Novel Gene-based Approach for Cartilage Repair

Existing pharmacologic, surgical and cell based treatments may offer temporary relief but are incapable of restoring damaged cartilage to its normal phenotype. Gene transfer provides the capability to achieve sustained, localized presentation of bioactive proteins or gene products to sites of tissue damage (Figure 8).
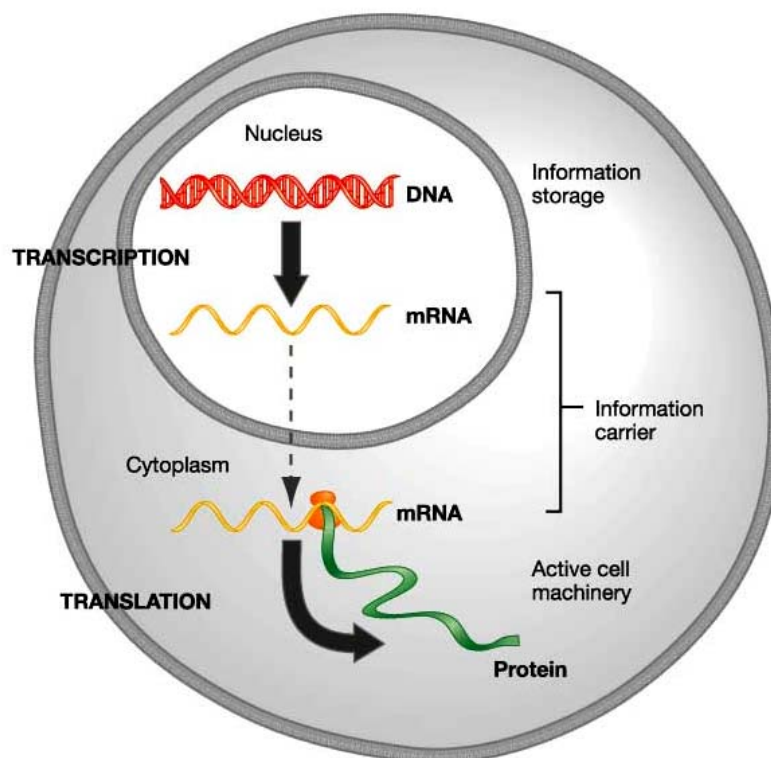
Figure 8 The central dogma of gene expressional molecular biology: Transcription of DNA to RNA and translation of RNA to protein.

A variety of cDNAs have been cloned which may be used to stimulate biological processes that improve cartilage healing. They are anabolic growth factors such as transforming growth factor (TGF-β superfamily), several of the bone morphogenetic proteins (BMPs), insulin-like growth factor (IGF), fibroblast growth factors (FGFs), and epidermal growth factor (EGF). Transcription factors such as Sox-9, L-Sox 5 and

Sox-6 that promote chondrogenesis or the maintenance of the chondrocyte phenotype present another class of biologics that may be useful. Signal transduction molecules, such as SMADs are also known to be important in chondrocyte differentiation. Because these regulatory molecules function intracellularly and cannot be delivered to cells in soluble form, gene transfer is perhaps the only way to which they might be directly applied for medical use [73, 74].

The challenge to gene-based treatment strategies is to devise methods that incorporate the correct gene or gene combination with the appropriate vector, delivered to specific target cells within the proper biological context to achieve a meaningful therapeutic response. Toward the treatment and repair of damaged articular cartilage, the three primary candidate cell types to target for genetic modification are synovial lining cells, chondrocytes and mesenchymal stem cells (MSCs) (Figure 9) [59].
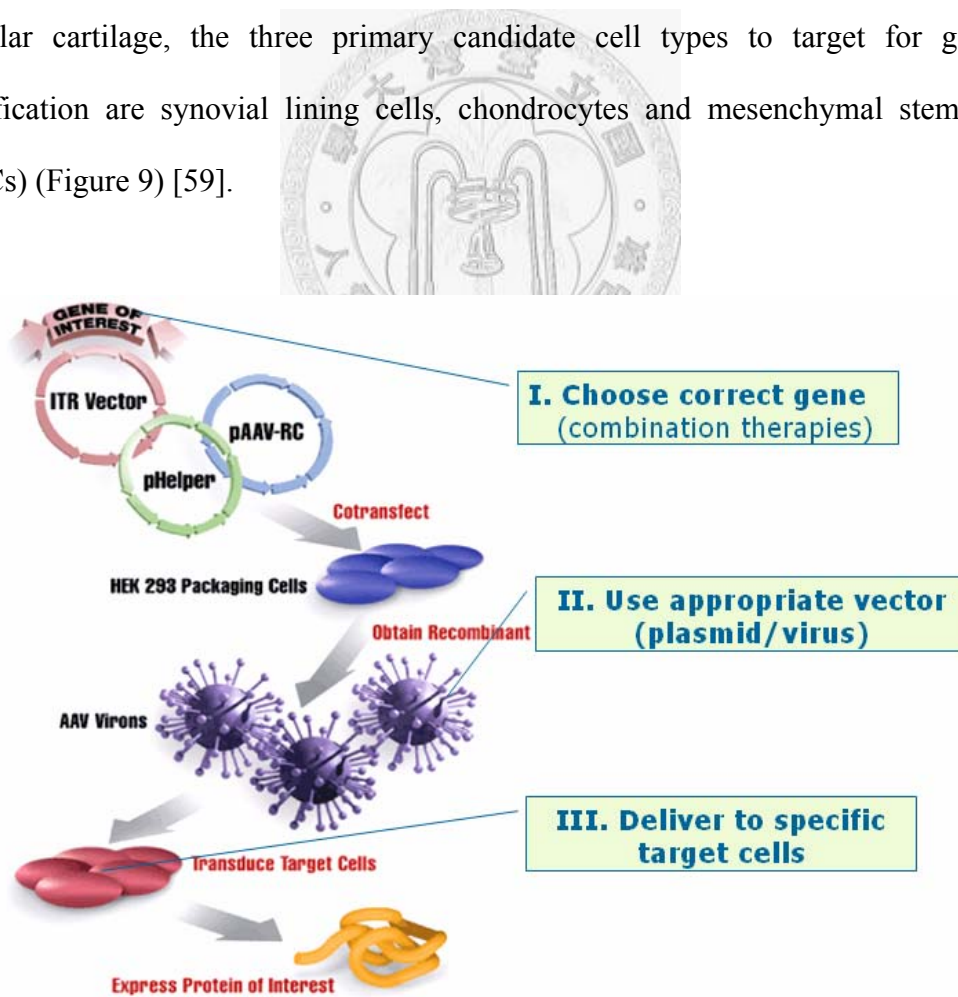
Figure 9 The key concept of gene-based cartilage repair. It provides a way to convert specific target cells into factories capable of sustained protein production.

1-5 Cartilage Tissue Engineering

Compared with the former two strategies for cartilage repair, the cell-based cartilage tissue engineering seems a better way to repair the cartilage for several reasons. One of them is that strategies for engineering cartilage tissues are mainly focused on the restoration of pathologically altered structures, which were based on the transplantation of the so-called tissue engineering triad: cells in combination with supportive matrix and biomolecules [73, 75]. Since this approach comprises the interactive tissue engineering triad of responsive cells, a supportive matrix template, bioactive molecules promoting differentiation, it can mimic and further regenerate the tissue structure (Figure 10) [76]. Moreover, the cell source can origin from autologous cells or stem cells, and the cell number can be further augmented *in vitro* environment. Furthermore, there are already lots of biodegradable materials can be used clinically. The detailed descriptions are in following paragraphs.
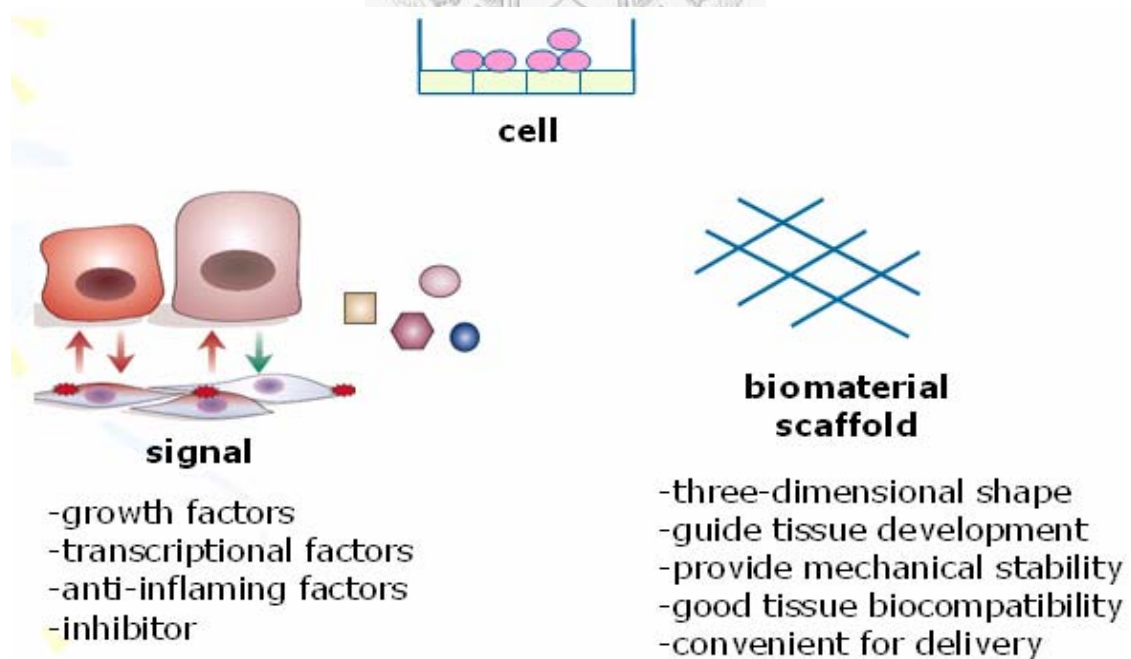
Figure 10 Tissue engineering triad and its characteristic.

1-5.1 Cell

The cell is the first important component of the tissue engineering triad. Just as mentioned, cells can be obtained from autologous cells or stem cells. Although the cell used in cartilage tissue engineering triad can be directly obtained from patients, chondrocytes are difficult to isolate in humans, and they are also replicate in a slow rate and are prone to phenotypic dedifferentiation *in vitro* culture [77]. This can be further affected by donor age and health status [78]. In view of this, tissue engineering based on adult stem cells (ASCs) for tissue engineering cartilage is highly considered recently. Stem cells are highly replicative cells that have multilineage differentiation capacity (Figure 11). ASCs are less tumorogenic than their embryonic stem cells and are accessible from many tissues including bone, deciduous teeth, adipose tissue, umbilical cord blood, synovium, brain, blood vessels and blood [79-81]. To date, mesenchymal stem cells can not only derive from the bone marrow, but can also obtain from adipose tissue, muscle, skin and synovium. They are capable of self-renewal and can differentiate into several different phenotypes including bone, cartilage, adipocytes, and haematopoiesis supporting stroma [74, 82].
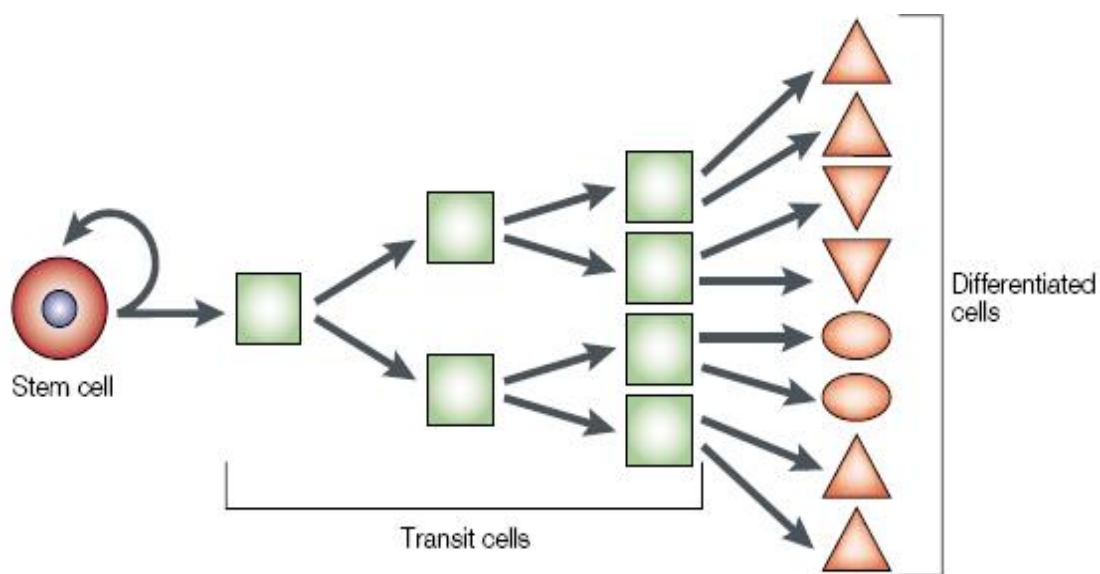
Figure 11 Definition of the stem cells [79].

1-5.2 Biomaterial Scaffold

A critical requirement of cartilage tissue engineering is the design of specific biomaterials and scaffold structures. Biomaterial scaffolds control three-dimensional shape, guide tissue development and permit the convenient delivery of cells into patients [83]. For cartilage and intervertebral disc engineering, a suitable biomaterial should provide or support initial mechanical stability, even cell distribution and good tissue biocompatibility [84].

Increasing evidence suggests that three-dimensional cell cultures provide the advantage of anchorage-independent cell growth, maintaining the differentiated phenotype that allows the synthesis of cell-specific pericellular or intercellular matrix. Furthermore, the macromolecular assembly of newly synthesized collagens and proteoglycans is critical for tissue engineering, as initially laden matrix serves as a template for subsequent matrix deposition and architecture. The polymers such as collagen, chondroitin sulfate, hyaluronate, fibrin, agarose, alginate and chitosan are often used in tissue engineering applications (Figure 12) [83]. Inclusion of chondroitin sulfate in scaffold may promote the secretion of proteoglycan and type II collagen [85], and using of hyaluronic acid can facilitates the integration of cells to the engineered cartilage [86].
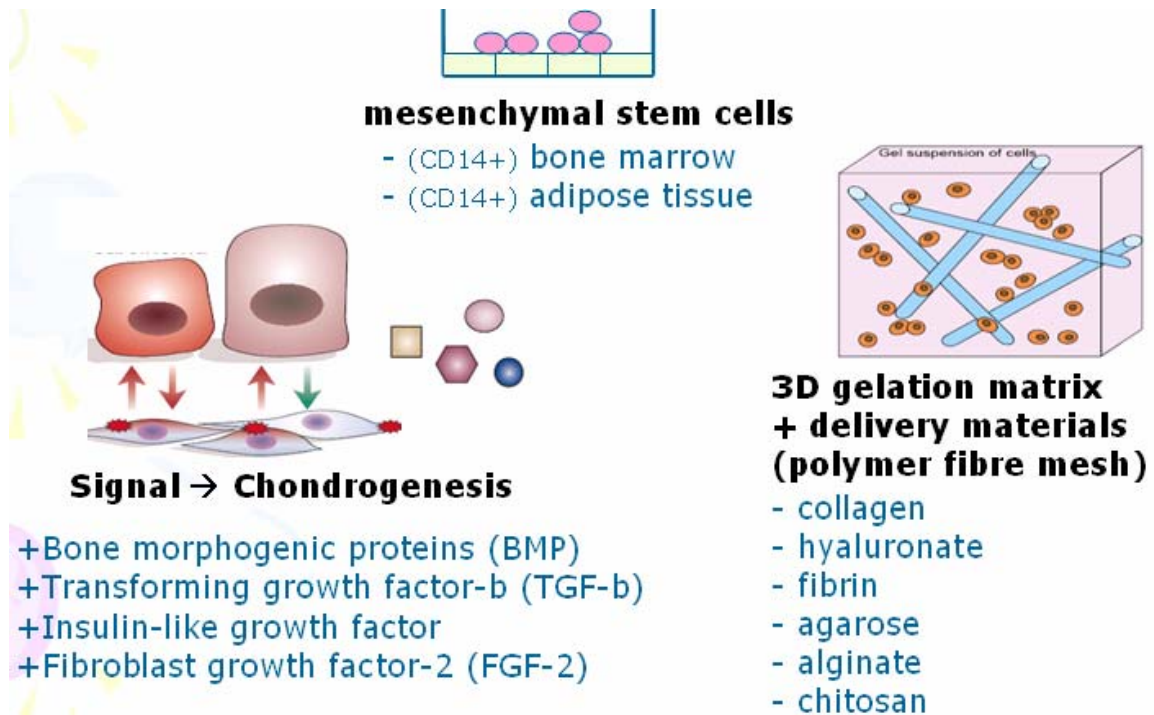
Figure 12 Tissue engineering triad of tissue engineered cartilage.

1-5.3 Chondrogenesis Signals

A multi-factors network of metabolic pathways governs chondrogenesis (Figure 12) [60]. TGF-β, BMPs, and the sonic hedgehog gene (members of TGF-β superfamily) were found to enhance chondrogenesis. Insulin-like growth factor was shown to have a synergistic effect with a member of the TGF-β family in promoting progenitor cell chondrogenesis. FGF-2 also has a role in chondrogenesis, inducing MSC proliferation and promoting retention of multilineage differentiation capacity [60].

CHAPTER 2

THEORETICAL BASIS

2-1 Reactive Oxygen Species in Cartilage

2-1.1 Introduction of Reactive Oxygen Species

Reactive oxygen species (ROS) are a group of oxygen-containing and highly reactive species which are partially reduced from molecular oxygen, including molecules such as hydrogen peroxide (H_2O_2), radicals such as hydroxyl radical ($^\bullet OH$), ions such as hypochlorite ion (OCl^-), and both an ion and a radical such as superoxide anion ($O_2^{\bullet -}$) [46, 87]. Under normal physiological conditions, the formation of ROS is a natural consequence of cellular metabolism, where about 1% to 3% of oxygen uptook by the body is reduced into ROS [88, 89]. The major source of ROS exists in the mitochondrial aerobic respiratory electron transport chain (ETC). Among four multi-protein complexes of ETC, Complex I, II, and III were believed to produced superoxide anion byproduct by leaking electrons to oxygen (Figure 13) [90, 91].
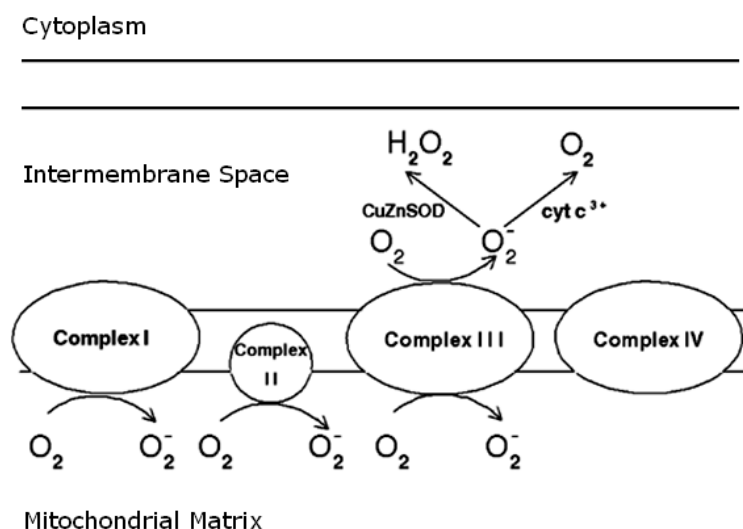
Figure 13 Generation of superoxide anion in the mitochondrial respiratory electron transport chain (ETC). (Modified from reference [91])

After reducing oxygen by one electron, the produced superoxide anion ($O_2^{\cdot-}$) can serve as the precursor of most other ROS. For example, superoxide anion can undergo dismutation to become hydrogen peroxide (H_2O_2), which can be further partially reduced to one of the strongest oxidants, hydroxyl radical ($^{\cdot}OH$) [92]. Furthermore, superoxide anion may also react with other radicals to produce new oxidants, such as peroxynitrite, an oxidant produced by the reaction of superoxide anion and nitric oxide ($^{\cdot}NO$) [93]. In addition to generating ROS by mitochondrial respiratory system, microsomal cytochrome P450 enzymes, flavoprotein oxidases, and peroxisomal enzymes involved in fatty acid metabolism also serve as the intracellular sources of ROS [88, 94].

According to current research, the biological functions of ROS constitute a paradox. They are not only involved in signal transduction and homeostasis of tissue turnover but also involved in cell death and cellular degradation (Figure 14) [67, 95]. Under normal physiological conditions, the toxic effects of ROS are prevented by various cellular anti-oxidant systems, which mean that the production of ROS and the scavenging of ROS by antioxidants are in balance. Therefore, the resulting low concentration of ROS within cells act as intracellular second messenger molecules which regulate the expression of a number of genes, such as ECM components, MMPs, and cytokines [96, 97]. However, in several pathological circumstances, the ROS are somehow over-produced and the antioxidants defenses become insufficient, which lead to destroy the balance between intracellular and extracellular redox state [67, 98]. The resulting so-called "oxidative stress" is an abnormal catabolic state which can induce structural or functional changes in cells and tissues by oxidizing polyunsaturated fatty acids to increase membrane fluidity and permeability, oxidizing guanine to 8-hydroxyguanine to cause DNA damage, and oxidizing amino acids such as proline, arginine, and cysteine to make protein dysfunction [46, 99-101].
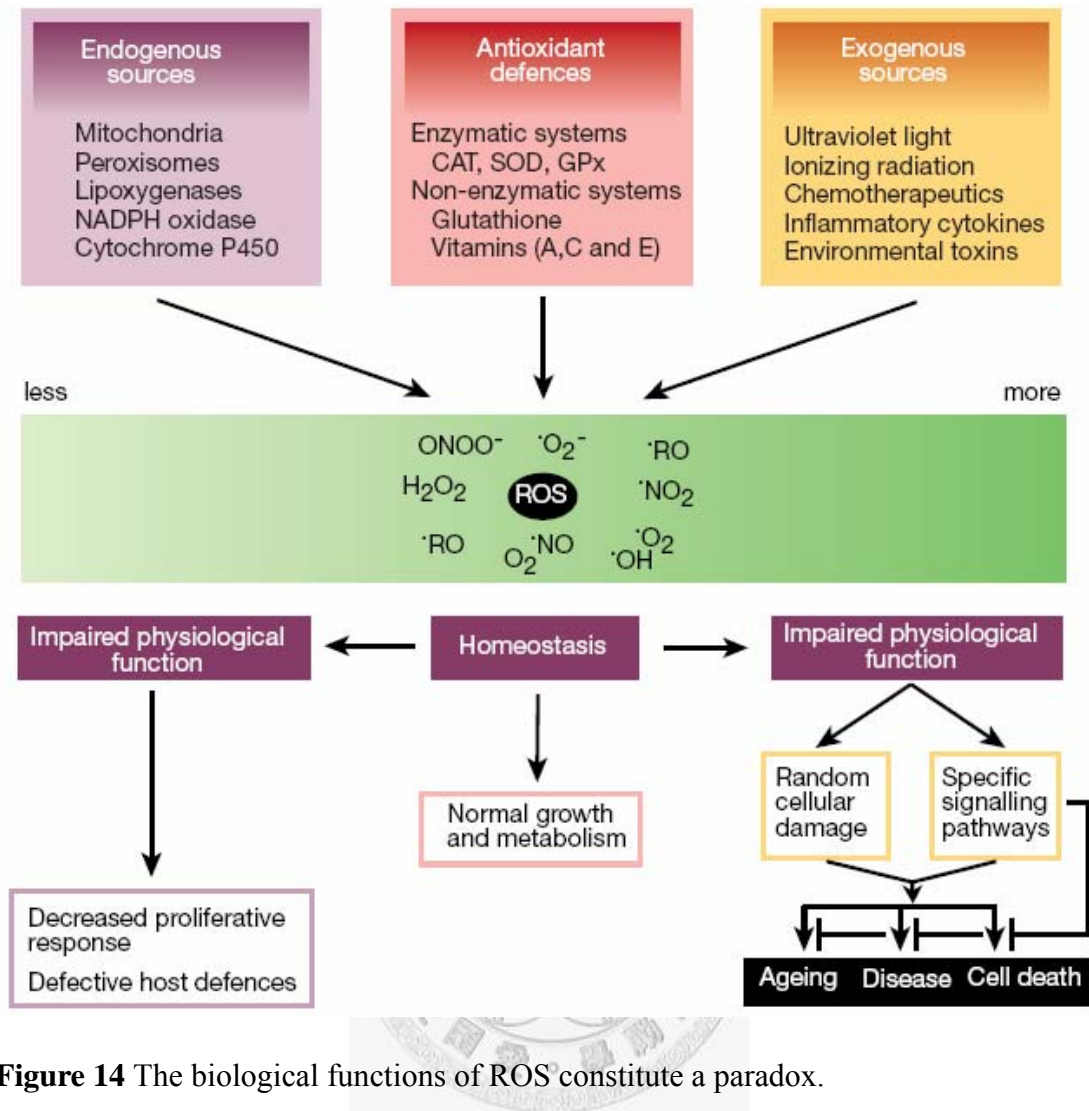
Figure 14 The biological functions of ROS constitute a paradox.

2-1.2 Reactive Oxygen Species Formation in Cartilage

The often produced ROS in chondrocytes are superoxide anion ($O_2{}^{\bullet-}$) and nitric oxide ($^\bullet NO$), which can further generate derivative radicals such as $ONOO^-$ and H_2O_2 (Figure 15) [102, 103]. Although $O_2{}^{\bullet-}$ *in vivo* can be enzymatically or nonenzymatically produced, in cartilage, $O_2{}^{\bullet-}$ is produced by the nicotinamide dinucleotide phosphate (NADPH) oxidase, which is a complex enzyme system consisting two membrane bound peptides: one is a two-peptide formed flavocytochrome, the other is a regulatory peptide called (Rap1A) [104]. Similarly, $^\bullet NO$ in cartilage is also produced by an enzyme system, called NO synthase (NOS) [105]. Among three isoforms of NOS, chondrocytes express endothelial NOS (eNOS) and inducible NOS (iNOS) to generate nitric oxide [106]. On the other hand, in an i*n vitro* environment, it was reported that $O_2{}^{\bullet-}$ may be generated by tumor necrosis factor-α (TNF-α) stimulation or by cyclic stretch [107], and $^\bullet NO$ generation may be stimulated by IL-1β, TNF-α, shear stress, or mechanical compression.
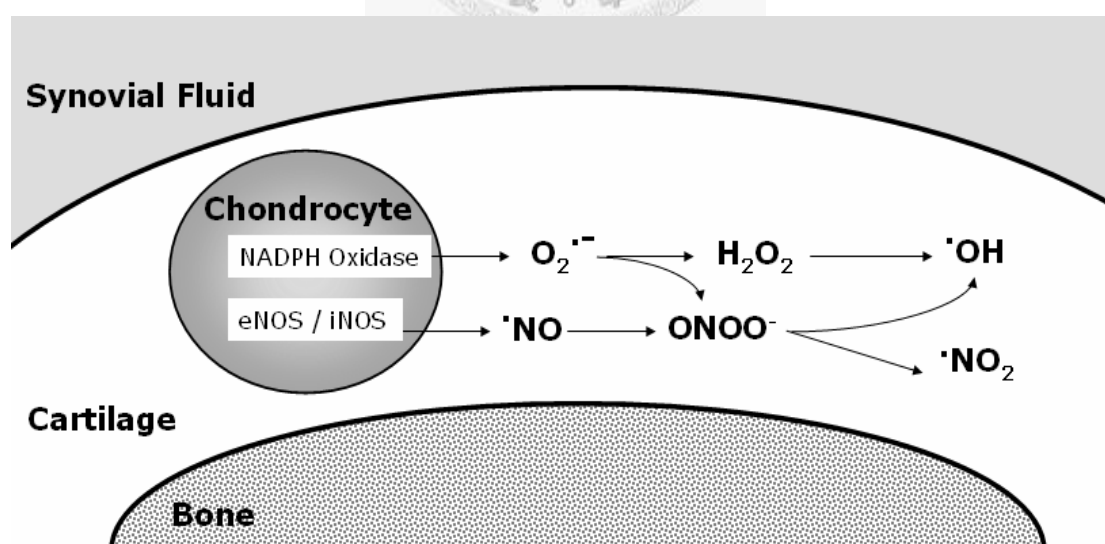
Figure 15 Schematic representation of the often produced ROS in chondrocytes.

(Modified from references [46] and [67])

2-1.3 Antioxidant Systems in Cartilage

In order to prevent the toxic effects of ROS, chondrocytes possess various anti-oxidant defensive systems to scavenge the over-produced ROS, which include superoxide dismutase (SOD), catalase (CAT), glutathione peroxidase (GPx), and peroxiredoxins (PRDX) (Figure 16) [108-111]. SODs are metalloproteins which possess metals in their reactive centers [112]. In chondrocytes, cytosolic Cu/Zn SOD and mitochondrial Mn SOD are constitutively expressed to catalyze two superoxide anions into one hydrogen peroxide and one molecular oxygen [113]. Because $O_2{}^{\bullet-}$ is the most frequent and abundant ROS produced by normal cellular metabolism, the breakdown of $O_2{}^{\bullet-}$ becomes the first defense mechanism against ROS [112]. However, the resulting hydrogen peroxide is also another kind of ROS and its accumulation is regarded as an oxidative stress as well. Therefore, catalase and glutathione peroxidase coexist and are functioned as scavengers of H_2O_2 [113, 114]. Besides this, peroxiredoxins, a newly found peroxidase family which possesses six isoforms in mammals, expresses type V isoform and eliminates H_2O_2 in cartilage [111].
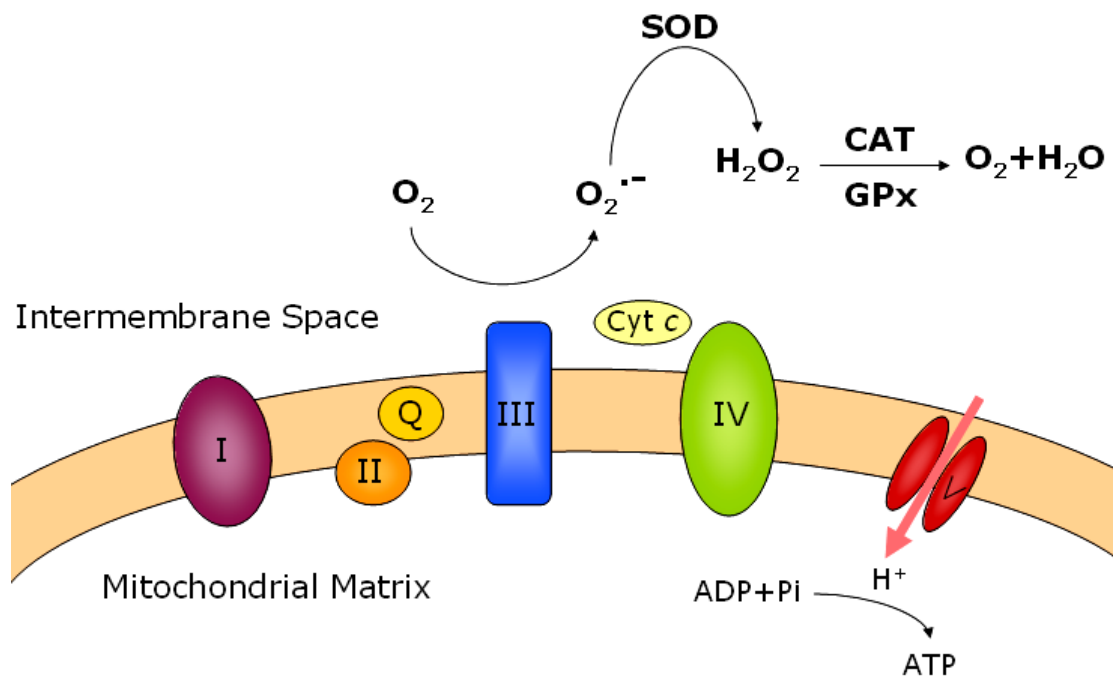
Figure 16 Schema of the antioxidant systems. (Modified from reference [91, 115])

2-1.4 Reactive Oxygen Species on Cartilage Matrix Degradation

In pathological conditions, such as OA, reactive oxygen species have been described as an important factor on cartilage matrix degradation because they can cause cellular or organic changes by either directly oxidizing the amino acids of collagen and proteoglycan molecules or by modifying the expression of anabolic and catabolic related enzymes [46, 99-101, 116]. From several *in vitro* experiments, it have been reported that ROS directly attacked ECM components. For example, when treating the incubated type I collagen with $O_2^{\bullet-}$, collagen was degraded and the ability of fibrils formation was lost [117, 118]. Moreover, in the $^{\bullet}OH$ and oxygen coexisting environment, collagen was degraded into small peptides where the cleavages often happened on proline or 4-hydroxyproline residues, and the increase of glutamic acid and aspartic acid in the peptides were also observed [119]. Furthermore, HOCl was discovered to possess the ability to cleave hyaluronic acid and hence decrease the viscosity of synovial fluid [120]. On the other hand, some data also showed that ROS can change the response of chondrocytes to ECM-related anabolic enzymes or upregulate the expression of ECM-related catabolic enzymes. For instance, the concurrent generation of $O_2^{\bullet-}$ and $^{\bullet}NO$ could decrease the sensitivity of chondrocytes to IGF-1 and hence inhibit the synthesis of proteoglycan [121, 122]. Moreover, $^{\bullet}NO$ could inhibit the sulfation of newly synthesized proteoglycan under the induction of IL-1 [123], and $^{\bullet}NO$ also played an important role in activation of metalloprotease enzymes in articular cartilage [124]. Besides this, HOCl could directly activate the proenzymes of metalloprotease and inactivate the tissue inhibitors of metalloprotease (TIMPs) [125, 126].

2-1.5 Reactive Oxygen Species on Cartilage Senescence

Oxidative stress is an important factor of the aging process in cartilage. Because adult articular cartilage is considered as a post-mitotic tissue with the characteristic of limited ability to achieve tissue turnover [127], its aging process is not attributed to intrinsic replicative senescence accompanying with telomere shortening but is related to oxidative stress-induced extrinsic senescence [66, 128]. Several reports showed that the ability of chondrocytes to detoxify ROS and turnover the damaged macromolecules is dramatically inefficient over time [112]. Therefore, oxidative damage products such as peroxidated lipids [129], nitrotyrosine [130], and mutagenic 8-oxoguanine [131] gradually accumulate in chondrocytes and disturb normal cellular functions until the chondrocytes can not endure these structural changes. Notably, the production of mutagenic 8-oxoguanine has been reported to result from $O_2^{\bullet-}$ attack which directly cause telomere erosion by injuring the guanine repeats in telomere DNA [132]. Moreover, it also has been reported that cell aging process correlates with the degeneration of mitochondria which may lead further leakage of electron transport chain and hence increase the production of ROS [133]. The accumulated ROS in mitochondria then attack mitochondrial 16-kilobase circular DNA, and the resulting mtDNA mutations contribute to the feature of accelerated aging [134].

2-1.6 Reactive Oxygen Species on Chondrocyte Death

In adult tissues, cell death plays an important role in maintenance of the balance of cell proliferation and the constancy of cell numbers [135]. Apoptosis is an active process of programmed cell death which is characterized by a series of morphological changes including DNA fragmentation, chromatin condensation, nucleus break-up, and cell fragmentation, while necrosis is the accidental death of cells that resulting from a pathologic injury [136].

It has been noted that aging [110], mechanical damage [137], and pathology such as osteoarthritis [138] often result in increased chondrocyte death in cartilage, and because of adult cartilage has limited ability for self-repair, the damaged cells may further accelerate the progression of the lesion [139]. From Blanco *et al.*'s research, it has been revealed that $^{\bullet}$NO is a primary inducer of chondrocyte apoptosis and is down-regulated by caspase-3 and tyrosine kinase activation [140]. However, from recent research, it has revealed that the toxicity of $^{\bullet}$NO needs to be further modulated by other ROS. For example, Del Carlo *et al.*'s research showed that the chondrocyte cell death mediated by $^{\bullet}$NO requires the generation of $O_2^{\bullet-}$, which suggests that $ONOO^-$ plays an important role in the process [141]. Moreover, in Kurz *et al.*'s finding, they found that both $O_2^{\bullet-}$ and H_2O_2 play important roles in mechanically induced cell death [142]. From these examples, it might be suggested that $O_2^{\bullet-}$ also plays an important role as $^{\bullet}$NO in chondrocyte cell death [46].

Several methods have been developed to detect cell death. However, it is often not sufficient to distinguish between apoptosis and necrosis by only applying a single assay. Therefore, combination of two to three methods is necessary to measure the morphological changes as well as the intracellular cell death parameters. Table 1 summarizes some methods for the characterization of cell death [136].

Table 2 Some methods for the characterization of cell death [136].
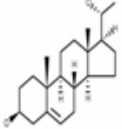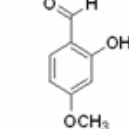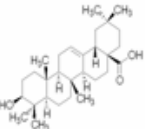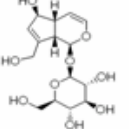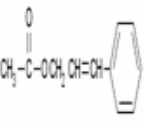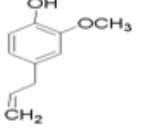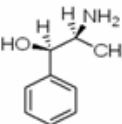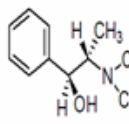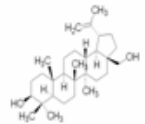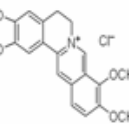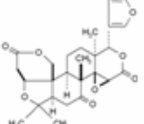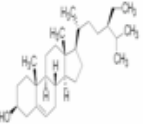
Cell Death Parameter	Method	Specific Detection of Apoptosis
Loss of cell attachment	Staining of cells with crystal violet or fluorescent DNA-binding dyes	−
Cellular ultrastructure	Electron Microscopy	+
Externalization of phosphatidyl serine	Annexin V binding	−
Release of cytosolic compounds	51Cr release, 3H-labeled proteins, enzymatic activities in culture supernatants	−
Uptake of dyes	Vital dyes (counting of cells) or fluorescent dyes for FACS	−
DNA laddering	Agarose gel electrophoresis	+
In situ DNA cleavage	TUNEL	−
Nuclear condensation and fragmentation	DAPI	+
DNA degradation	DNA content in sub G1 cells (FACS), agarose gel electrophoresis, DNA fragmentation ELISA	−
Internucleosomal DNA fragmentation	DNA fragmentation ELISA, agarose gel electrophoresis	+
Oxidative phosphorylation	MTT, Alomar Blue	−
Mitochondrial membrane polarization	Aggregation, uptake, sequestration of fluorescent dyes	−
Caspase activity	Conversion of fluorogenic substrates	+
Caspase processing	Western blot, immunhistochemistry	+
Cleavage of caspase substrates	Western blot, immunhistochemistry	+

2-2 Chondrogenesis-related Chinese Herbal Medicine

Circumstances that impair chondrocyte function can disrupt the balance of synthesis and catabolism in favor of cartilage degradation, which over time can lead to OA. The changes can result in joint symptoms such as pain, stiffness and loss of function. The symptoms vary with time and between joint sites and individuals. The main risk factors for OA are age, obesity and any form of joint trauma. In some families, OA seems to be inherited [143].

In Chinese herbal medicines, a number of herbs are used for treating joint symptoms in a long time treatment, and more and more researches have shown that the effective chemicals extracted from them possess various biological activities [144, 145]. From traditional Chinese herbal medicine ancient literatures and records, we preliminarily compared the prescriptions which have been used to treat the degeneration of the cartilage and targeted on 12 single chemical compounds which are extracted from 7 chondrogenesis-related Chinese herbal medicines (Table 1).

Table 3 Twelve single chemical compounds extracted from 7 chondrogenesis-related Chinese herbal medicines.

Then, by furthering systematic computer-aided search of the Medline database for the period 1990 through June 2006 and considering the commercializing achievability, we investigated the involved mechanism of 2 major single chemical compounds extracted from *Plantago asiatica* and *Ampelopsis brevipedunculata (Maxim.) Trautv.* by focusing on their antioxidant activity on cartilage tissue engineering. (Table 2)

Table 4 Four chondrogenesis-related single chemical compounds extracted from *Plantago asiatica* and *Ampelopsis brevipedunculata (Maxim.) Trautv.*

Plantago asiatica   Ampelopsis brevipedunculata
                           (Maxim.) Trautv.
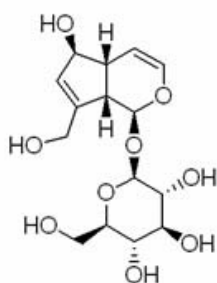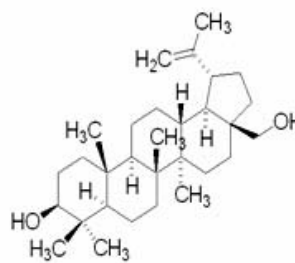
Aucubin   Betulin

2-3 Purpose of this study

The objective of this study was to modify the current cartilage tissue engineering triad and find a better combination for regeneration the articular cartilage *in vitro* environment. We searched for the new signals which are more stable in structure and cheaper in price than the traditionally used signals such as TGF-β1 and IGF, and suggested that because of the ROS were scavenged in cultured chondrocytes, the life span of cartilage tissue hybrids would be longer. Also, we modified the components of original gelatin-C6S-HA tricopolymer to the one which is more mimic the really ECM in organisms. We hope that the newly designed cartilage tissue engineering triad will improve the antioxidant and proliferation activity of chondrocytes.

In the beginning, we had to find the optimal concentration of these single chemical compounds when they were added in culture medium, and the experiment is divided into two parts: one part is 2D cell-based experiment, and the other part is 3D tissue engineering. In the 2D cell-based experiment, the important role in scavenging free radicals by these extracted chemical compounds was detected by the chemiluminescence method, and the proliferation and matrix productivity of chondrocytes were evaluated by real-time reverse-transcriptase polymerase chain reaction, ELISA assays, and immuno-histochemical staining. In the 3D tissue engineering experiment, also, the proliferation and matrix productivity were double evaluated by ELISA assays, real-time reverse-transcriptase polymerase chain reaction, and immuno-histochemical staining.

Table 5 Experiment Design.

2D Cell-based Experiment
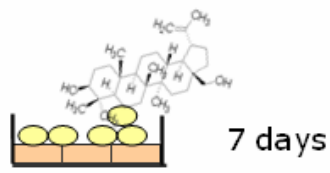
| MTT、LDH |
| Total DNA |
| Quantitative PCR |
| Superoxide anion: O_2^- |
| GAGs conc. (DMMB) |
| Histostain (HE&AB) |
| Immunostain (S100 & II col) |

7 days

3D Tissue Engineering
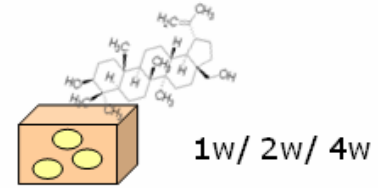
| SEM |
| WST-1 |
| Total DNA |
| GAGs conc. (DMMB) |
| Quantitative PCR |
| Histostain (HE&AB) |
| Immunostain (S100 & II col) |

1w/ 2w/ 4w

CHAPTER 3

MATERIALS AND METHODS

3-1 Two-dimensional Cell-based Experiments

3-1.1 Isolation and Culture of Chondrocytes

3-1.1.1 Specimen Isolation

The articular cartilage used in the experiment was obtained aseptically from adult porcine knee joints which had no macroscopic signs of osteoarthritis. Within 4 h of slaughter, the integral part of adult porcine knee joint was cleaned by 75% ethanol (E7148, Sigma Co., St. Louis, MO, U.S.A.), iodine solution (35089, Sigma Co.) and phosphate-buffered saline (PBS, pH 7.2) in sequence. After trimming the undesired connective tissue with sterile scalpels, the cartilage tissue was sliced into 5mm×5mm×0.5mm pieces, and the action of slicing was avoided cutting deep into the subchondral bone [146]. Then the thin slices were washed three times in sterile PBS and were further sterilized by soaking in 5-fold antibiotics-added (50 units/mL penicillin, 50 μg/mL streptomycin, 100 μg/mL neomycin, P4083, Sigma Co.) PBS for 15 minutes.

3-1.1.2 Matrix Digestion

Enzymatic digestion of articular cartilage has been a feasible and useful technique for isolating chondrocytes based on degrading the extracellular matrix between cells. [147, 148]. In this experiment, the thin slices of cartilage were subjected to 0.2% collagenase (C0130, Sigma Co.) digestion in order to degrade the native collagen between animal cells and get the sufficient amount of cells after digestion [149-151]. The collagenase was dissolved in DMEM (31600-026, Gibco

Invitrogen Co., Burlington, Ontario, Canada) which was supplemented with 3.7 mg/ml sodium bicarbonate (S5761, Sigma Co.), 50 μg/ml ascorbic acid (A5960, Sigma Co.) [152], 50 units/50 μg/100 μg/mL penicillin/ streptomycin/ neomycin (P4083, Sigma Co.), and 10% heat-inactivated fetal bovine serum (100-106 Gemini Bio-Products, Woodland, CA) and filter-sterilized by passing through a 0.22 μm filter (SCGPT05RE, Millipore Co., Bedford, MA, U.S.A.). After incubating the sliced cartilage in a humidified incubator at 37°C, 5% carbon dioxide for 16 hours, the resulting chondrocytes/collagenase solution suspension was collected and centrifuged at 1500 rpm for 5 min (KUBOTA 5101, Canada). The supernatant was discarded and the pelleted cells were gently washed once in PBS to neutralize remaining collagenase. Cells were centrifuged at 1500 rpm for 5 min again and resuspended in 10 ml of the same medium mentioned above. Cell number and viability was assessed by hemocytometer and trypan blue dye (T8154, Sigma Co.) exclusion.

3-1.1.3 Cell Culture

The chondrocytes were plated out to sterile 10cm tissue culture petri dishes (Cellstar, Greiner Bio-One, Longwood, Florida, United States) at 1×10^6 cells per dish as monolayer culture in the same DMEM mentioned above and maintained in a humidified incubator at 37°C, with 5% carbon dioxide [153]. Usually, the healthy chondrocytes would begin to adhere within the first two days, so in the 3rd day the culture medium was refreshed to discard the dead cells [154]. Moreover, often in the 7th day the cultured chondrocytes reached confluence and were detached by 0.05% trypsin with EDTA•4Na (15400-054, Invitrogen Co.) for passage. Because most of the *in vitro* cultured chondrocytes lost their phenotype after the third passage [155], the cells used in the experiment were all in the beginning of the second passage.

3-1.2 Effective Single Compound Treatment

In two-dimensional cell-based experiments, two commercially available effective single compounds: aucubin (55561, Fluka, St. Louis, MO, USA) and betulin (B9757, Sigma Co.) were chosen. Because previous researches have shown that the concentration of aucubin and betulin around 0.03 μM and 1 μM created no biochemically toxic to cells [156, 157], 5 mg of aucubin and 10 mg of betulin were separately dissolved in 50 ml of PBS to serve as a 0.1 mg/mL and a 0.2 mg/mL stock solution, respectively. Then, aucubin stock solution was further diluted with culture medium to get a starting concentration at 0.005 mg/mL, and betulin stock solution was also diluted with culture medium to get a starting concentration at 0.02 mg/mL. In order to assess the safe and effective concentration ranges of two compounds for treating chondrocytes, four-fold serial dilution with culture medium of the starting concentration of aucubin and betulin were performed to achieve twelve different concentrations, and the cytotoxicity effects of different concentrations of aucubin and betulin on chondrocytes were assessed by LDH assay and MTT assay (detailed methods and results were shown later). After this, only three different concentrations of aucubin (5μg, 80μg, and 1280μg of aucubin/L culture medium) and betulin (0.02μg, 0.32ug, and 5.12ug betulin/mL culture medium) were chosen for further experiment.

For the subsequent experiment, chondrocytes in their beginning of passage two were trypsinized and re-plated out to sterile optimal cell culture microplates (Greiner Bio-One) for further 7-day effective single compounds treatment. Aucubin-treated experimental groups were separately treated with a concentration of a 5μg, 80μg, and 1280μg of aucubin/L culture medium while betulin-treated experimental groups were separately treated with a concentration of a 0.02μg, 0.32ug, and 5.12ug betulin/mL culture medium. Chondrocytes cultured with no chemical added culture medium served as the control group.

3-1.3 LDH Cytotoxicity Assay for Cytotoxicity

Lactate dehydrogenase (LDH) is a stable cytoplasmic enzyme retained within intact plasma membranes [158]. However, when cells are exposure to toxic substances which may somehow induce the loss of plasma membrane integrity, LDH begins to release into culture medium from leaky membrane [159]. Therefore, the amount of LDH released in culture medium can be used as the indicator of necrotic cells [158]. Here, a commercially available CytoTox 96® Non-Radioactive Cytotoxicity Assay (G1780, Promega Co., Madison, WI, U.S.A.) was chosen for LDH leakage detection. Briefly, released LDH converts NAD^+ and lactate to NADH and pyruvate, and in the presence of a coupled enzymatic assay, NADH and the added tetrazolium salt (INT) turn into a red formazan product. The chemical reactions of the CytoTox 96® Assay are as follows:

$$NAD^+ + lactate \quad \xrightarrow{\text{LDH}} \quad pyruvate + NADH$$

$$NADH + INT \quad \xrightarrow{\text{Diaphorase}} \quad NAD^+ + formazan \text{ (red)}$$
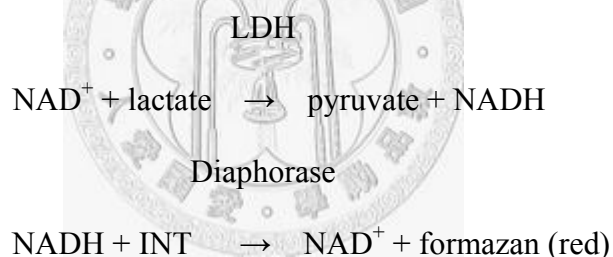
The amount of red formazan product correlates with LDH activity, and the data can be collect in a change in visible wavelength absorbance at 490 nm. Briefly, chondrocytes in their beginning of passage two were trypsinized and re-plated out to sterile 48-well cell culture microplates at 2×10^4 cells per well for further 7-day effective single compounds treatment. Each aucubin-treated experimental group, betulin-treated experimental group, and the control group were all performed in quadruplicate. At the end of 7-day cultivation, 50 ml of aliquots of media and total 100 ml of reagent were mixed in a 96-well plate (Greiner Bio-One), and absorbance at 490 nm was recorded using a MicroElisa reader (Emax Science Corp., CA, U.S.A.).

3-1.4 MTT Assay for Cell Viability

MTT (3-[4,5-dimethylthiazol-2-yl]-2,5-diphenyltetrazolium bromide) is a yellow water soluble tetrazolium salt, which can be endocytosed by metabolically active cells and chemically reduced to an insoluble purple formazan crystal by cleavage of its tetrazolium ring [160-162]. The reduction of MTT is accomplished by NADPH and NADH which are produced by the succinate dehydrogenase system of metabolically active mitochondria and also by other enzyme systems within the viable cells outside the mitochondria [162-164]. Therefore, the amount of insoluble purple formazan crystal produced is directly proportional to metabolically-active cell number which can be served as an indicator of cell viability in cell proliferation and cytotoxicity [165, 166]. Moreover, because the insoluble purple formazan crystals are impermeable to the cell membranes, they accumulate in healthy cells and were further solubilized by organic solvent for spectrophotometrical measurement. Briefly, chondrocytes in their beginning of passage two were trypsinized and re-plated out to sterile 48-well cell culture microplates at 2×10^4 cells per well. Each aucubin-treated experimental group, betulin-treated experimental group, and the control group were all performed in quadruplicate. MTT was freshly prepared with 0.01M PBS (pH 7.2) to obtain a concentration of 5 mg/ml and sterilized by passing through a 0.22 μm filter. At the end of 7-day cultivation, after removing the culture media, chondrocytes were washed once by PBS and added with 125 uL MTT solution and then incubated at 37°C again for 4 h. Then, the MTT solution was removed, chondrocytes were washed again by PBS, and 100 μl of 1M HCl were added to each well. The absorbance at 570 nm was recorded using a MicroElisa reader (Emax Science Corp., CA, U.S.A.).

3-1.5 Total DNA for Cell Proliferation Quantification

The Wizard® Genomic DNA Purification Kit (A2360, Promega Co., Madison, WI, U.S.A.) was chosen for DNA extraction. Chondrocytes in their beginning of passage two were trypsinized and re-plated out to sterile 24-well cell culture microplates at 4×10^4 cells per well for further 7-day effective single compounds treatment. Each aucubin-treated experimental group, betulin-treated experimental group, and the control group were all performed in triplicate. Briefly, at the end of 7-day cultivation, after discarding the culture medium and washing cells with $1\times$ PBS, lysis buffer was added to lyse the cells, and each lysate was transferred to a separate Wizard® SV minicolumn assembly. The assembly was centrifuged at $13,000 \times$ g for 3 min to bind genomic DNA to the membrane, and liquid in the collection tube of assembly was discarded. 650 mL of Wizard® SV Wash Solution was then added to wash the membrane of each assembly followed by centrifuging at $13,000 \times$ g for 1 min, and this step was repeated four times. Finally, extracted total DNA were dissolved in 65°C 250 uL nuclease-free water, and the absorbance at 230 nm, 260 nm, 280 nm, and 320 nm were measured by UV spectrophotometer (Beckman Instrument Inc., Fullerton, CA, U.S.A.). DNA quality was determined at the ratio of 260 nm and 280 nm absorption which should be in the range of 1.8 to 2.0 demonstrating good deproteinization [167], and the ratio of 260 nm to 230 nm help evaluate the level of salt carryover in the purified DNA [168]. DNA concentration was calculated by assuming 1 O.D. at 260 nm was equivalent to 50 ug of DNA per mL. Therefore, total DNA concentration was estimated with formula O.D. 260 - O.D. 320 × dilute factor × 50ug/ml, where the subtraction of A320 was for adjusting the A260 measurement for turbidity [169].

3-1.6 DMMB Assay for Quantitative Measurement of Sulfated GAGs Content

The 1,9-Dimethyl-Methylene Blue (DMMB) was used to determine the content of sulphate-glycosaminoglycans (sGAG), such as chondroitin sulphate and keratan sulphate, in the media to estimate the amount of cell-secreted proteoglycan [170, 171]. Positive charge of DMMB and the negative charge of sulfate of sGAG interact to form DMMB-GAG complexes which alter light absorbance at 595 nm and can thus be measured by spectrophotometer [172]. Briefly, the DMMB solution was prepared by dissolving 21 mg of DMMB (341088, Sigma Co.) in 5 mL of 95% ethanol (E7148, Sigma Co.), and the dissolved dye was further added with 2 g sodium formate (107603, Sigma Co.) and 800 ml of ddH$_2$O. The solution was adjusted to a pH of 3.5 by drop-by-drop addition of 0.1 M formic acid (33015, Sigma Co.), and ddH$_2$O was added to reach a final volume of 1 L. The stock DMMB solution was stored at 4°C in an aluminum foil-wrapped glass bottle. A standard curve was made using serial dilutions of chondroitin-6-sulfate with culture medium to final concentrations of 0.1, 1, 10, and 100 μg C6S/mL, and the absorbance at 595 nm of the DMMB-C6S complexes were measured triplicate and plotted against known concentrations [173]. Chondrocytes in their beginning of passage two were trypsinized and re-plated out to sterile 24-well cell culture microplates at 4×10^4 cells per well for further 7-day effective single compounds treatment. Each aucubin-treated experimental group, betulin-treated experimental group, and the control group were all performed in quadruplicate. At the end of 7-day cultivation, 40 ml of aliquots of media and 250 ml of DMMB solution were mixed in a 96-well microplate at room temperature, and absorbance at 595 nm was recorded using a MicroElisa reader (Emax Science Corp., CA, U.S.A.). Sulfated GAGs concentration of each sample was then calculated with use of the regression equation obtained from the linear standard curve.

3-1.7 Real-time Reverse-Transcriptase Polymerase Chain Reaction for mRNA Expression Quantification

Real-time Polymerase Chain Reaction (PCR) is a quantitative method to detect the amplification of a target sequence as it is amplified in real time during the progress of PCR cycling [174, 175] Because of the use of additional fluorescent reporter dye [174, 175], the amount of amplicon produced is collected during PCR cycles, rather than at the end of the PCR (i.e. the traditional agarose-gel-running semi-quantitative PCR) [176], and the result can be plotted as a representative amplification plot which reports the fluorescence of each cycle (Figure 17). Often used reporter dye includes SYBR® Green I dye. SYBR® Green I Dye is a small molecule which specifically binds to double-stranded DNA resulting in the increase of fluorescence. During PCR cycling, when new copies of the double-stranded target are created, the SYBR Green I dye then binds to each of them (Figure 18). Hence, the amount of amplicon is proportional to the increase in fluorescence intensity and can be detected in real time by the photo multiplier tube (PMT) of the real-time PCR instrument [177].
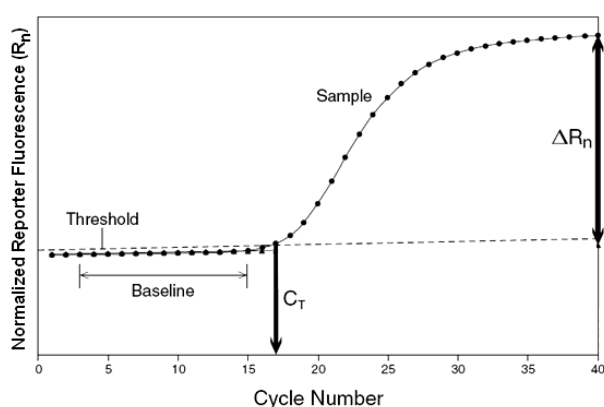
Figure 17 A representative real time PCR amplification plot and some definiendum. (Modified from Applied Biosystems User Bulletin #2: Relative Quantitation of Gene Expression (PN 4303859)).

(a) The SYBR® Green I dye fluoresces when binds to double-stranded DNA

(b) When DNA is denatured, the SYBR® Green I dye is released and fluorescence is drastically reduced

Forward Primer

(c) During extension, primers anneal and PCR product is generated

Reverse Primer

(d) SYBR® Green I dye binds to each new copy of the double-stranded DNA, resulting in a net increase in fluorescence detected by the instrument
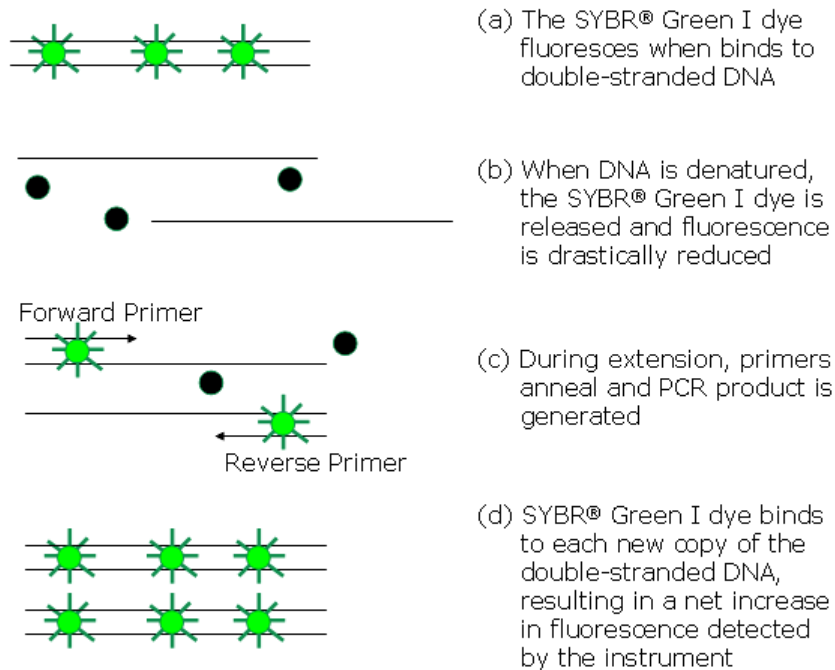
Figure 18 Mechanisms of the SYBR® Green I Dye chemistry. (Modified from Applied Biosystems User Bulletin #2: Relative Quantitation of Gene Expression (PN 4303859)).

In real-time PCR quantitation assay, both absolute and relative quantitation can be used to calculate the results, but relative quantitation assay is especially used to analyze changes in gene expression in a chemically treated experimental sample relative to an untreated control sample, and relative quantitation provides accurate comparison between the initial level of template in each sample without requiring the exact copy number of the template. Often, comparative C_T method is used for relative quantitation by using the arithmetic formula, $2^{-\Delta\Delta C_T}$, and the result is drawn as gene expression plot which shows the fold-difference of the treated experimental sample relative to the untreated control sample. The threshold cycle (C_T) here is defined as the fractional cycle number where the fluorescence passes the fixed threshold, and the threshold is set in the region of an exponential growth of PCR product.

In this study, chondrocytes in their beginning of passage two were trypsinized and re-plated out to sterile 12-well cell culture microplates at 8×10^4 cells per well for further 7-day effective single compounds treatment. Each aucubin-treated experimental group, betulin-treated experimental group, and the control group were all performed in quadruplicate. Briefly, at the end of 7-day cultivation, total RNA of each sample was isolated by TRI REAGENT^{TM} (T9424, Sigma Co.), and two-step real-time RT-PCR was used to measure specific mRNA expressed by chondrocytes, where the SuperScript^{TM} III First-Strand Synthesis System for RT-PCR (18080-044, Invitrogen Co.) and the 2X SYBR Green Master Mix (4309155, Applied Biosystems, Foster City, CA,. USA) were used for reverse transcription and PCR, respectively. The list of target genes for real-time RT-PCR in this study is in Table 4, and the primer sequence of those target genes are listed in Table 5. The detailed procedures were described in the following paragraphs.

Table 6 List of target genes for real-time RT-PCR in two-dimensional chondrocytes culture.

Target gene	Description
GAPDH	Housekeeping gene
I collagen	Absent in healthy cartilage, present when fibrously transformed
II collagen	Major collagen type in the cartilage
Aggrecan	Key component of aggregated proteoglycans
Decorin	Small proteoglycans
TIMP-1	Tissue inhibitor of MMPs
MT1-MMP	Degradative enzyme
MMP-2	Degradative enzyme
Sox9	Master chondro-regulatory gene
IL-1beta	Regulator of catabolism
TGF-beta1	Regulator of anabolism

Table 7 Primer Sequences of two-dimensional chondrocytes culture.

Name	Sequences
GAPDH	5'- GTCATCCATGACAACTTCGG-3'
	5'- GCCACAGTTTCCCAGAGG-3'
I collagen	5'- CAGAACGGCCTCAGGTACCA -3'
	5'- CAGATCACGTCATCGCACAAC -3'
II collagen	5'- GAGAGGTCTTCCTGGCAAAG -3'
	5'- AAGTCCCTGGAAGCCAGAT -3'
Aggrecan	5'- CGAAACATCACCGAGGGT- 3'
	5'- GCAAATGTAAAGGGCTCCTC-3'
Decorin	5'-GCATTTGCACCTTTGGTGAA-3'
	5'-GACACGCAGCTCCTGAAGAG-3'
TIMP-1	5'- AACCAGACCGCCTCGTACA -3'
	5'- GGCGTAGATGAACCGGATG -3'
MT1-MMP	5'- GCTGTGGTGTTCCAGACAAG -3'
	5'- GGATGCAGAAAGTGATCTCG -3'
MMP-2	5'- GTTCTGGAGGTACAATGA -3'
	5'- ACCACGGCGTCCAGGTTA -3'
Sox9	5'-ACCTGAAGAAGGAGAGC-3'
	5'-CACCGGCATGGGTACCA-3'
IL-1beta	5'- ACCTCAGCCCTCTGGGAGA -3'
	5'- CCTCCTTTGCCACAATCAC -3'
TGF-beta1	5'- GCACGTGGAGCTATACCAGA -3'
	5'- ACAACTCCGGTGACATCAAA -3'

In total RNA isolation, after discarding the culture medium and washing cells with 1× PBS, 500 μL of TRI REAGENT^{TM} was directly added to each well to dissociating nucleoprotein complexes for 5 minutes, and the cell lysate was homogenized by pipetting and transferred to separate microcentrifuge tubes. Then 100 μL of chloroform (C2432, Sigma Co.) was added, and the tubes were vigorously shake for 15 seconds and allowed to stand at room temperature for 15 minutes. The mixture was centrifuged at 12000 × g for 15 minutes at 4°C, and the colorless upper aqueous phase was transfer separately to a fresh microcentrifuge tube followed by adding 250 μL of isopropanol (I9516, Sigma Co.) and staying at room temperature for 10 minutes. The mixture was then centrifuged at 12000 × g for 10 minutes at 4°C, and the RNA precipitate would form a pellet on the bottom of the tube. After removing the supernatant, the RNA pellet was washed by 500 μL of 75% ethanol (E7148, Sigma Co.), vortexed and centrifuged at 7500 × g for 5 minutes at 4°C. Finally, the RNA pellet was dried for 10 minutes by air-drying and dissolved in 20 μL of the RNA Storage Solution (7001, Ambion, Austin, TX, USA). RNA content was determined at 260 nm by UV spectrophotometer (Beckman Instrument Inc., Fullerton, CA, U.S.A.) and RNA quality was evaluated at the ratio of 260 nm and 280 nm absorption which should be higher than 1.7.

In complement DNA synthesis, 8 μL of extracted RNA, 1 μL of 50 μM oligo(dT)$_{20}$, and 1 μL of 10mM dNTP were mixed and incubated at 65°C for 5 minutes, then placed on ice for 5 minutes. Next, 2 μL of 10× RT buffer, 4 μL of 25 mM MgCl$_2$, 2 μL of 0.1M DTT, 1 μL of RNaseOUT^{TM}, and 1 μL of SuperScript^{TM} III RT (200 U/ μL) were added into the mixture. After this, the mixture was incubated at 50°C for 50 minutes and followed by terminating the reaction at 85°C for 5mins. Finally, the synthesized cDNA was chilled on ice, and 1 μL of RNase H was added to each tube for 20 minutes at 37°C.

In real-time PCR, each reaction was performed with 10 mL of cDNA with 100 ng of cDNA in content, 12.5 μL of 2X SYBR Green Master Mix (4309155, Applied Biosystems Co.), 0.75 μL of 1 μM forward primer solution, 0.75 μL of 1 μM reverse primer solution, and 6 μL of nuclease-free water (P1193, Promega Co.). In order to avoid pipetting errors, three replicates of each sample were amplified. PCR cycles were performed on an ABI PRISM 7900 Sequence Detection System with ABI PRISM 7900 Sequence Detection Software 2.2.2 (Applied Biosystems, Foster City, CA, USA). Briefly, real-time PCR reaction was divided into three stages. In the first initiation stage, after the SYBR® Green I dye was activated at 50°C for 2 minutes, samples were then heated to 95°C for double-strand cDNA denaturation for 10 minutes. Next, in the second cycling stage, the samples were undergone melting at 95°C for 15 seconds followed by annealing/extension at 60°C for 1 minute for 40 cycles to produce the amplicons. Finally, in the last termination stage, the samples were hold at 37°C for 10 minutes for the SYBR® Green I dye inactivation.

Real-time PCR was amplified for GAPDH, type I collagen (COL1), type II collagen (COL2), aggrecan, decorin, tissue inhibitor of metalloproteinase-1 (TIMP-1), matrix metalloproteinase-2 (MMP-2), membrane-type matrix metalloproteinases-1 MMP (MT1-MMP), Sox9, IL-1β, and TGF-β1. GAPDH served as the endogenous control, and the level of mRNA expression of each target gene was normalized to GAPDH. The results were analyzed by comparative C_T method, where ΔCt value of each target gene was first normalized by subtracting the Ct value of GAPDH from the Ct value of each target gene, ΔΔCt value were then obtained by subtracting the ΔCt value of the untreated control sample from the ΔCt value of each aucubin or betulin treated experimental sample, and by using the arithmetic formula, $2^{-\Delta\Delta C_T}$, the fold-expression change of each mRNA was obtained.

3-1.8 Chemiluminescence Method for Detecting Free Radicals Scavenging

In order to assess the ROS scavenging effects of chondrocytes after treated with different concentrations of aucubin or betulin, luminal- and lucigenin- dependent chemiluminescences (CL) methods were used as indicators of ROS detection.

Luminol (5-amino-2,3-dihydro-1,4-phthalazinedione) is a water-soluble and slightly yellow crystalline solid which can exhibit chemiluminescence when activated with an appropriate oxidizing agent. Usually, the appropriate oxidizing agents are a solution of H_2O_2 or a hydroxide salt in water. When luminol reacts with H_2O_2, a series of reaction will lead to produce a very unstable intermediate product, and as the excited state product relaxes to the ground state, the excess energy is liberated as a photon which is visible as a striking blue glow (Figure 19).
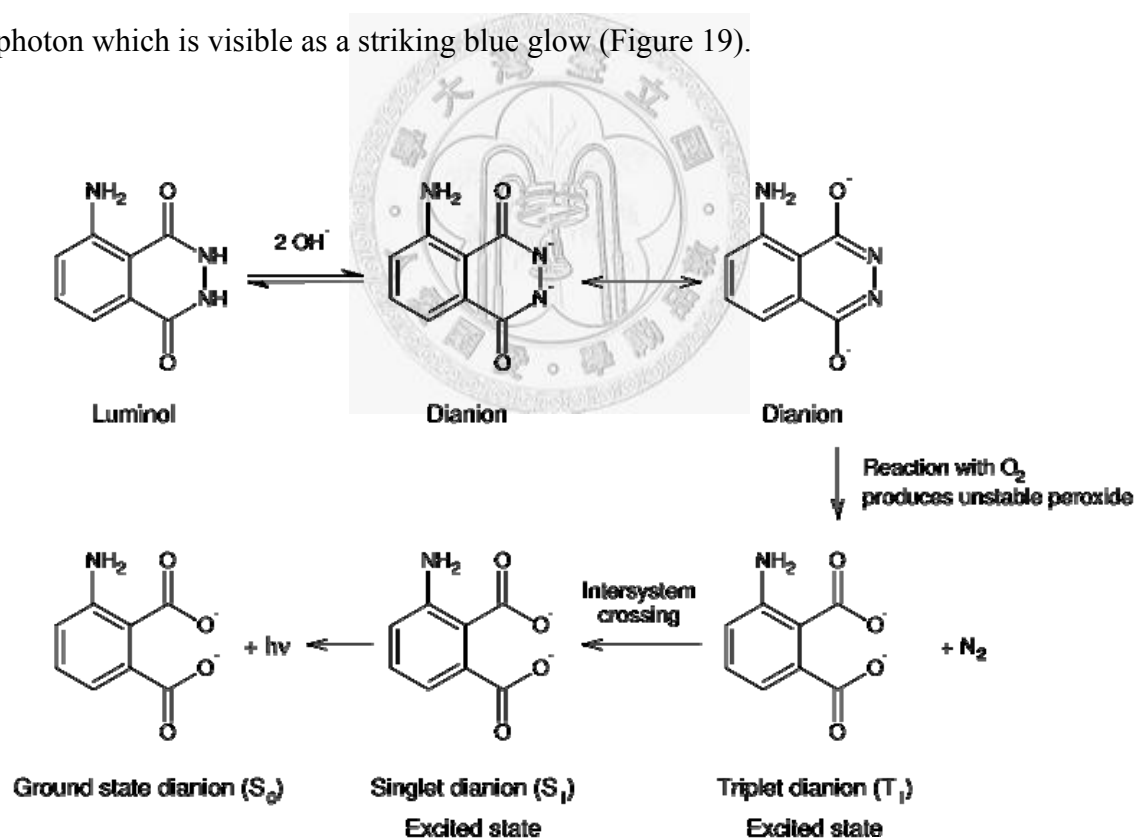
Figure 19 Reactions leading to the chemiluminescence of luminol.

Lucigenin (9,9'-Bis-N-methylacridinium nitrate) is an aromatic compound and is an specific reagent used for the generation of chemiluminescence in the presence of superoxide anion radical. It will react with $O_2^{\bullet-}$ and result in the formation of an excited intermediate product, and as the excited state product relaxes to the ground state, the excess energy is liberated as a photon which is visible as emits a bluish green glow.

In the experiment, 0.2 mM of luminol (09253, Fluka) was used to detect the existence of H_2O_2 or ROO, while 0.2 mM lucigenin (M8010, Sigma Co.) was specifically used to detect the existence of $O_2^{\bullet-}$. The measurements were made at room temperature using the Multi Luminescence Spectrometer (Tohoku Electronic Industrial Co., Ltd, Japan).

Briefly, at the end of 7-day cultivation, after discarding the culture medium and washing cells twice with PBS, specimens were put into the TEI CL Sample Chamber for background measurement for 180 sec. At the 181st second, 1 mL of lucigenin or luminol was added separately to each specimen, and the CL counts were obtained for further 6 min at 10 sec intervals. Finally, the results were given as the area under curve (AUC) for a counting period of 6 min, where the CL count was corrected for subtracting the AUC of the baseline.

3-1.9 Histochemical Staining Evaluation

Histological staining and characterization of cartilage tissue is used to provide a general evaluation of the morphology, structure, and arrangement of cells and matrix. Hematoxylin & eosin staining is used to characterize the morphology of chondrocytes, while alcian blue staining is used to characterize proteoglycans in the ECM. Briefly, chondrocytes in their beginning of passage two were trypsinized and re-plated out to sterile 8-well Lab-Tek II chamber slides (154534, Nalge Nunc International Co., Naperville, IL, USA) at 1.6×10^4 cells per well for further 7-day effective single compounds treatment. Each aucubin-treated experimental group, betulin-treated experimental group, and the control group were all performed in quadruplicate. At the end of 7-day cultivation, each group was fixed by 10% neutral buffered formalin (NBF) solution and then evaluated by Hematoxylin & Eosin staining and alcian blue staining.

The fixation step used here is a chemical process that allows the phenotypes of cells or tissue can be maintained as similar as they are in the *in vivo* environment. An appropriate fixative can stop the activity of intracellular enzyme which may cause autolysis after death, inhibit the infection of bacteria and molds, and protect cells or tissue from excessive shrinkage and swelling. Because formalin is a trade name which contains about 40% of formaldehyde gas in water, a 10% NBF solution contains approximate 4% formaldehyde. NBF can irreversibly crosslink DNA and RNA to nearby protein by combining the nitrogen atoms in DNA or RNA with primary amine groups through a -CH$_2$- linkage.

3-1.9.1 Hematoxylin & Eosin staining

Hematoxylin & Eosin staining is the basic and most common procedure for most tissues. Hematoxylin stains basophilic structures such as the nucleic acids-containing cell nucleus with blue-purple color, while eosin stains eosinophilic structures such as intracellular protein or extracellular protein with bright pink color. The structures of hematoxylin and eosin are shown in Figure 20.

Briefly, after the *in vitro* cultured 7-day chondrocytes were washed once by PBS and fixed in 10% NBF solution for 15 min, each sample slide was washed briefly in distilled water and then stained in hematoxylin solution for 2 min. The slides were then washed in running tap water for 2 minutes and then covered with 0.5% hydrogen chloride solution for 1 second to avoid over-staining. After washing the slides in running tap water for 15 minutes, each sample slide was then stained in eosin solution for 2 min, and the samples were dehydrated through 95% alcohol and two changes of absolute alcohol with 30 sec for each. Finally, each sample slide was dried by air, cleared in three changes of non-xylene solution with 30 sec for each, and then mounted with xylene based mounting medium.
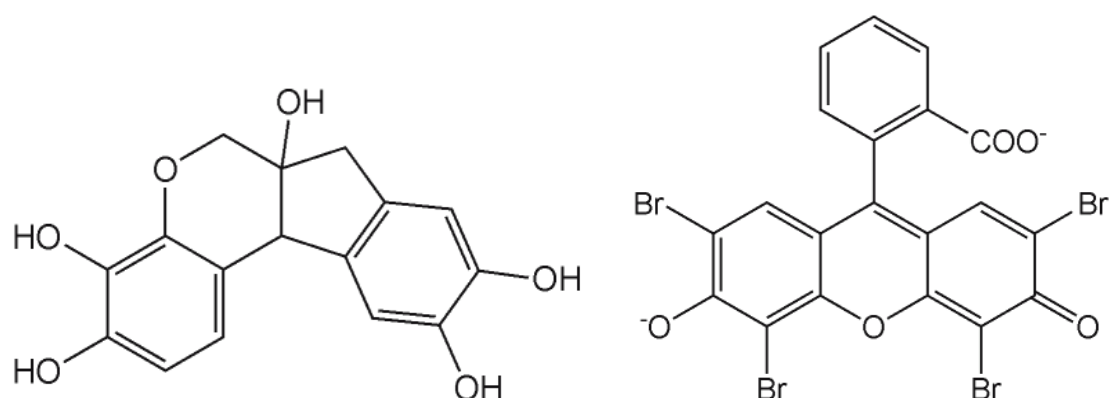
Figure 20 The structures of hematoxylin and eosin. Left one is hematoxylin, and right one is eosin.

3-1.9.2 Alcian blue Staining

Alcian blue is a widely used cationic dye and is a phthalocyanine dye which contains copper (Figure 21). It selectively stains the acid parts of polysaccharides and glycosaminoglycans (GAGs) by making electrostatic forces between the negatively charge of macromolecules (such as the sulfate group) and its cations. The stained parts usually become blue to bluish-green. Alcian blue staining can also be combined with H&E staining method.

Figure 21 The chemical structure of alcian blue.

Briefly, after the *in vitro* cultured 7-day chondrocytes were washed once by PBS and fixed in 10% NBF solution for 15 min, each sample slide was washed briefly in PBS and covered with 3% acetic acid for 2 min and washed by PBS again. The slides were then stained with alcian blue (pH 1.0, MUTO PURE CHEMICALS, Japan) for 30 min to let the alcian blue make electrostatic forces with the sulfate group of GAGs and then washed in running tap water for 1 minute. Hematoxylin staining was used here as a counterstain, so each sample slide was stained in hematoxylin solution for 2 min followed by being washed in running tap water for 15 min. Finally, the samples were dehydrated through 95% alcohol and two changes of absolute alcohol with 30 sec for each, dried by air, cleared in three changes of non-xylene solution with 30 sec for each, and then mounted with xylene based mounting medium.

3-1.10 Immunohistochemical Staining Evaluation

Immunohistochemical staining techniques have been developed in recent years to examine specific biochemicals such as type I, type II collagen, and other proteins in tissues. In immunohistochemistry, the biologic targets of interest are localized by the precise attachment of a complex or label, and the results can be subsequently visualized by either bright-field microscopy or by UV microscopy depending on whether the product is a chromogenic reaction product or a fluorescent coupled product. Common macromolecules in cartilage such as the ECM proteins and S100 protein have been successfully localized in the specimens by immunohistochemical staining.

The fixation step in immunohistochemical staining is much more restrict than in histochemical staining because of the successful of antibody localization may be fixative-sensitive. Often, fixation by ethanol or the sections treated by non-fixed frozen method may be needed for successful immunohistochemistry.

3-1.10.1 S100 Protein Immunohistochemical Staining

S100 protein is a calcium binding protein and exists in the cytoplasm and/or nucleus of cells derived from the neural crest, chondrocytes, adipocytes, myoepithelial cells, macrophages, dendritic cells, and keratinocytes. S100 proteins are involved in a variety of intracellular and extracellular functions including the regulation of cell cycle progression, protein phosphorylation, Ca^{2+} homeostasis, the dynamics of cytoskeleton constituents, enzyme activities, and the inflammatory response.

Briefly, after the *in vitro* cultured 7-day chondrocytes were washed once by PBS, each sample slide was fixed in acetone at -20℃ for 20 min. This step was used to directly break the cell membrane and let the intracellular components may directly

contact with the following reagents. Then, each sample slide was covered with PBS, incubated with 3% H_2O_2 to eliminate the activity of endogenous peroxidase for 10 min, and retrieved into the citrate buffer solution (pH 7) at 95°C for 20 min. The commercialized Histostain® Plus Kits (85-9643, Zymed, South San Francisco, CA, USA) was used in the following steps. 10% non-immune goat serum was used to block nonspecific antigen on each sample slide for 30 min at room temperature, and the sample slides were then incubated with 50-fold diluted mouse monoclonal [B32.1] to S100 antibody (ab7852, Abcam, Cambridge, MA, USA) for 1 hour. Subsequently, each sample slide was washed with PBS and incubated with the biotinylated goat anti-rabbit secondary antibody for 10 min, and then washed by PBS again and incubated with streptavidin-peroxidase conjugate for another 10 min. Finally, each sample slide was incubated with the 3, 3'-diaminobenzidine tetrahydrochloride (DAB) solution until the brown color developed around the antigen/antibody/enzyme complex, dehydrated through 95% alcohol and two changes of absolute alcohol with 30 sec for each, dried by air, cleared in three changes of non-xylene solution with 30 sec for each, and then mounted with xylene based mounting medium.

3-1.10.2 Type II Collagen Immunohistochemical Staining

Type II collagen is a fibrous structural protein and is an important component in ECM which adds structure and strength to connective tissues. It is found primarily in cartilage, inner ear, nucleus pulposus, and the vitreous of eyeball. In articular cartilage, type II collagen is the major protein which occupies 50% of the total proteins and makes up around 85% to 90% of collagen of articular cartilage.
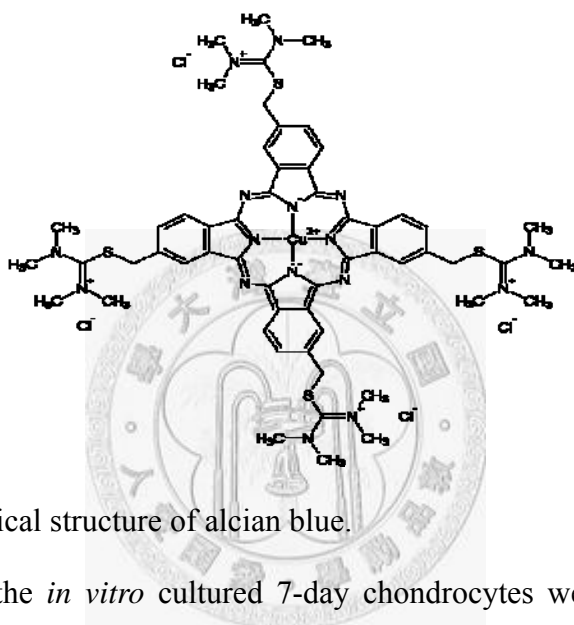
Briefly, after the *in vitro* cultured 7-day chondrocytes were washed once by PBS and fixed in 10% NBF solution for 15 min, each sample slide was covered with PBS, incubated with 3% H_2O_2 to eliminate the activity of endogenous peroxidase for

10 min, and retrieved into the citrate buffer solution (pH 7) at 95°C for 20 min. Also, the commercialized Histostain® Plus Kits (85-9643, Zymed, South San Francisco, CA, USA) was used in the following steps. 10% non-immune goat serum was used to block nonspecific antigen on each sample slide for 30 min at room temperature, and the sample slides were then incubated with 100-fold diluted rabbit polyclonal collagen type II antibody (NCL-COLL-IIp, Novocastra Laboratories Ltd., Newcastle, UK) for 1 hour. Subsequently, each sample slide was washed with PBS and incubated with the biotinylated goat anti-rabbit secondary antibody for 10 min, and then washed by PBS again and incubated with streptavidin-peroxidase conjugate for another 10 min. Afterward, each sample slide was incubated with the 3, 3'-diaminobenzidine tetrahydrochloride (DAB) solution until the brown color developed around the antigen/antibody/enzyme complex. Hematoxylin staining was used here as a counterstain, so each sample slide was stained in hematoxylin solution for 2 min followed by being washed in running tap water for 15 min. Finally, the samples were dehydrated through 95% alcohol and two changes of absolute alcohol with 30 sec for each, dried by air, cleared in three changes of non-xylene solution with 30 sec for each, and then mounted with xylene based mounting medium.

3-1.10 Statistical analysis

The paired Student's t-test was employed for determining the statistical significance of OD values detected in the LDH assay, MTT assay, Total DNA assay, and DMMB assay between each experimental group and the control group, where a p value of less than 0.05 was considered to be statistically significant. Similarly, the differences in mRNA expression and the ROS scavenging effects in each experimental group and the control group were also analyzed by using a paired Student's t-test, but the p value of less than 0.01 was considered to be statistically significant.

3-2 Three-dimensional Tissue-based Experiments

3-2.1 Isolation and Culture of Chondrocytes

3-2.1.1 Specimen Isolation

The articular cartilage used in the experiment was obtained aseptically from adult porcine knee joints which had no macroscopic signs of osteoarthritis. Within 4 h of slaughter, the integral part of adult porcine knee joint was cleaned by 75% ethanol (E7148, Sigma Co., St. Louis, MO, U.S.A.), iodine solution (35089, Sigma Co.) and phosphate-buffered saline (PBS, pH 7.2) in sequence. After trimming the undesired connective tissue with sterile scalpels, the cartilage tissue was sliced into 5mm×5mm×0.5mm pieces, and the action of slicing was avoided cutting deep into the subchondral bone [146]. Then the thin slices were washed three times in sterile PBS and were further sterilized by soaking in 5-fold antibiotics-added (50 units/mL penicillin, 50 μg/mL streptomycin, 100 μg/mL neomycin, P4083, Sigma Co.) PBS for 15 min.

3-2.1.2 Matrix Digestion

Enzymatic digestion of articular cartilage has been a feasible and useful technique for isolating chondrocytes based on degrading the extracellular matrix between cells [147, 148]. In this experiment, the thin slices of cartilage were subjected to 0.2% collagenase (C0130, Sigma Co.) digestion in order to degrade the native collagen between animal cells and get the sufficient amount of cells after digestion [149-151]. The collagenase was dissolved in DMEM (31600-026, Gibco Invitrogen Co., Burlington, Ontario, Canada) which was supplemented with 3.7 mg/ml sodium bicarbonate (S5761, Sigma Co.), 50 μg/ml ascorbic acid (A5960, Sigma Co.) [152], 50 units/50 μg/100 μg/mL penicillin/ streptomycin/ neomycin (P4083, Sigma Co.),

and 10% fetal bovine serum (100-106 Gemini Bio-Products, Woodland, CA) and filter-sterilized by passing through a 0.22 μm filter (SCGPT05RE, Millipore Co., Bedford, MA, U.S.A.). After incubating the sliced cartilage in a humidified incubator at 37°C, 5% carbon dioxide for 16 hours, the resulting chondrocytes/collagenase solution suspension was collected and centrifuged at 1500 rpm for 5 min (KUBOTA 5101, Canada). The supernatant was discarded and the pelleted cells were gently washed once in PBS to neutralize remaining collagenase. Cells were centrifuged at 1500 rpm for 5 min again and resuspended in 10 ml of the same medium mentioned above. Cell number and viability was assessed by hemocytometer and trypan blue dye (T8154, Sigma Co.) exclusion.

3-2.1.3 Cell Culture

The chondrocytes were plated out to sterile 10cm tissue culture petri dishes (Cellstar, Greiner Bio-One, Longwood, Florida, United States) at 1×10^6 cells per dish as monolayer culture in the same DMEM mentioned above and maintained in a humidified incubator at 37°C, with 5% carbon dioxide [153]. Usually, the healthy chondrocytes would begin to adhere within the first two days, so in the 3rd day the culture medium was refreshed to discard the dead cells [154]. Moreover, often in the 7th day the cultured chondrocytes reached confluence and were detached by 0.05% trypsin with EDTA•4Na (15400-054, Invitrogen Co.) for passage. Because most of the *in vitro* cultured chondrocytes lost their phenotype after the third passage [155], the cells used in the experiment were all in the beginning of the second passage.

3-2.2 Preparation of Modified Tri-copolymer Scaffolds

Modified tri-co-polymer scaffolds were made up by gelatin (G2500, Sigma Co., St. Louise, USA), chondroitin-6-sulfate (C6S) (C4384, Sigma Co.), hyaluronic acid (H7630, Sigma Co.), and a newly added component: chondroitin-4-sulfate (C4S) (27042, Fluka, St. Gallen, Switzerland) in order to mimic the real extracellular matrix of cartilage [178]. 1 g gelatin, 0.12 g C6S, 0.08 g C4S, and 10 mg HA were sequentially dissolved into 13.8 ml ddH_2O at the temperature of 40°C, and the mixture was then well mixed by stir for 20 min. After the solution became yellow colored colloid, it was further cross-linked by the crosslinking agents. 0.1 g 1-ethyl-3-(3-dimethylaminopropyl) carbodiimide (EDC) (E1769, Sigma Co.) and 12 mg N-hydroxysuccinimide (NHS) (56480, Fluka) were dissolved into 10 ml ddH_2O as the crosslinking agents. At room temperature, 4 ml of the crosslinking agents were slowly dropped into the previous yellow colored colloid, and the newly formed solution was well mixed and stirred for two to three minutes. After the solution was cooled at 4°C for 1 h for gelation, gel was frozen at 20°C for 2 h followed 80°C overnight to form a sponge and then lyophilized for 72 h. After drying, the modified tri-co-polymer scaffold sponge was cut into 0.5x0.5x0.5 cm cubes and soaked in 100 mL of 5-fold dilution of the crosslinking agents at 4°C for 24 h for re-crosslinking. Again, the cubes were frozen at 20°C for 2 h followed 80°C overnight and then lyophilized for 72 h to get the dry sponge scaffolds. Finally, the modified tri-co-polymer scaffolds were sterilized by soaking in 70% ethanol (E7148, Sigma Co.) overnight and were washed five times by PBS and then pre-wetted by soaking in culture medium at 37°C for 30 min before cell seeding.

3-2.3 Seeding and Culturing Porcine Chondrocytes in the Modified

Tri-Copolymer Scaffolds

Porcine chondrocytes were expanded by two-dimensional monolayer culture for one week in DMEM medium (31600-026, Gibco Invitrogen Co., Burlington, Ontario, Canada) containing 3.7 mg/ml sodium bicarbonate (S5761, Sigma Co.), 50 μg/ml ascorbic acid (A5960, Sigma Co.) [152], 50 units/50 μg/100 μg/mL penicillin/ streptomycin/ neomycin (P4083, Sigma Co.), and 10% fetal bovine serum (100-106 Gemini Bio-Products, Woodland, CA). At the 7th day, monolayer-cultured porcine chondrocytes were trypsinized and re-suspended in the culture medium, where the final concentration was about 1×10^6 chondrocytes/10 uL culture medium. A volume of 10 uL of cell suspension containing 1×10^6 cells was then injected into each scaffold. After this, cell-scaffold hybrids were cultured in 48-well plates for the first three days for cell attachment and then transfer to 6-well plates for further culture. Culture medium was changed twice a week during the first three days and two times a week during the subsequent culture period. Here, experimental groups were cell-scaffold hybrids treated with betulin-added culture medium, and positive control group was cell-scaffold hybrids treated with normal culture medium and was incubated under the same conditions as the experimental group. Furthermore, negative control groups were scaffolds which were not seeded with chondrocytes and incubated under the same conditions as the experimental groups and the positive control group. At the end of 1, 2, and 4-week in vitro cultivation, Duplicate samples from each experimental group were removed at the end of a 6-week cultivation for immunohistochemical study on Type II collagen and measurement of DNA content. The other quadruplicate samples from each group were removed at the end of 12 weeks for measurement of DNA and sulfated GAG content, WST-1 assays and immunohistochemical study on Type II collagen.

3-2.4 Preparation of scaffold for scanning electron microscopy (SEM)

SEM was performed for morphological observation of the gelatin/C6S/C4S/hyaluronan modified tri-copolymer scaffold. The modified tri-copolymer scaffold was dehydrated by treatment with a series of graded ethanol solutions (50% for 12 h, then 75%, 85%, and 95%, each for 2 h), and then placed overnight in a vacuum oven at 50∞C before coating with gold for SEM examination. The scaffold was then examined using a JEOL JXA-804 A scanning electron microscope (JEOL-USA, Inc., Peabody, MA, U.S.A.).

3-2.5 WST-1 Assay for Cell Proliferation in Cell-Scaffold Hybrids

Water soluble tetrazolium salt, 4-[3-(4-iodophenyl)-2-(4-nitrophenyl)-2H-5-tetrazolio]-1, 3-benzen disulfonate (WST-1), had been demonstrated to be a simple and rapid measurement of cell proliferation with extremely low cytotoxicity. A 10% working solution was made by mixing 1 volume of cell proliferation reagent WST-1 (Roche Molecular Biochemicals, Mannheim, Germany) with 9 volumes of DMEM/F-12 medium. Cell viability and proliferation in cell–scaffold hybrids were tested at the end of the second and fourth weeks of cultivation. Tricopolymer scaffolds with no cell seeded served as controls, and were regulated in the same culture condition as the cell–scaffold hybrids. Each scaffold, including cell–scaffold hybrids and control scaffolds, was incubated with 1 mL of WST-1 working solution in a 12-well plate at 37∞C for 2 h. Then 100 mL of reacted solution was transferred to a 96-well microplate. OD450 was measured using a VERSAmax microplate absorbance reader (Molecular Devices Corp., Sunnyvale, CA, U.S.A.).

3-2.6 Total DNA for Cell Proliferation Quantification

The Wizard® Genomic DNA Purification Kit (A2360, Promega Co., Madison, WI, U.S.A.) was chosen for DNA extraction. Both betulin-treated experimental group and control group were performed in quadruplicate. At the end of 1, 2, and 4-week cultivation, each cell-scaffold hybrid were places into 1.5 mL microcentrifuge tubes and digested by 275 uL of digestion solution for 18 h at 55°C. The digestion solution was composed of 200 uL of Nuclei Lysis Solution, 50 uL of 0.5M EDTA (pH 8.0), 20 uL of proteinase K (20 mg/mL), and 5 uL of RNase A solution (4 mg/mL). After this, 250 uL Lysis Buffer was added into microcentrifuge tubes, and each lysate was transferred to a separate Wizard® SV minicolumn assembly. The assembly was centrifuged at 13,000 × g for 3 min to bind genomic DNA to the membrane, and liquid in the collection tube of assembly was discarded. 650 mL of Wizard® SV Wash Solution was then added to wash the membrane of each assembly followed by centrifuging at 13,000 × g for 1 min, and this step was repeated four times. Finally, extracted total DNA were dissolved in 65°C 250 uL nuclease-free water, and the absorbance at 230 nm, 260 nm, 280 nm, and 320 nm were measured by UV spectrophotometer (Beckman Instrument Inc., Fullerton, CA, U.S.A.). DNA quality was determined at the ratio of 260 nm and 280 nm absorption which should be in the range of 1.8 to 2.0 demonstrating good deproteinization [167], and the ratio of 260 nm to 230 nm help evaluate the level of salt carryover in the purified DNA [168]. DNA concentration was calculated by assuming 1 O.D. at 260 nm was equivalent to 50 ug of DNA per mL. Therefore, total DNA concentration was estimated with formula O.D. 260 - O.D. 320 × dilute factor × 50ug/ml, where the subtraction of A320 was for adjusting the A260 measurement for turbidity [169].

3-2.7 DMMB Assay for Quantitative Measurement of Sulfated GAGs Content

The 1,9-Dimethyl-Methylene Blue (DMMB) was used to determine the content of sulphate-glycosaminoglycans (sGAG), such as chondroitin sulphate and keratan sulphate, in the media to estimate the amount of cell-secreted proteoglycan [170, 171]. Positive charge of DMMB and the negative charge of sulfate of sGAG interact to form DMMB-GAG complexes which alter light absorbance at 595 nm and can thus be measured by spectrophotometer [172]. Briefly, the DMMB solution was prepared by dissolving 21 mg of DMMB (341088, Aldrich-Chemie GmbH, Steinheim, Germany) in 5 mL of 95% ethanol (E7148, Sigma Co.), and the dissolved dye was further added with 2 g sodium formate (107603, Sigma Co.) and 800 ml of ddH_2O. The solution was adjusted to a pH of 1.5 by drop-by-drop addition of 0.1 M formic acid, and ddH_2O was added to reach a final volume of 1 L. The stock DMMB solution was stored at 4°C in an aluminum foil-wrapped glass bottle. A standard curve was made using serial dilutions of chondroitin-6-sulfate with HBSS to final concentrations of 0.1, 1, 10, and 100 μg C6S/mL, and the absorbance at 595 nm of the DMMB-C6S complexes were measured triplicate and plotted against known concentrations. At the end of 1, 2, and 4-week cultivation, positive and negative control group and quadruplicate betulin-treated experimental group were digested with 0.1% papain (#CAT, Sigma Co.) in HBSS solution (Sigma Co.) at 60°C for 16 h. Then 40 ml of sample digests and 250 ml of DMMB solution were mixed in a 96-well microplate at room temperature, and absorbance at 595 nm was recorded using a MicroElisa reader (Emax Science Corp., CA, U.S.A.). Sulfated GAGs concentration of each sample was then calculated with use of the regression equation obtained from the linear standard curve.

3-2.8 Real-time Reverse-Transcriptase Polymerase Chain Reaction for mRNA Expression Quantification

In three-dimensional tissue-based experiments, at the end of 1, 2, and 4-week cultivation, quadruplicate betulin-treated experimental cell-scaffold hybrids and the untreated control cell-scaffold hybrids and were immediately immersed into 1.5 mL of RNAlater RNA Stabilization Reagent (76104, QIAGEN GmbH, Hilden, Germany) in microcentrifuge tubes after removing from the culture medium. Briefly, total RNA of each sample was isolated by using RNeasy Protect Mini Kit (74124, QIAGEN GmbH), and two-step real-time RT-PCR was used to measure specific mRNA expressed by chondrocytes, where the SuperScript^{TM} III First-Strand Synthesis System for RT-PCR (18080-044, Invitrogen Co.) and the 2X SYBR Green Master Mix (4309155, Applied Biosystems, Foster City, CA,. USA) were used for reverse transcription and PCR, respectively. The list of target genes for real-time RT-PCR in this study is in Table 6, and the primer sequence of those target genes are listed in Table 7. The detailed procedures were described in the following paragraphs.

Table 8 List of target genes for real-time RT-PCR in three-dimensional scaffold culture.

Target gene	Description
GAPDH	Housekeeping gene
I collagen	Absent in healthy cartilage, present when fibrously transformed
II collagen	Major collagen type in the cartilage
X collagen	Marker of cellular hypertrophy
Aggrecan	Key component of aggregated proteoglycans
Decorin	Small proteoglycans
TIMP-1	Tissue inhibitor of MMPs
MT1-MMP	Degradative enzyme
MMP-2	Degradative enzyme
Sox9	Master chondro-regulatory gene
IL-1beta	Regulator of catabolism
TGF-beta1	Regulator of anabolism
BMP-7	Promote growth and expression of the chondrocytes phenotype
IGF-1	Regulate normal chondrocytes matrix secretion
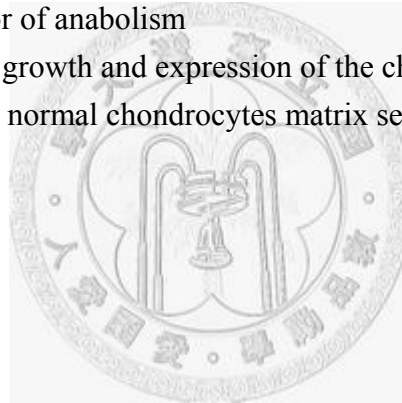
Table 9 Primer Sequences of three-dimensional scaffold culture.

Name	Sequences
GAPDH	5'- GTCATCCATGACAACTTCGG-3'
	5'- GCCACAGTTTCCCAGAGG-3'
I collagen	5'- CAGAACGGCCTCAGGTACCA -3'
	5'- CAGATCACGTCATCGCACAAC -3'
II collagen	5'- GAGAGGTCTTCCTGGCAAAG -3'
	5'- AAGTCCCTGGAAGCCAGAT -3'
X collagen	5'- CAGGTACCAGAGGTCCCATC -3'
	5'- CATTGAGGCCCTTAGTTGCT -3'
Aggrecan	5'- CGAAACATCACCGAGGGT- 3'
	5'- GCAAATGTAAAGGGCTCCTC-3'
Decorin	5'-GCATTTGCACCTTTGGTGAA-3'
	5'-GACACGCAGCTCCTGAAGAG-3'
MT1-MMP	5'- GCTGTGGTGTTCCAGACAAG -3'
	5'- GGATGCAGAAAGTGATCTCG -3'
MMP-2	5'- GTTCTGGAGGTACAATGA -3'
	5'- ACCACGGCGTCCAGGTTA -3'
TIMP-1	5'- AACCAGACCGCCTCGTACA -3'
	5'- GGCGTAGATGAACCGGATG -3'
Sox9	5'-ACCTGAAGAAGGAGAGC-3'
	5'-CACCGGCATGGGTACCA-3'
IL-1beta	5'- ACCTCAGCCCTCTGGGAGA -3'
	5'- CCTCCTTTGCCACAATCAC -3'
TGF-beta1	5'- GCACGTGGAGCTATACCAGA -3'
	5'- ACAACTCCGGTGACATCAAA -3'
BMP-7	5'- CCATGTTCATGCTGGACCTG -3'
	5'- GATCAAACCGGAACTCCCGG -3'
IGF-1	5'-CTCTTCAGTTCGTGTGCGGA-3'
	5'-GAGCCTTGGGCATGTCCGTG-3'

In total RNA isolation, after immersing each cell–scaffold hybrids into 1.5 mL of RNAlater RNA Stabilization Reagent (76104, QIAGEN GmbH, Hilden, Germany), the samples were then disrupted and homogenized in 600 mL of Buffer RLT by using a rotor–stator homogenizer () to shear high-molecular-weight genomic DNA and other high-molecular-weight cellular components. Next, the lysate was centrifuged at full speed for 3 min, and the supernatant which had RNA dissolve in it was transfer to a new microcentrifuge tube followed by adding 600 mL of 70% ethanol for promoting selective binding of RNA to the RNeasy membrane. The mixture was then transfer to an RNeasy spin column placed in a 2 ml collection tube and centrifuge at 8,000 × g for 15 seconds. Subsequently, the column were washed once by 700 µl of Buffer RW1 and twice by 500 µl Buffer RPE accompanying centrifuge at 8,000 × g for 15 seconds, 8,000 × g for 15 seconds, and 8,000 × g for 2 minutes, respectively. Finally, extracted total RNA was dissolved in 50 uL nuclease-free water and was eluting by centrifuge at 8,000 × g for 1 minute. RNA content was determined at 260 nm by UV spectrophotometer (Beckman Instrument Inc., Fullerton, CA, U.S.A.), and RNA quality was evaluated at the ratio of 260 nm and 280 nm absorption which should be higher than 1.7.

In complement DNA synthesis, 8 µL of extracted RNA, 1 µL of 50 µM oligo(dT)$_{20}$, and 1 µL of 10mM dNTP were mixed and incubated at 65°C for 5 minutes, then placed on ice for 5 minutes. Next, 2 µL of 10× RT buffer, 4 µL of 25 mM MgCl$_2$, 2 µL of 0.1M DTT, 1 µL of RNaseOUT^{TM}, and 1 µL of SuperScript^{TM} III RT (200 U/ µL) were added into the mixture. After this, the mixture was incubated at 50°C for 50 minutes and followed by terminating the reaction at 85°C for 5mins. Finally, the synthesized cDNA was chilled on ice, and 1 µL of RNase H was added to each tube for 20 minutes at 37°C.

In real-time PCR, each reaction was performed with 10 mL of cDNA with 100 ng of cDNA in content, 12.5 μL of 2X SYBR Green Master Mix (4309155, Applied Biosystems Co.), 0.75 μL of 1 μM forward primer solution, 0.75 μL of 1 μM reverse primer solution, and 6 μL of nuclease-free water (P1193, Promega Co.). In order to avoid pipetting errors, three replicates of each sample were amplified. PCR cycles were performed on an ABI PRISM 7900 Sequence Detection System with ABI PRISM 7900 Sequence Detection Software 2.2.2 (Applied Biosystems, Foster City, CA, USA). Briefly, real-time PCR reaction was divided into three stages. In the first initiation stage, after the SYBR® Green I dye was activated at 50°C for 2 minutes, samples were then heated to 95°C for double-strand cDNA denaturation for 10 minutes. Next, in the second cycling stage, the samples were undergone melting at 95°C for 15 seconds followed by annealing/extension at 60°C for 1 minute for 40 cycles to produce the amplicons. Finally, in the last termination stage, the samples were hold at 37°C for 10 minutes for the SYBR® Green I dye inactivation.

Real-time PCR was amplified for glyceraldehyde-3-phosphate dehydrogenase (GAPDH), type I collagen (COL1), type II collagen (COL2), type X collagen (COL10), aggrecan, decorin, tissue inhibitor of metalloproteinase-1 (TIMP-1), matrix metalloproteinase-2 (MMP-2), membrane-type matrix metalloproteinases-1 MMP (MT1-MMP), sex determining region Y-box 9 (Sox9), interleukin-1β (IL-1β), transforming growth factor-β1 (TGF-β1), bone morphogenic protein-7 (BMP-7), and insulin-like growth factor-1 (IGF-1). The mRNA expressions were analyzed by numbers of threshold cycles (Ct), where the Ct value of each target gene were normalized by the Ct value of endogenous control: GAPDH, and the results were shown as -ΔCt in means ± SD. The mRNA expression between betulin-treated experimental group and the untreated control group was analyzed statistically by Student's t-test with a level of significance of $\alpha = 0.01$.

3-2.9 Statistical analysis

A Student's t-test was employed for determining the statistical significance of sulfated GAG content and OD values detected in the WST-1 assay between the cell–scaffold hybrids and the control scaffolds. The differences in mRNA expression in the cell-scaffold hybrids control groups and cell-scaffold hybrids experimental groups were also analyzed by using a Student's t-test matched-pairs signed rank test. A p value of less than 0.05 was considered to be statistically significant.

CHAPTER 4

RESULTS

4-1 Two-dimensional Chondrocytes Culture

4-1.1 LDH Cytotoxicity Assay

The OD_{490} obtained from 2D cultured porcine chondrocytes which were treated with aucubin and betulin are summarized in Figure 22 and Figure 23, respectively. In the aucubin-treated experimental groups, the chondrocytes treated with the lowest concentration of aucubin showed a significantly higher OD value than the control group (0.725 ± 0.081 vs. 0.690 ± 0.073, P = 0.045). However, the chondrocytes treated with the middle and the highest concentrations of aucubin lowered the OD value compared with the control group.
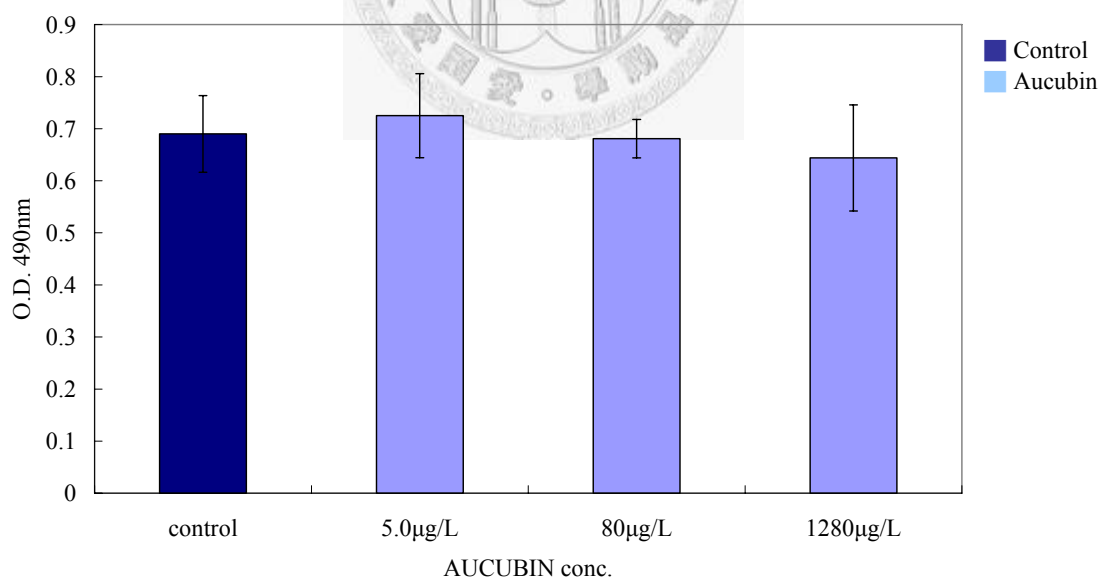
Figure 22 LDH cytotoxicity assay of aucubin-treated chondrocytes. The absorbances at 490 nm were obtained from one-week chondrocytes which were treated with different concentrations of aucubin.

In the betulin-treated experimental groups, the higher the concentrations of betulin, the lower the OD values. However, these differences are not statistically significant.
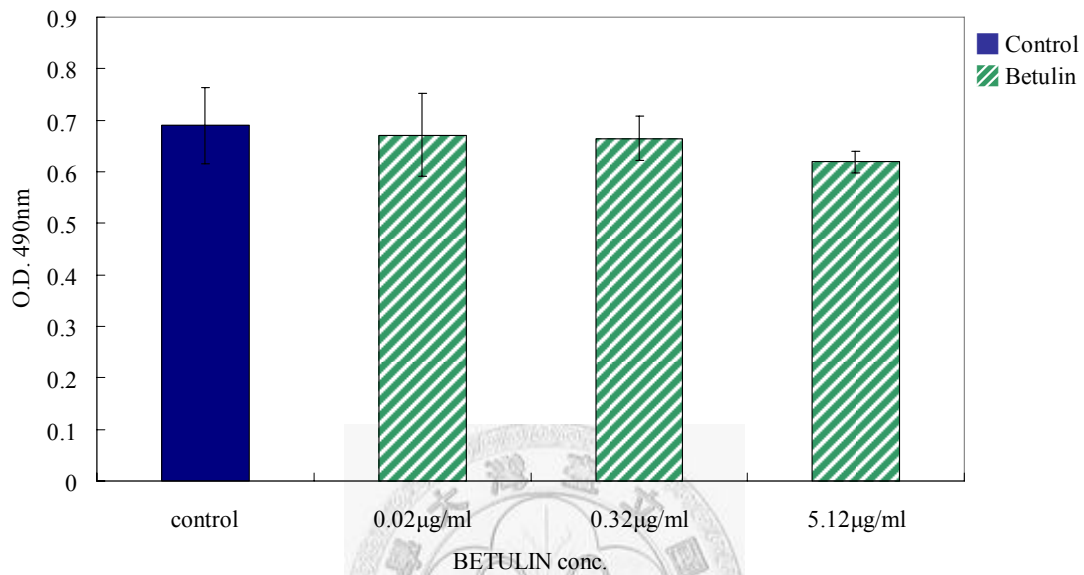
Figure 23 LDH cytotoxicity assay of betulin-treated chondrocytes. The absorbances at 490 nm were obtained from one-week chondrocytes which were treated with different concentrations of betulin.

4-1.2 MTT Cell Proliferation Assay

The OD_{570} obtained from 2D cultured porcine chondrocytes which were treated with aucubin and betulin are summarized in Figure 24 and Figure 25, respectively. In the aucubin-treated experimental groups, the chondrocytes treated with the lowest concentration of aucubin showed very little and not significantly higher OD value than the control group, and the chondrocytes treated with the middle concentration of aucubin showed a little but not significant lower OD value than the control group. In contrast, the chondrocytes treated with the highest concentration of aucubin showed a significantly higher OD value than the control group (0.253 ± 0.03 vs. 0.220 ± 0.03, P = 0.0004).
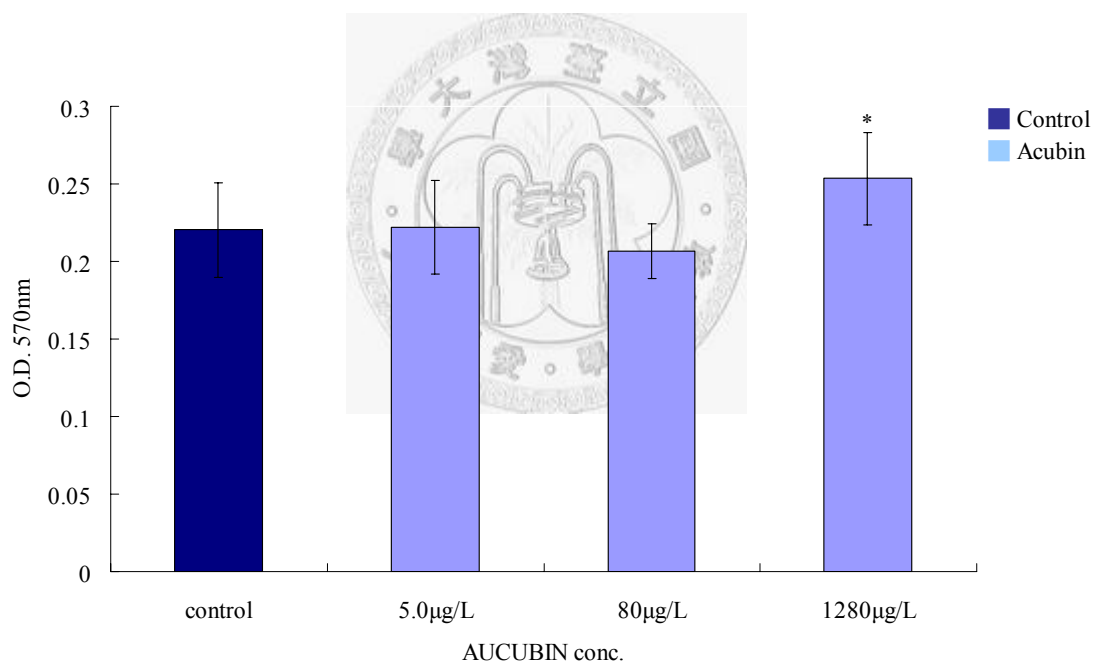
Figure 24 MTT cell proliferation assay of aucubin-treated chondrocytes. The absorbances at 570 nm were obtained from one-week chondrocytes which were treated with different concentrations of aucubin.

In the betulin-treated experimental groups, the chondrocytes treated with the lowest and the highest concentrations of betulin both showed significantly lower OD values than the control group (0.168 ± 0.023 vs. 0.220 ± 0.03, P = 0.003, and 0.176 ± 0.028 vs. 0.220 ± 0.03, P = 0.046), and the chondrocytes treated with the middle concentration of betulin showed lower but not statistical significant OD values than the control group.
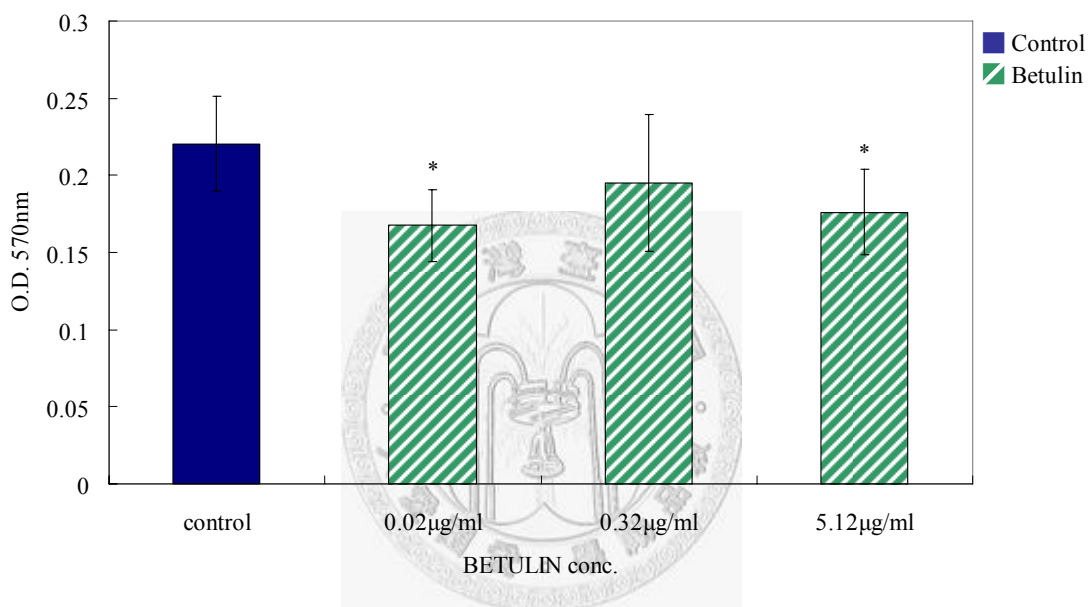
Figure 25 MTT cell proliferation assay of betulin-treated chondrocytes. The absorbances at 570nm were obtained from one-week chondrocytes which were treated with different concentrations of betulin.

4-1.3 Total DNA for Cell Proliferation Quantification

After the genomic DNA was isolated from cultured cells, genomic DNA concentration was calculated by using the formula: DNA concentration = O.D. 260 − O.D. 320 × dilute factor × 50 ug/ml. Total genomic DNA content obtained from 2D cultured porcine chondrocytes which were treated with aucubin and betulin are summarized in Figure 26 and Figure 27, respectively. In the aucubin-treated experimental groups, the chondrocytes treated with the lowest and the highest concentrations of aucubin both increased the DNA content in a statistical insignificant level than the control group. However, the chondrocytes treated with the middle concentration of betulin decreased the DNA content in a statistical significant level compared with the control group (2.322 ± 0.005 μg/mL vs. 2.682 ± 0.135 μg/mL, $p = 0.006$).
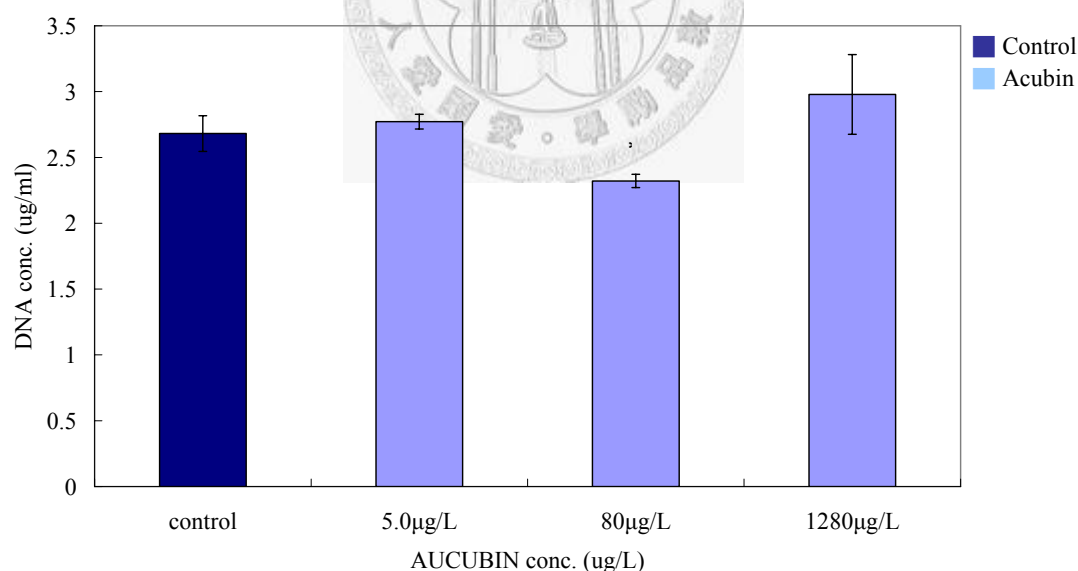
Figure 26 Total DNA content of one-week chondrocytes treated with different concentrations of aucubin. DNA concentration was calculated by equation: O.D. 260 - O.D. 320 x dilute factor x 50 ug/ml.

In the betulin-treated experimental groups, betulin increased the total DNA content of chondrocytes in every experimental group. Total DNA content in chondrocytes treated with the lowest and the middle concentrations of betulin averaged 3.05 ± 0.240 µg/mL and 3.185 ± 0.318 µg/mL respectively, which showed significant increase than the control group ($p = 0.041$ and $p = 0.033$). Total DNA content in chondrocytes treated with the highest concentrations of betulin averaged 2.711 ± 0.118 µg/mL, but this increase of DNA content was not statistically significant. ($p = 0.393$).
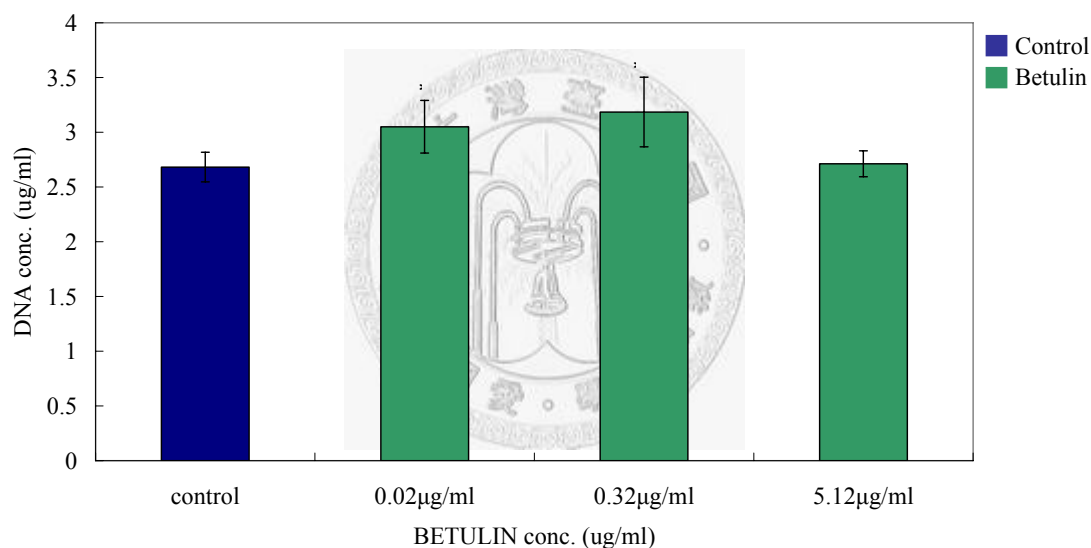
Figure 27 Total DNA content of one-week chondrocytes treated with different concentrations of betulin. DNA concentration was calculated by equation: O.D. 260 - O.D. 320 x dilute factor x 50 ug/ml.

4-1.4 DMMB Assay for Sulfated Glycosaminoglycans Content

Before conducting DMMB assay, a linear standard curve was obtained from GAG standards: 0–100 mg/mL of chondroitin-6-sulfate (C-4384, Sigma), which were then used to estimate the GAG content in each experimental sample. The OD_{525} obtained from C6S standards are summarized in Figure 28. The linear regression trend line of C6S standards was: $y = 0.0043x + 0.4292$.

GAGs Standard Curve

$y = 0.0043x + 0.4292$
$R^2 = 0.9839$
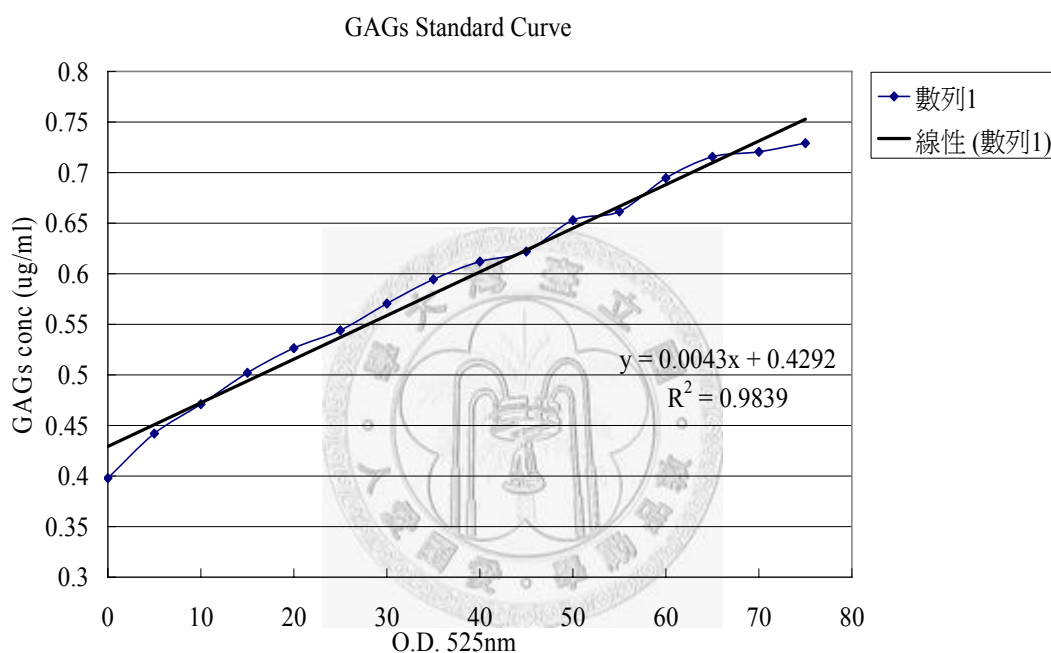
Figure 28 Linear standard curve of glycosaminoglycans standards. The absorbance at 525 nm was measured. The linear regression trend line of glycosaminoglycans standards was: $y = 0.0043x + 0.4292$.

Sulfated glycosaminoglycans content obtained from 2D cultured porcine chondrocytes which were treated with aucubin and betulin are summarized in Figure 29 and Figure 30, respectively. Both in the aucubin-treated experimental groups and the betulin-treated experimental groups, sulfated GAG content didn't show any significantly change. The average sulfated GAG content in the control group was 0.43128 ± 0.052 ug/ml, and the average sulfated GAG content in chondrocytes treated with the lowest, middle, and highest concentrations of aucubin were 0.43126 ± 0.006 ug/ml, 0.43133 ± 0.019 ug/ml, and 0.43134 ± 0.001 ug/ml, respectively.
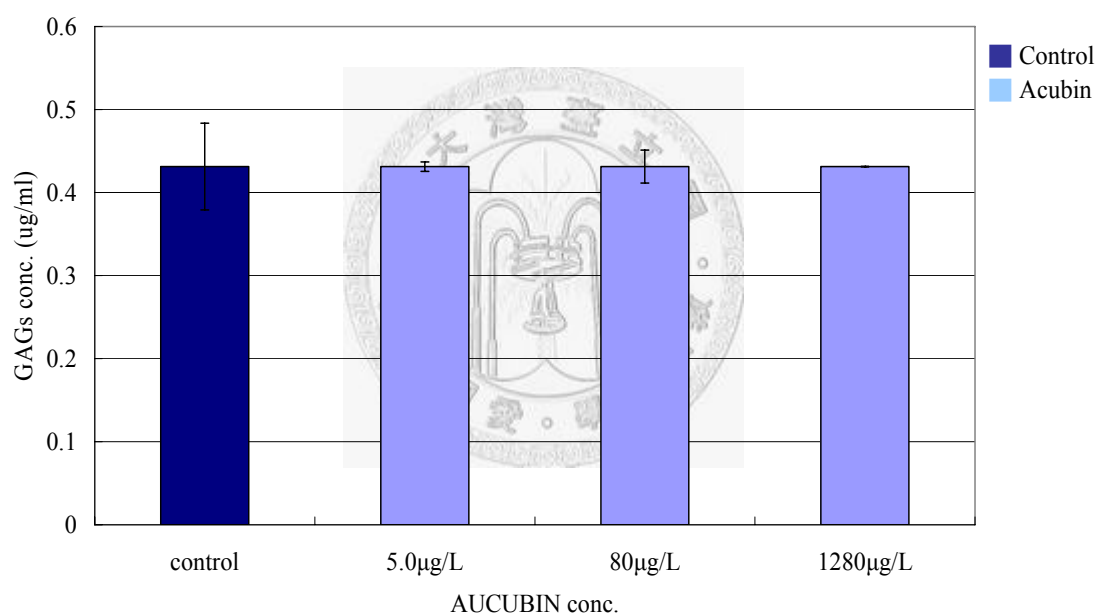
Figure 29 Glycosaminoglycans content of one-week chondrocytes treated with different concentrations of aucubin.

In the betulin-treated experimental groups, the average sulfated GAG content in chondrocytes treated with the lowest, middle, and highest concentrations of betulin were 0.43126 ± 0.006 ug/ml, 0.43125 ± 0.001 ug/ml, and 0.43136 ± 0.002 ug/ml, respectively.
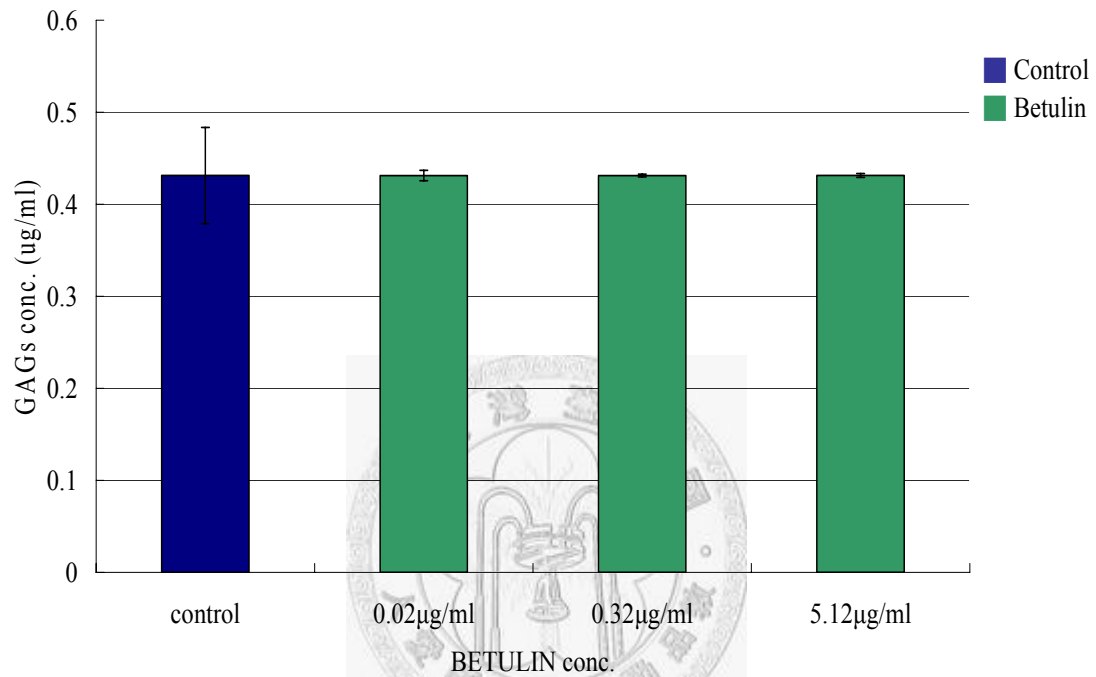
Figure 30 Glycosaminoglycans content of one-week chondrocytes treated with different concentrations of betulin.

4-1.5 Real-time Reverse-Transcriptase Polymerase Chain Reaction for mRNA Expression Quantification

In real-time PCR, the -$\triangle$Ct values of each target gene were normalized by the house-keeping gene, GAPDH, and relative expressions of each target gene between the experimental groups and the control group are shown by the comparative CT ($\triangle\triangle$CT) changes and summarized as follows.

4-1.5.1 Gene Expression of Type I collagen

In the aucubin-treated experimental groups, gene expression of type I collagen showed a 1.33-fold increase under the lowest concentration of aucubin treatment. Also, there was a 1.36-fold increase under the middle concentration of aucubin treatment. In contrast, the chondrocytes treated with the highest concentration of aucubin lowered the gene expression of type I collagen to a 0.94-fold compared with the control group.
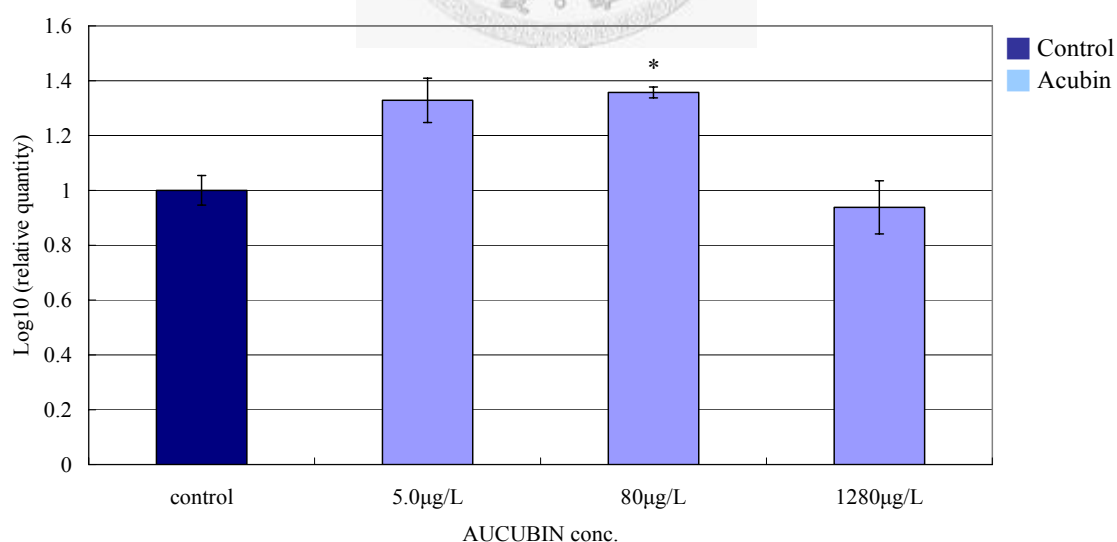
Figure 31 The mRNA expression of type I collagen of one-week chondrocytes under different concentrations of aucubin treatment.

In the betulin-treated experimental groups, gene expression of type I collagen showed a 0.91-fold decrease under the lowest concentration of aucubin treatment, while there was a 1.26-fold and 1.21-fold increase under the treatment of the middle and highest concentrations of aucubin, respectively.
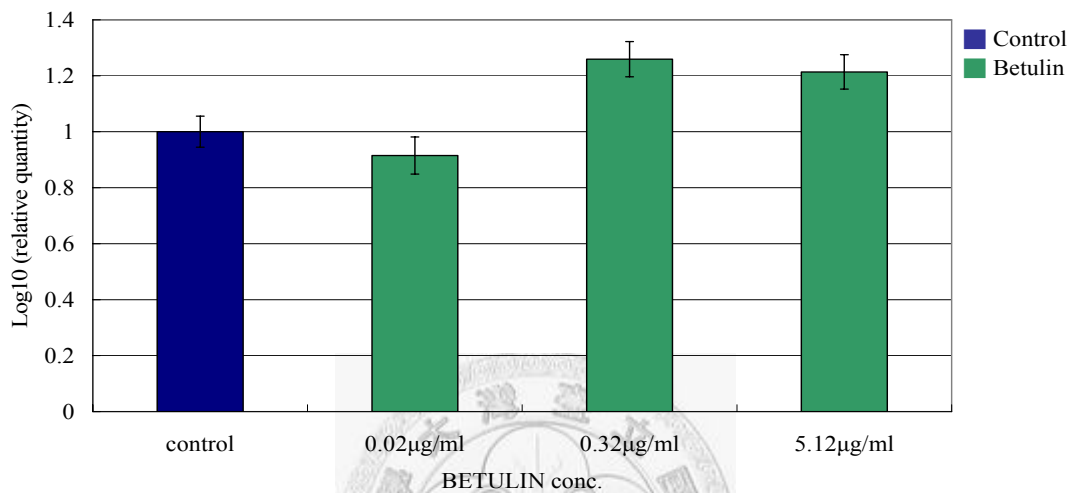
Figure 32 The mRNA expression of type I collagen of one-week chondrocytes under different concentration of betulin treatment. The data was shown by the comparative CT ($\triangle\triangle$CT) changes in gene expression of type I collagen protein.

4-1.5.2 Gene Expression of Type II collagen

In the aucubin-treated experimental groups, gene expression of type II collagen showed a 1.26-fold and a 1.14-fold increases under the treatment of the lowest and middle concentration of aucubin, respectively. However, there was a 0.95-fold decrease under the highest concentration of aucubin treatment.

Figure 33 The mRNA expression of type II collagen of one-week chondrocytes under different concentrations of aucubin treatment. The data was shown by the comparative CT ($\triangle\triangle$CT) changes in gene expression of type II collagen protein.

In the betulin-treated experimental groups, gene expression of type II collagen increased in each experimental group. Moreover, the result showed that the higher the concentration of betulin added, the higher the gene expression of type II collagen in chondrocytes. The chondrocytes treated with the lowest concentration of betulin showed a 1.04-fold increase, and the chondrocytes treated with the middle and highest concentrations of betulin showed significant increases up to a 1.307-fold and 1.311-fold, respectively.
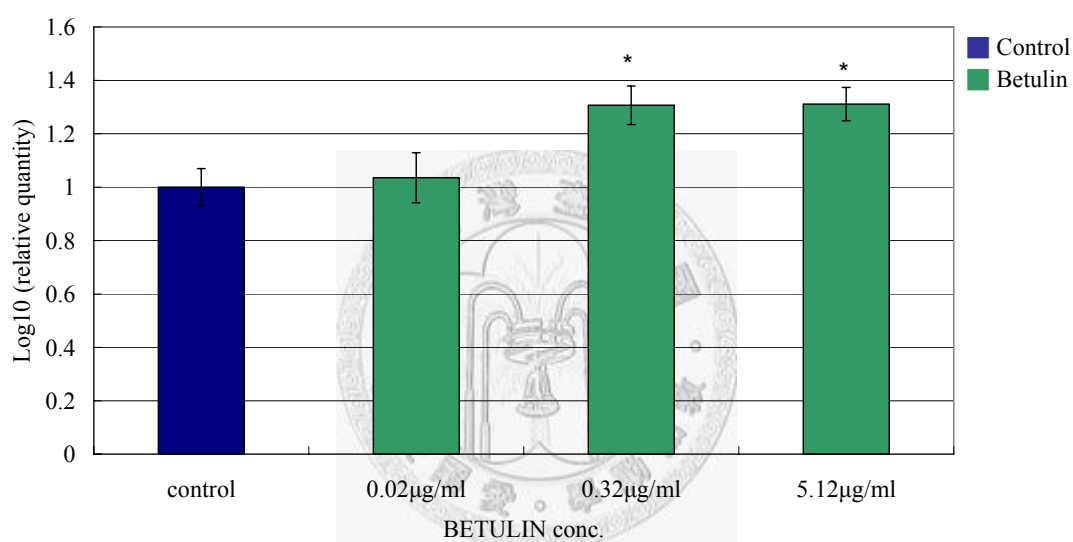
Figure 34 The mRNA expression of type II collagen of one-week chondrocytes under different concentration of betulin treatment. The data was shown by the comparative CT ($\triangle\triangle$CT) changes in gene expression of type II collagen protein.

4-1.5.3 Gene Expression of Aggrecan

In the aucubin-treated experimental groups, gene expression of aggrecan showed a 1.58-fold increase under the treatment of the lowest concentration of aucubin. Also, there was a 1.11-fold increase under the treatment of the middle concentration of aucubin. However, gene expression of aggrecan under the highest concentration of aucubin treatment showed a 0.96-fold decrease compared with the control group.
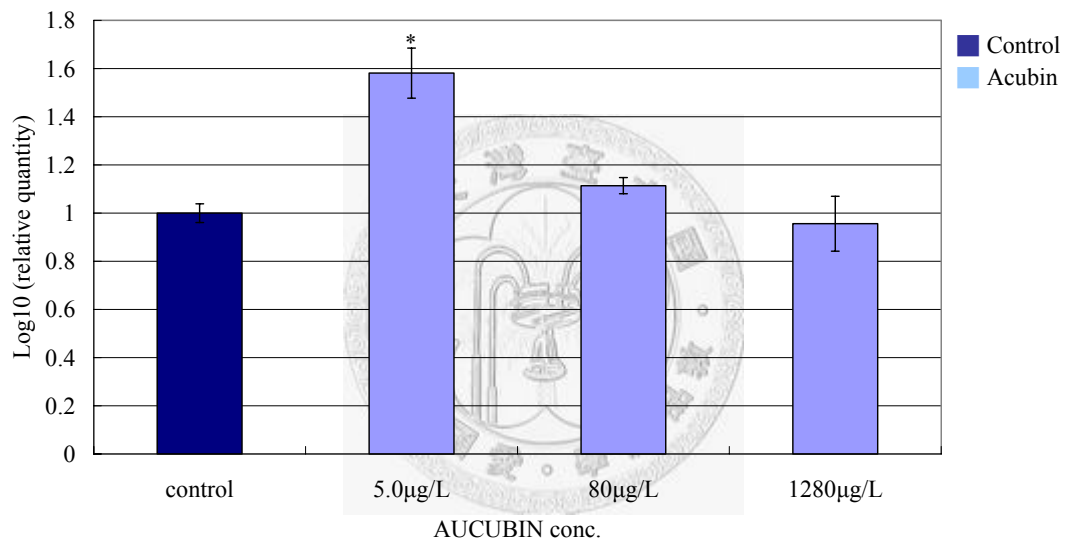
Figure 35 The mRNA expression of aggrecan of one-week chondrocytes under different concentration of aucubin treatment. The data was shown by the comparative CT ($\triangle\triangle$CT) changes in gene expression of aggrecan protein.

In the betulin-treated experimental groups, although gene expression of aggrecan showed a 0.79-fold decrease under the treatment of the lowest concentration of betulin, gene expression of aggrecan showed a 1.31-fold and a 1.54-fold under the treatment of the middle and highest concentration of betulin, respectively. The result showed that the higher the concentration of betulin added, the higher the gene expression of aggrecan in chondrocytes.
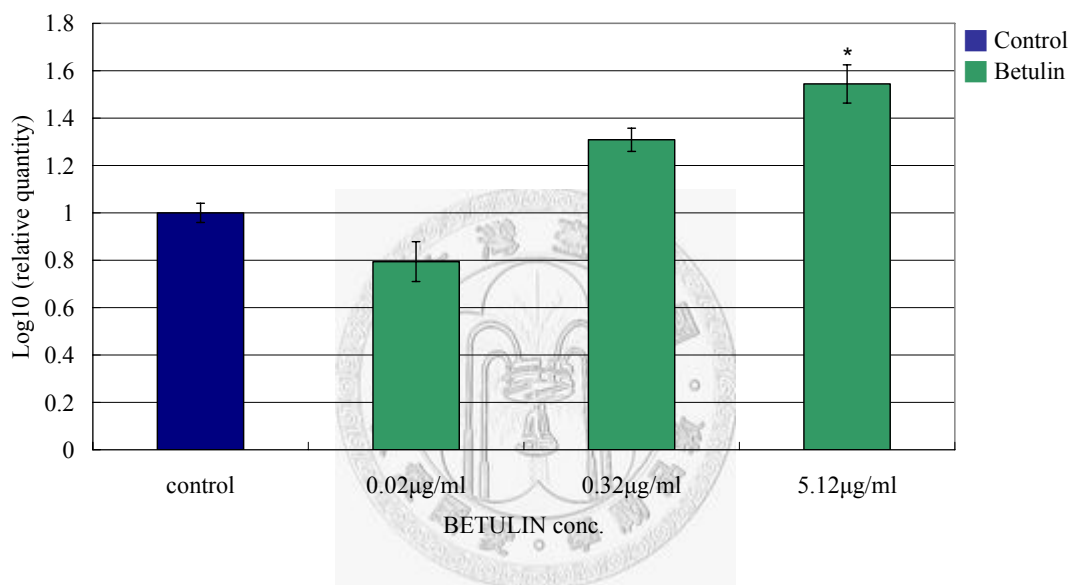
Figure 36 The mRNA expression of aggrecan of one-week chondrocytes under different concentration of betulin treatment. The data was shown by the comparative CT ($\triangle\triangle$CT) changes in gene expression of aggrecan protein.

4-1.5.4 Gene Expression of Decorin

In the aucubin-treated experimental groups, gene expression of decorin increased in each experimental group, although the result showed that the higher the concentration of aucubin added, the lower the gene expression of decorin in chondrocytes. The chondrocytes treated with the lowest and middle concentrations of aucubin showed significant increases up to a 1.39-fold and 1.33-fold, respectively. Also, the chondrocytes treated with the highest concentration of betulin showed a 1.06-fold increase.

Figure 37 The mRNA expression of decorin of one-week chondrocytes under different concentration of aucubin treatment. The data was shown by the comparative CT ($\triangle\triangle$CT) changes in gene expression of decorin protein.
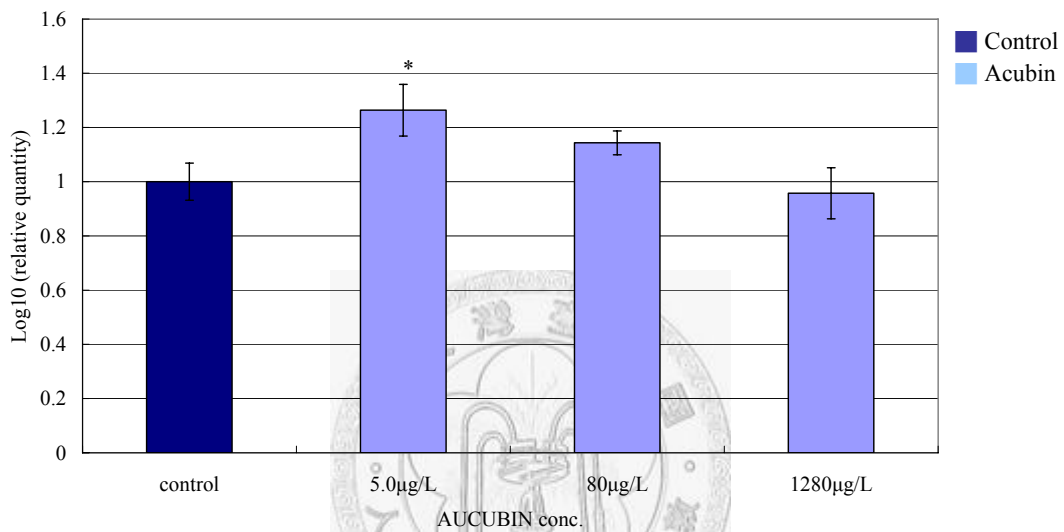
In the betulin-treated experimental groups, although gene expression of decorin decreased in each experimental group, the chondrocytes treated with the middle concentration of betulin still showed a 0.99-fold expression compared with the control group. The chondrocytes treated with the lowest and the highest concentrations of betulin showed a 0.82-fold and a 0.94-fold decrease, respectively.

Figure 38 The mRNA expression of decorin of one-week chondrocytes under different concentration of betulin treatment. The data was shown by the comparative CT ($\triangle\triangle$CT) changes in gene expression of decorin protein.

4-1.5.5 Gene Expression of Sox9

In the aucubin-treated experimental groups, gene expression of sox9 decreased lower than a 0.4-fold in each experimental group. The gene expression of sox9 in chondrocytes treated with the lowest, middle, and highest concentrations of aucubin showed 0.35-fold, 0.14-fold, and 0.23-fold decreases, respectively.

Figure 39 The mRNA expression of Sox9 of one-week chondrocytes under different concentration of aucubin treatment. The data was shown by the comparative CT ($\triangle\triangle$CT) changes in gene expression of Sox9 protein.

Also, in the betulin-treated experimental groups, gene expression of sox9 decreased lower than a 0.35-fold in each experimental group. The gene expression of sox9 in chondrocytes treated with the lowest, middle, and highest concentrations of betulin showed 0.14-fold, 0.12-fold, and 0.33-fold decreases, respectively.
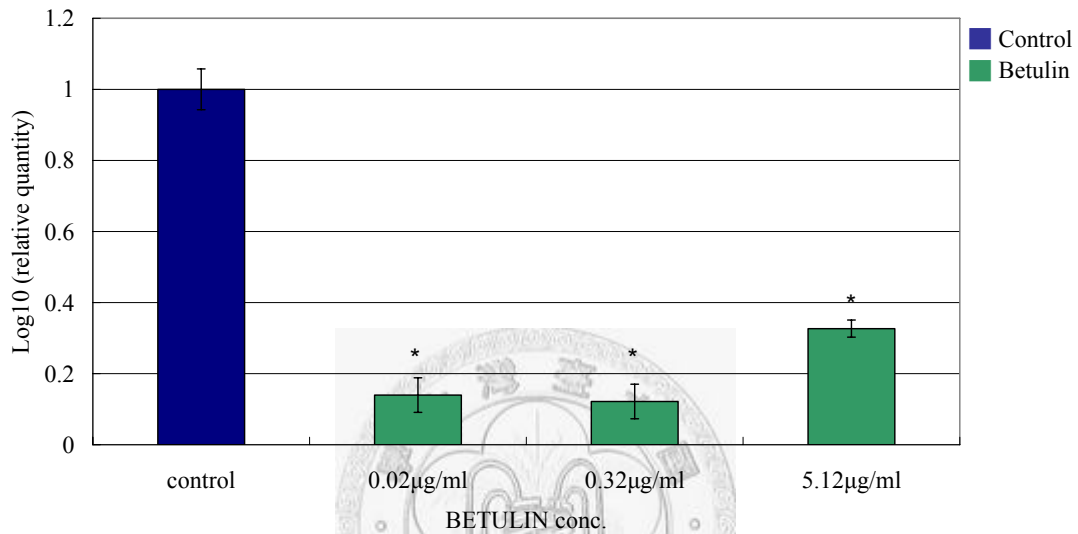
Figure 40 The mRNA expression of Sox9 of one-week chondrocytes under different concentration of betulin treatment. The data was shown by the comparative CT ($\triangle\triangle$CT) changes in gene expression of Sox9 protein.

4-1.5.6 Gene Expression of MT1-MMP

In the aucubin-treated experimental groups, gene expression of MT1-MMP increased in each experimental group. However, real-rime PCR analysis demonstrated that MT1-MMP mRNA levels were slightly but not significantly increased in chondrocytes treated with the lowest concentration of aucubin compared with the control group. Furthermore, the gene expression of mt1-mmp in chondrocytes treated with the middle, and highest concentrations of aucubin showed 1.14-fold and 1.24-fold increases, respectively.

Figure 41 The mRNA expression of MT1-MMP of one-week chondrocytes under different concentration of aucubin treatment. The data was shown by the comparative CT ($\triangle\triangle$CT) changes in gene expression of MT1-MMP protein.
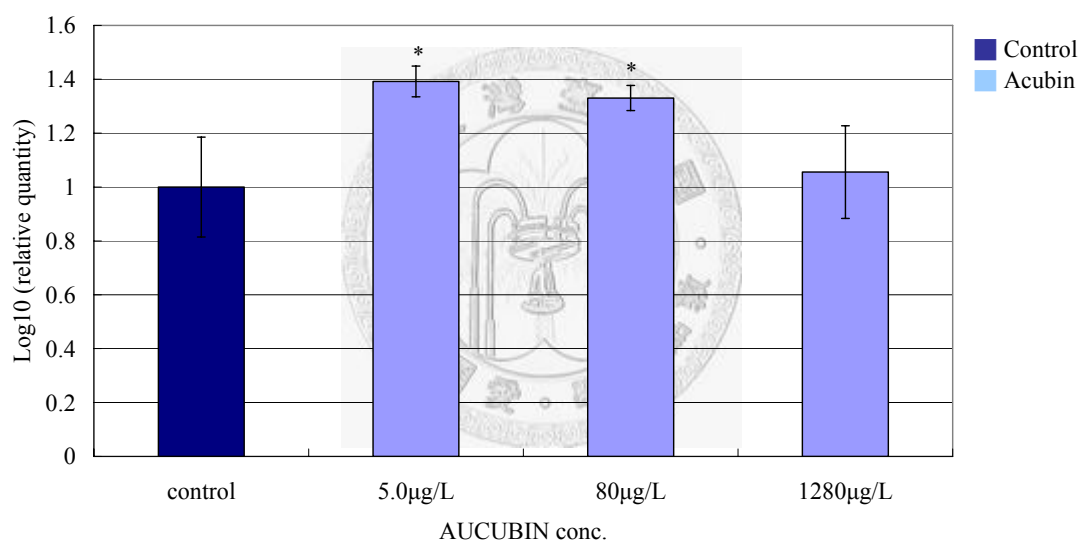
In the betulin-treated experimental groups, although gene expression of mt1-mmp showed a 0.82-fold decrease under the treatment of the lowest concentration of betulin, gene expression of mt1-mmp showed a 1.16-fold and a 1.13-fold increases under the treatment of the middle and highest concentration of betulin, respectively.
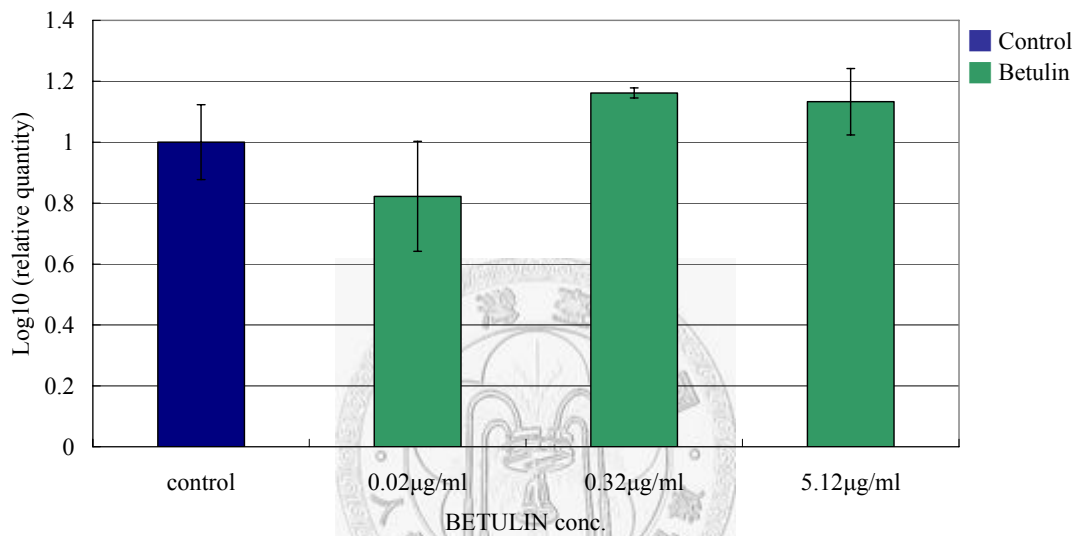
Figure 42 The mRNA expression of MT1-MMP of one-week chondrocytes under different concentration of betulin treatment. The data was shown by the comparative CT (△△CT) changes in gene expression of MT1-MMP protein.

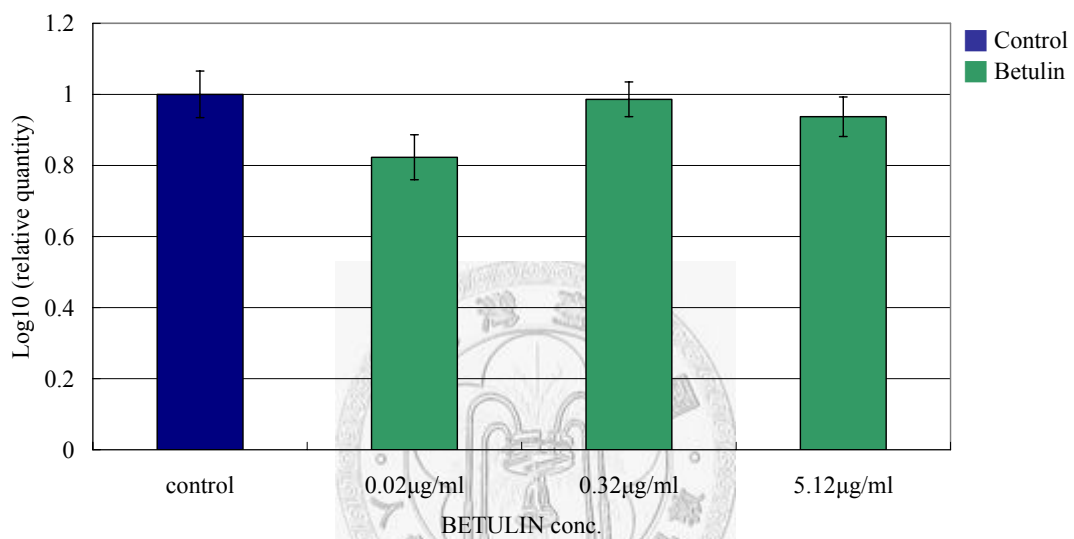**4-1.5.7 Gene Expression of MMP-2**

In the aucubin-treated experimental groups, gene expression of mmp-2 decreased in each experimental group. The chondrocytes treated with the lowest concentration of aucubin showed a 0.72-fold decrease. Moreover, the chondrocytes treated with the middle and highest concentrations of aucubin showed significant decreases to a 0.15-fold and 0.22-fold, respectively.
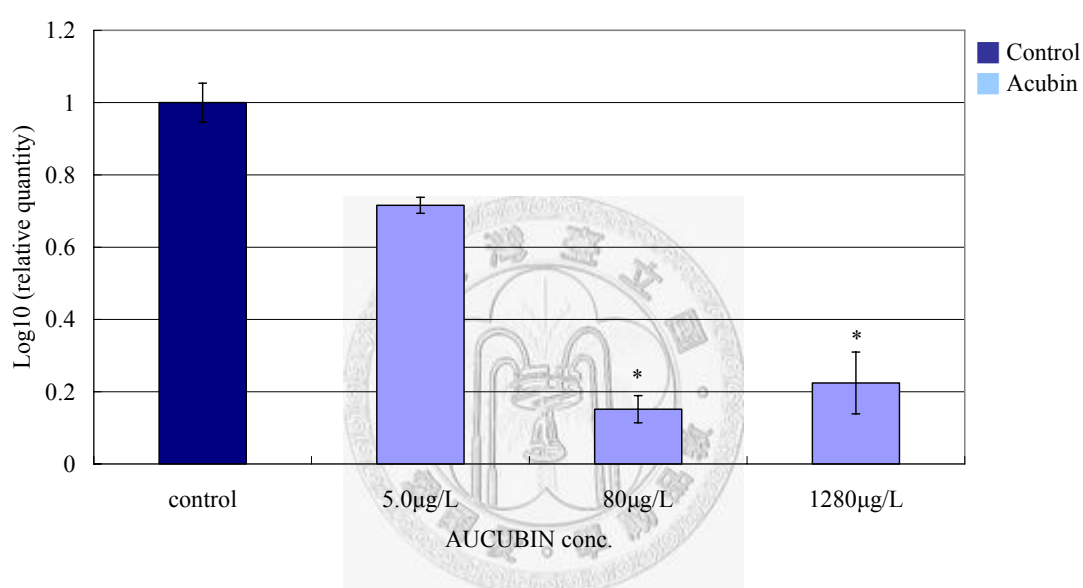
Figure 43 The mRNA expression of MMP-2 of one-week chondrocytes under different concentration of aucubin treatment. The data was shown by the comparative CT ($\triangle\triangle$CT) changes in gene expression of MMP-2 protein.
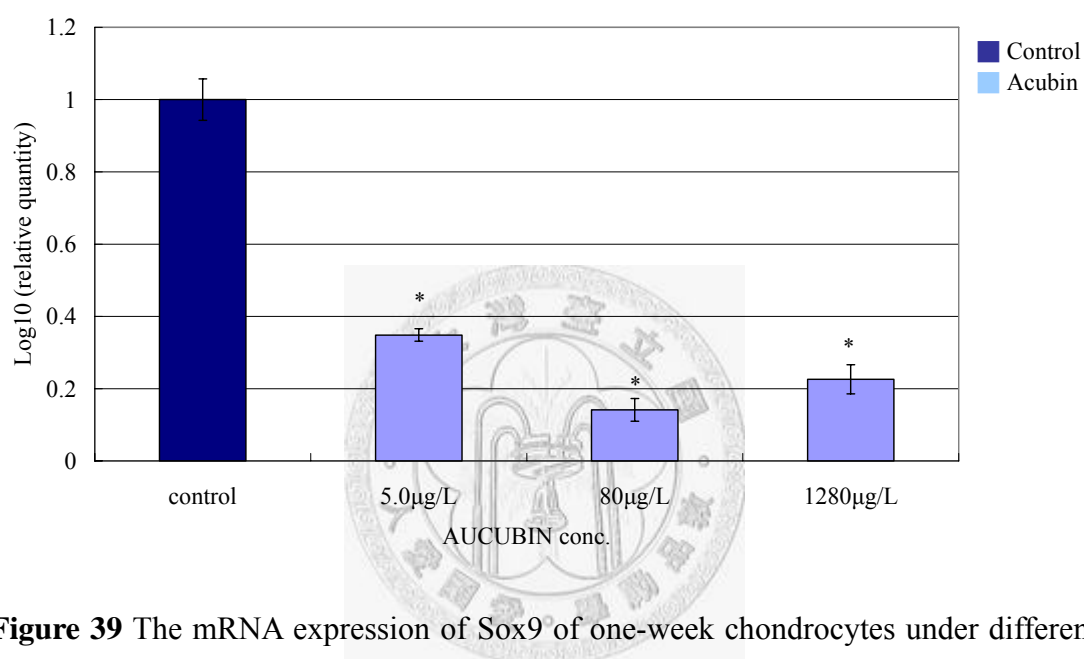
Similarly, in the betulin-treated experimental groups, gene expression of mmp-2 decreased in each experimental group. The chondrocytes treated with the lowest concentration of betulin showed a 0.48-fold decrease. Moreover, the chondrocytes treated with the middle and highest concentrations of betulin showed significant decreases to a 0.13-fold and 0.21-fold, respectively.

Figure 44 The mRNA expression of MMP-2 of one-week chondrocytes under different concentration of betulin treatment. The data was shown by the comparative CT ($\triangle\triangle$CT) changes in gene expression of MMP-2 protein.

4-1.5.8 Gene Expression of T1MP-1

In the aucubin-treated experimental groups, although gene expression of timp-1 showed a 0.79-fold decrease under the treatment of the lowest concentration of aucubin, gene expression of timp-1 showed a 1.13-fold increase under the treatment of the middle concentration of aucubin. The chondrocytes treated with the highest concentration of aucubin showed a little decrease to a 0.98-fold.

Figure 45 The mRNA expression of TIMP-1 of one-week chondrocytes under different concentrations of aucubin treatment. The data was shown by the comparative CT ($\triangle\triangle$CT) changes in gene expression of TIMP-1 protein.
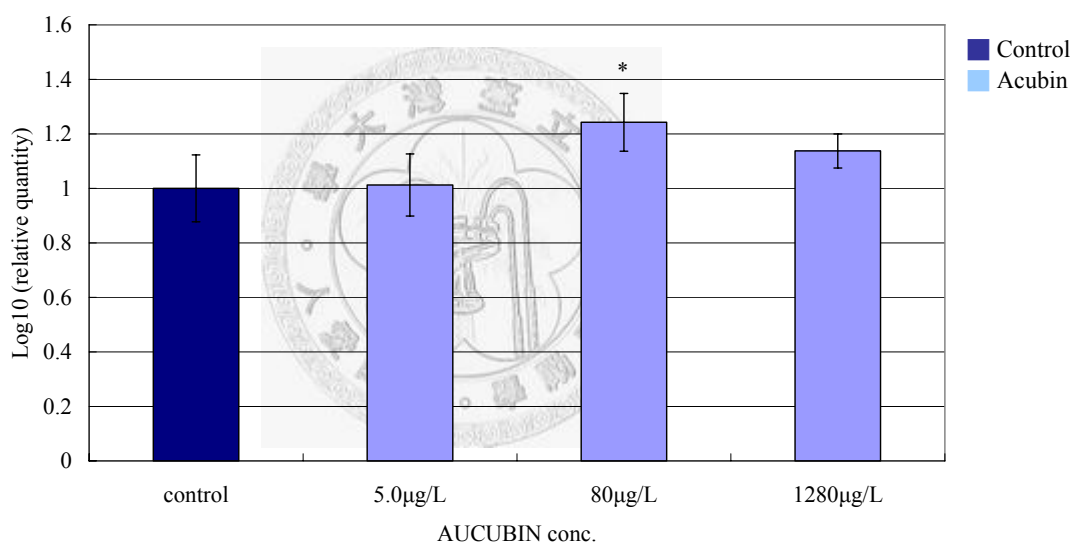
In the betulin-treated experimental groups, the chondrocytes treated with the lowest concentration of aucubin showed a 1.13-fold increase in mRNA expression of timp-1 compared with the control group. Although gene expression of timp-1 showed a 0.82-fold and a 0.92-fold decreases under the treatment of the middle and highest concentration of betulin respectively, the value were still kept above 0.8-fold.
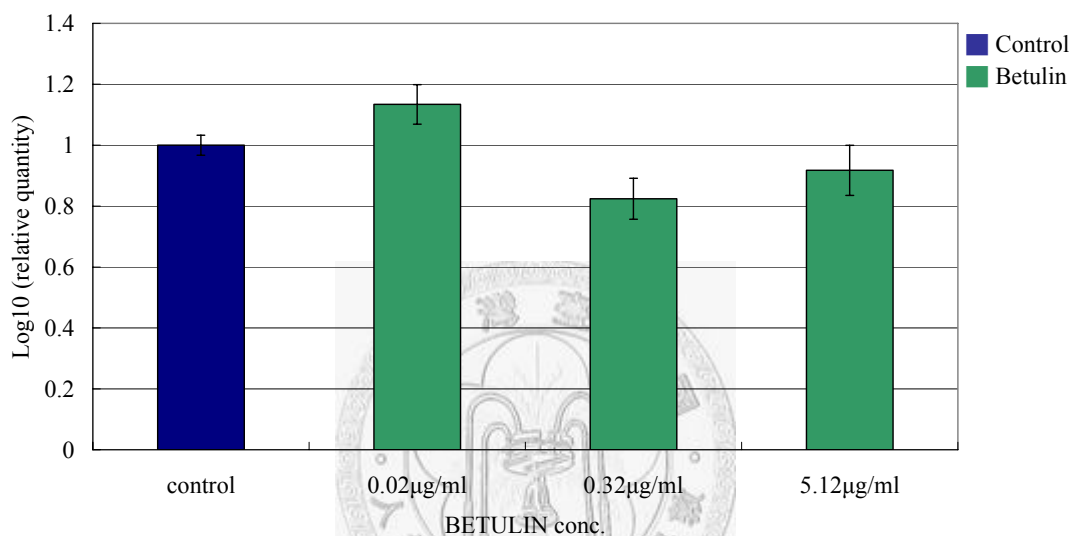
Figure 46 The mRNA expression of TIMP-1 of one-week chondrocytes under different concentration of betulin treatment. The data was shown by the comparative CT ($\triangle\triangle$CT) changes in gene expression of TIMP-1 protein.

4-1.5.9 Gene Expression of IL-1beta

In the aucubin-treated experimental groups, gene expression of IL-1 beta extremely increased higher than a 100-fold in each experimental group. The gene expression of IL-1 beta in chondrocytes treated with the lowest, middle, and highest concentrations of aucubin showed 103-fold, 170-fold, and 144-fold increases, respectively.
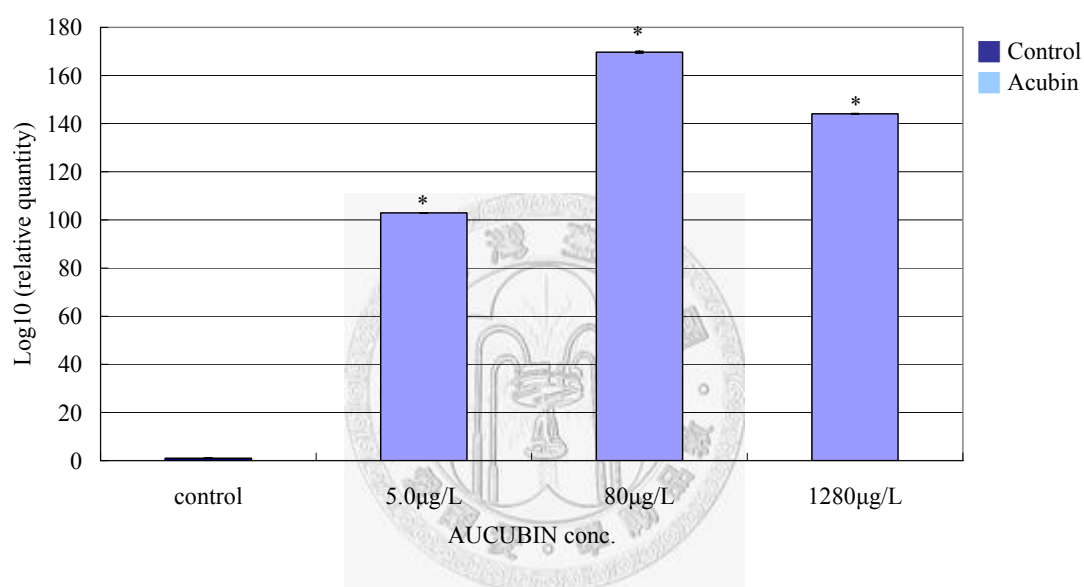
Figure 47 The mRNA expression of IL-1beta of one-week chondrocytes under different concentration of aucubin treatment. The data was shown by the comparative CT ($\triangle\triangle$CT) changes in gene expression of IL-1beta protein.

On the other hand, gene expression of IL-1 beta also increased in each betulin-treated experimental group. Nevertheless, the increasing extent is not as high as in each aucubin-treated experimental group. The result showed that when chondrocytes were treated with betulin, there were about 20-fold to 50-fold increases in mRNA expression of IL-1 beta compared with the control group. The gene expression of IL-1 beta in chondrocytes treated with the lowest, middle, and highest concentrations of betulin showed 22-fold, 23-fold, and 47-fold increases, respectively.
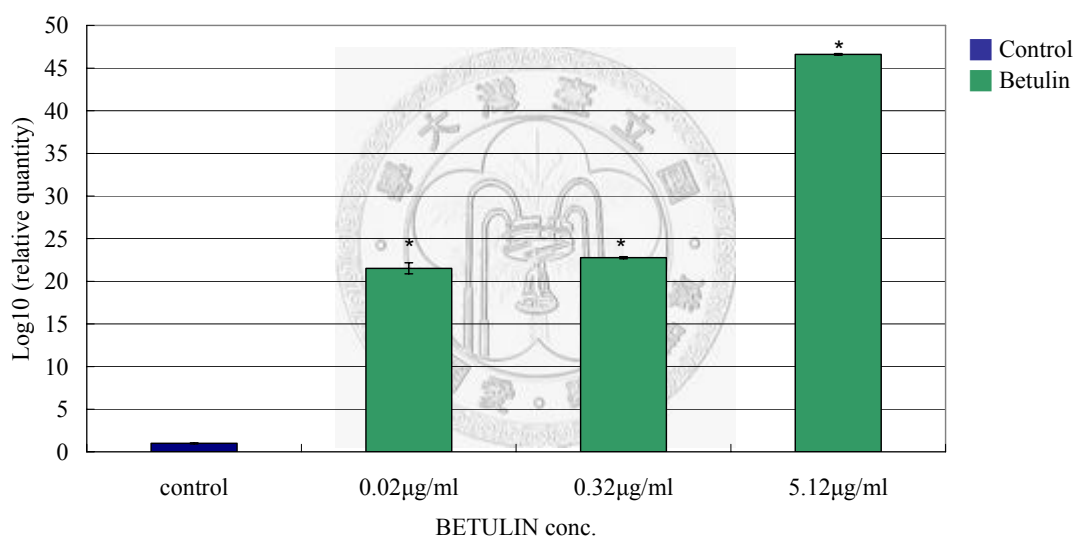
Figure 48 The mRNA expression of IL-1beta of one-week chondrocytes under different concentration of betulin treatment. The data was shown by the comparative CT ($\triangle\triangle$CT) changes in gene expression of IL-1beta protein.
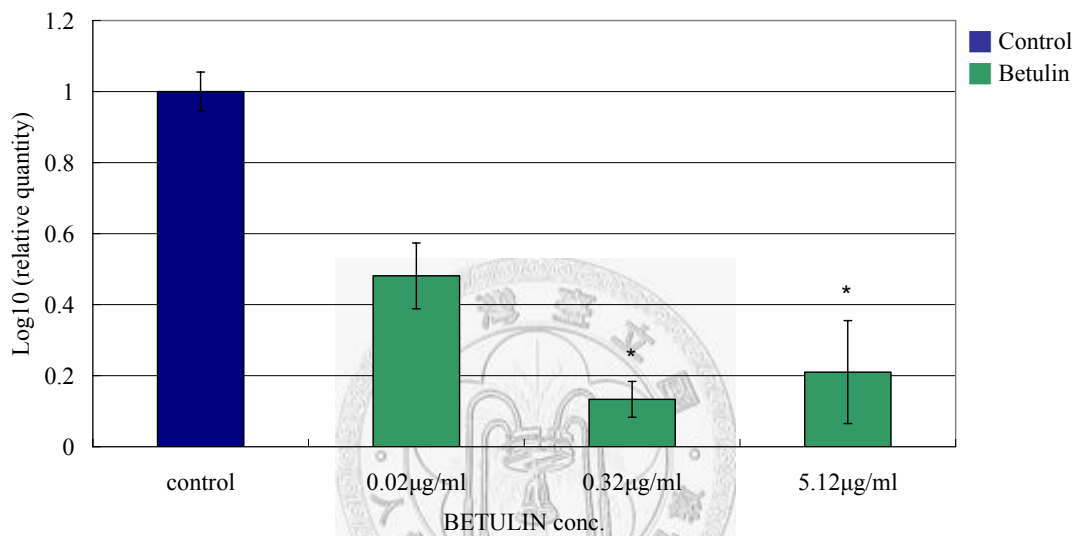
4-1.5.10 Gene Expression of TGF-beta1

In the aucubin-treated experimental groups, although gene expression of TGF-beta1 showed a 0.82-fold and 0.92-fold decreases under the treatment of the middle and highest concentration of betulin respectively, the TGF-beta1 mRNA levels were still kept above 0.85-fold. However, the chondrocytes treated with the highest concentration of aucubin showed a 0.60-fold decrease in TGF-beta1 mRNA levels compared with the control group.
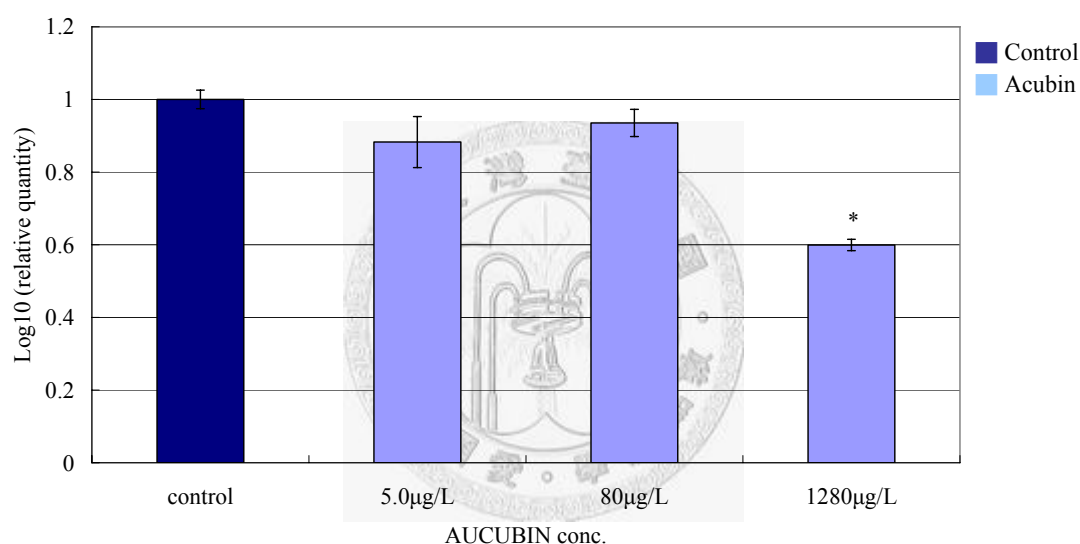
Figure 49 The mRNA expression of TGF-beta1 of one-week chondrocytes under different concentration of aucubin treatment. The data was shown by the comparative CT (△△CT) changes in gene expression of TGF-beta1 protein.
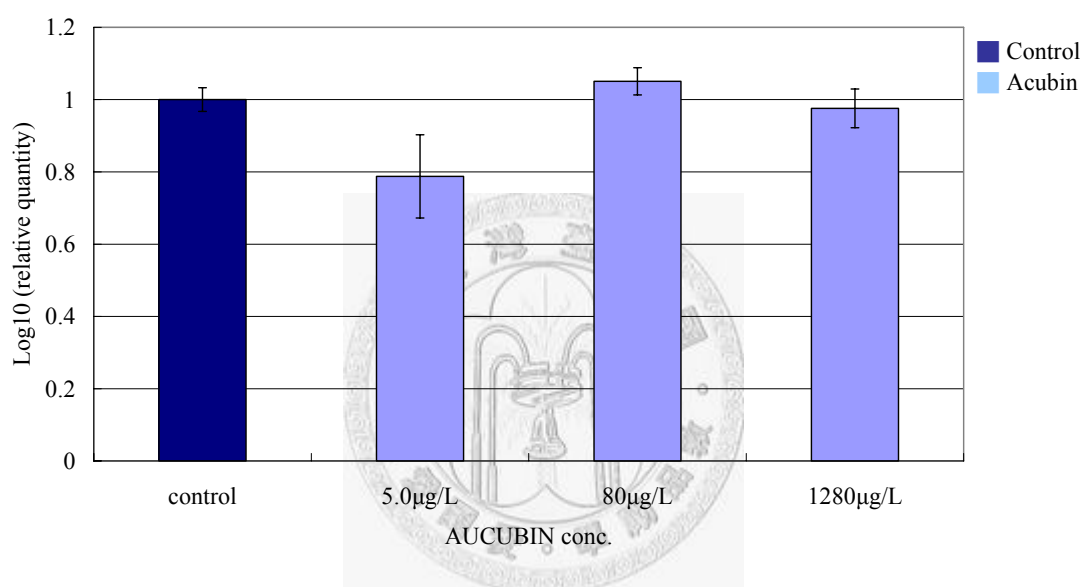
In the betulin-treated experimental groups, gene expression of TGF-beta1 showed a 1.25-fold increase under the treatment of the lowest concentration of aucubin, and the chondrocytes treated with the highest concentration of betulin kept the gene expression of TGF-beta1 just as the control group (1.00-fold). In contrast, there was a 0.75-fold decrease in TGF-beta1 mRNA levels under the highest concentration of betulin treatment.
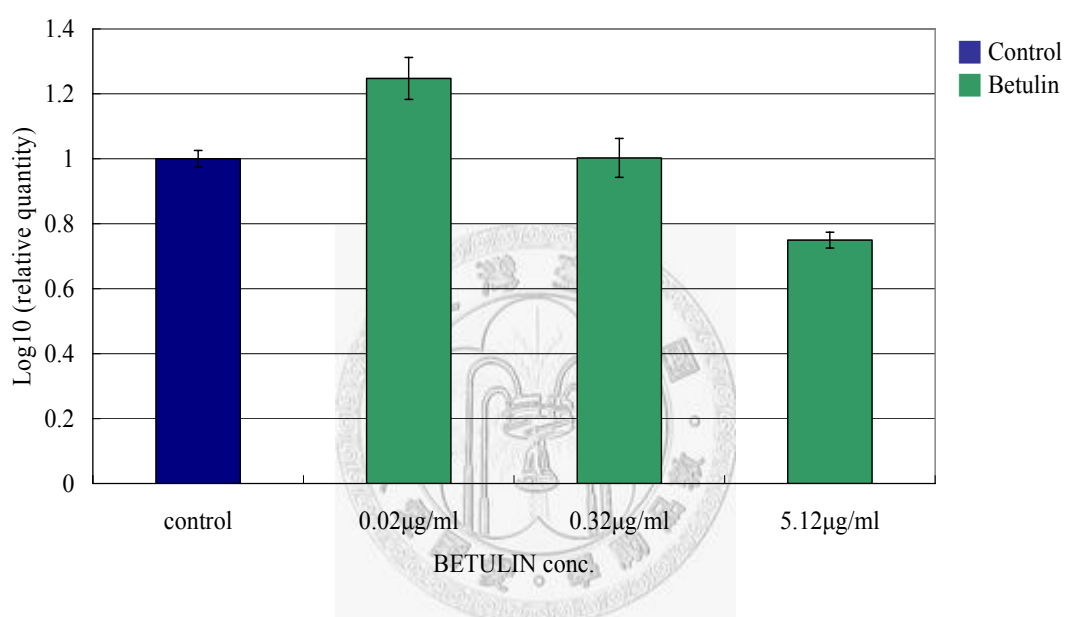
Figure 50 The mRNA expression of TGF-beta1 of one-week chondrocytes under different concentration of betulin treatment. The data was shown by the comparative CT ($\triangle\triangle$CT) changes in gene expression of TGF-beta1 protein.

4-1.6 Chemiluminescence Method for Detecting Free Radicals Scavenging

Formation of reactive oxygen species in 2D cultured chondrocytes was demonstrated by using chemiluminescence (CL) technique with luminol and lucigenin chemical probes. Luminol was used to detect the existence of hydrogen peroxide in cells, while lucigenin was selective to the existence of superoxide anion in cells. Because there was no significant detection of hydrogen peroxide existing in 2D cultured chondrocytes of the control groups and the experimental groups, the luminol-dependent chemiluminescence results were not shown here.

In the aucubin-treated experimental groups, lucigenin-dependent chemiluminescence demonstrated that lucigenin CL levels were slightly decreased in the group treated with the lowest concentration of aucubin compared with the control group (54.82±4.8 vs. 60.5±4.04 CL count/10sec, $p = 0.165 > 0.01$), but the lucigenin CL levels were slightly but not significantly increased in the group treated with the middle concentration of aucubin (88.35±6.63 vs. 60.5±4.04 CL count/10sec, $p = 0.018 > 0.01$). In the group treated with the highest concentration of aucubin, the lucigenin CL levels were dramatically and significantly decreased compared with the control group (-53.81±6.16 vs. 60.5±4.04 CL count/10sec, $p = 0.001 < 0.01$).
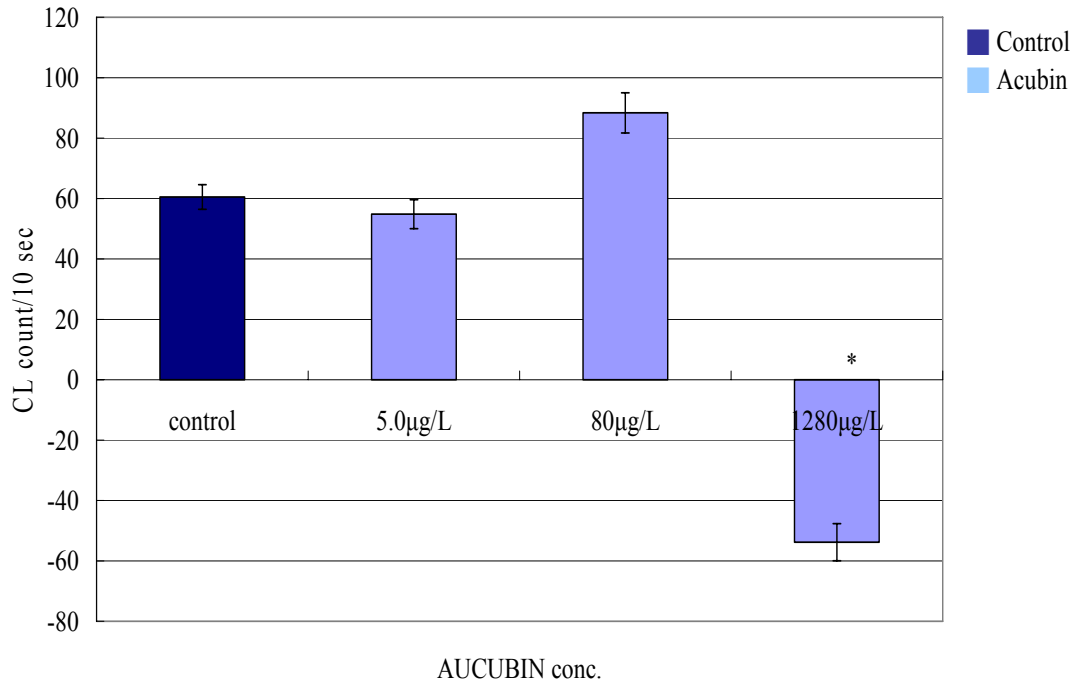
Figure 51 The free radicals scavenging effect of different concentrations of aucubin on lucigenin-dependent chemiluminescence of one-week chondrocytes.

In the betulin-treated experimental groups, lucigenin CL levels significantly decreased to negative values in all experimental groups, which meant that after the addition of lucigenin enhancer to the experimental groups, the quantity of O_2^- obtained in 5 min was lower than the baseline. In the group treated with the lowest concentration of betulin, that lucigenin CL levels were significantly decreased compared with the control group (-25.06±2.21 vs. 60.5±4.04 CL count/10sec, $p = 0.0007<0.01$). Furthermore, the lucigenin CL levels were extremely and significantly decreased in the group treated with the middle concentration of betulin (-172.96±6.95 vs. 60.5±4.04 CL count/10sec, $p =0.0003<0.01$). Also, in the group treated with the highest concentration of betulin, the lucigenin CL levels were decreased when compared with the control group (-3.06±9.16 vs. 60.5±4.04 CL count/10sec, $p =0.006<0.01$).
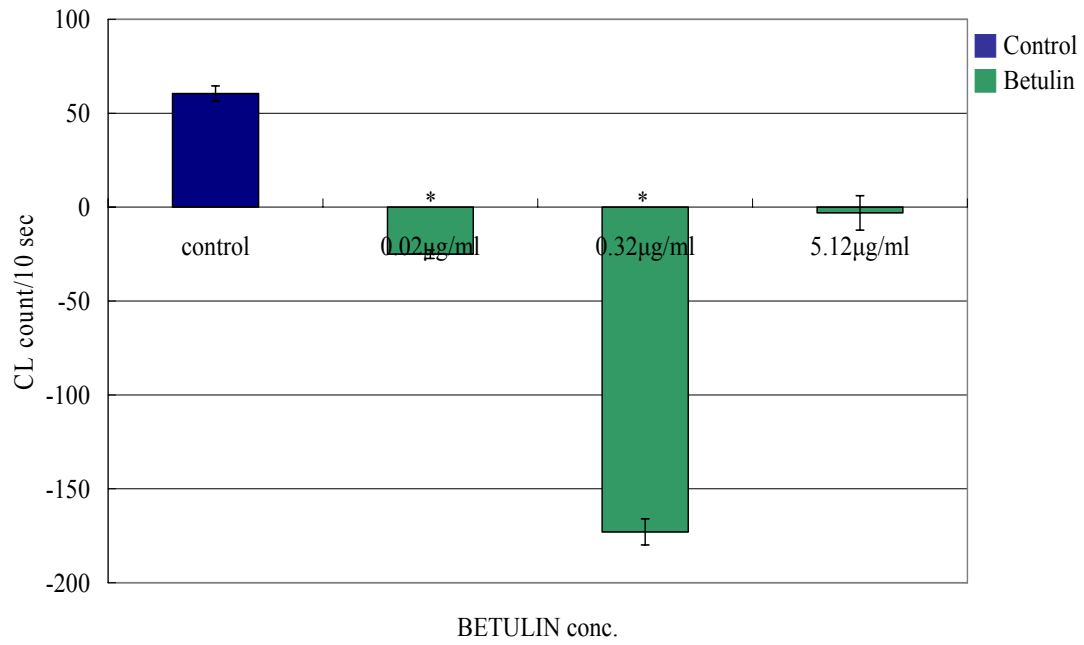
Figure 52 The free radicals scavenging effect of different concentrations of betulin on lucigenin-dependent chemiluminescence of one-week chondrocytes.
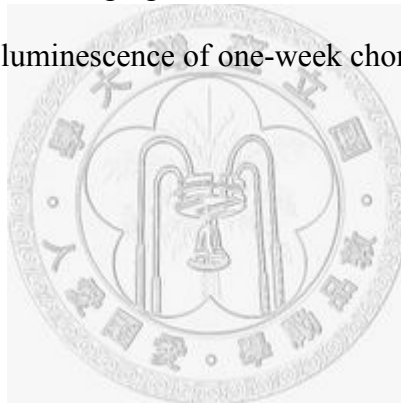
4-1.7 Histochemical Staining Evaluation

After one-week culture, the control group and the experimental group treated with the middle concentration of betulin were evaluated by H&E staining and Alcian blue staining. H&E staining was used to check the cell morphology, and the results are shown in Figure 53.

<table>
<tr><td>(a)</td><td>(b)</td></tr>
</table>
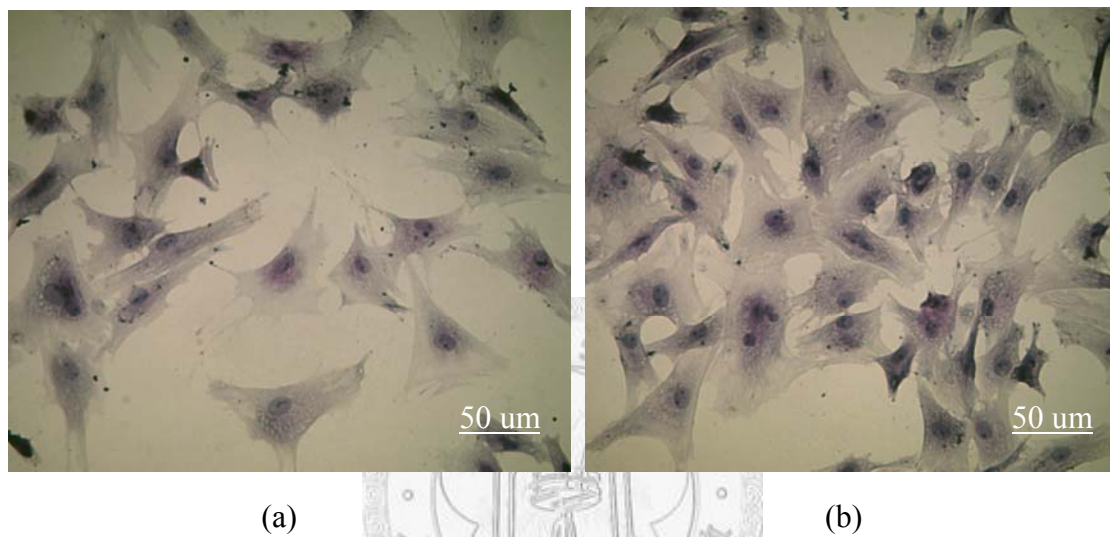
Figure 53 H&E staining of one-week cultured chondrocytes (100×). (a) Control group (b) Cells treated with 0.32ug/ml betulin experimental group.

Alcian blue staining targeted on the glycosaminoglycans of extracellular matrix, and the results are shown in Figure 54. In Alcian blue staining, the light blue color showed the existence of GAGs, and the light blue regions were both found in either control group or the experimental group.

<table>
<tr><td>(a)</td><td>(b)</td></tr>
</table>
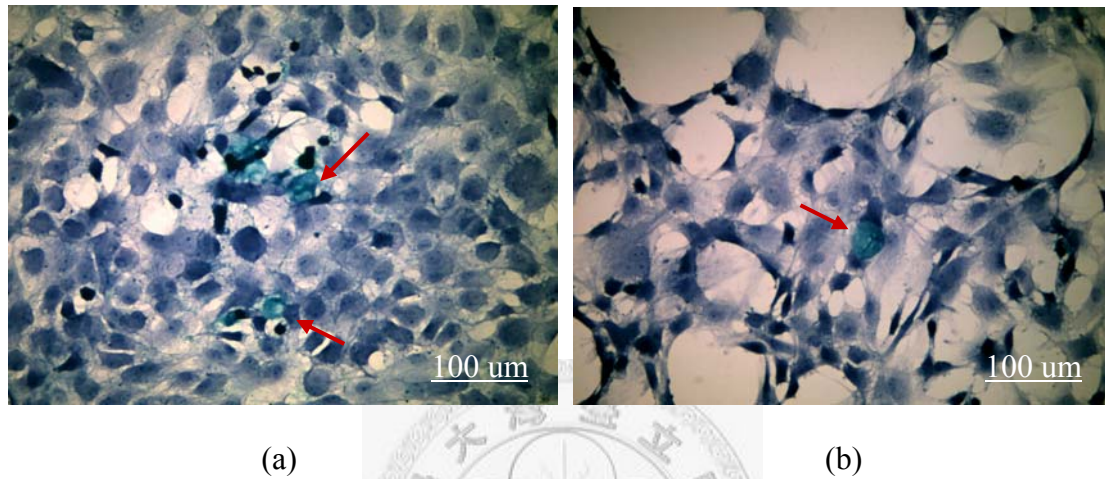
Figure 54 Alcian Blue staining of one-week cultured chondrocytes (40×). (a) Control group (b) Cells treated with 0.32ug/ml betulin experimental group.

4-1.8 Immunohistochemical Staining Evaluation

After one-week culture, the control group and the experimental group treated with the middle concentration of betulin were evaluated by S-100 protein antibody immunochemical stain and type II collagen antibody stain. Here, S-100 protein antibody immunochemical stain was doubled checked by the labeled-(strept) avidin-biotin (LAB-SA) method and immunofluorescence method. The results of S-100 protein antibody immunochemical staining are shown in Figure 55 and Figure 56, and the results of type II collagen antibody staining are shown in Figure 57.

(a)   (b)
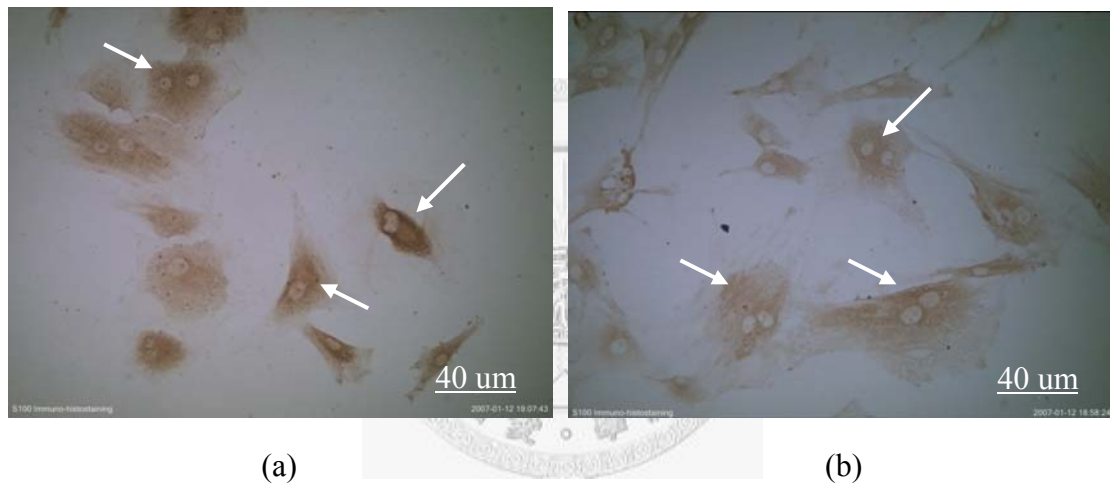
Figure 55 S-100 protein antibody immunochemical stain of one-week cultured chondrocytes (200×). (a) Control group (b) Cells treated with 0.32ug/ml betulin experimental group.
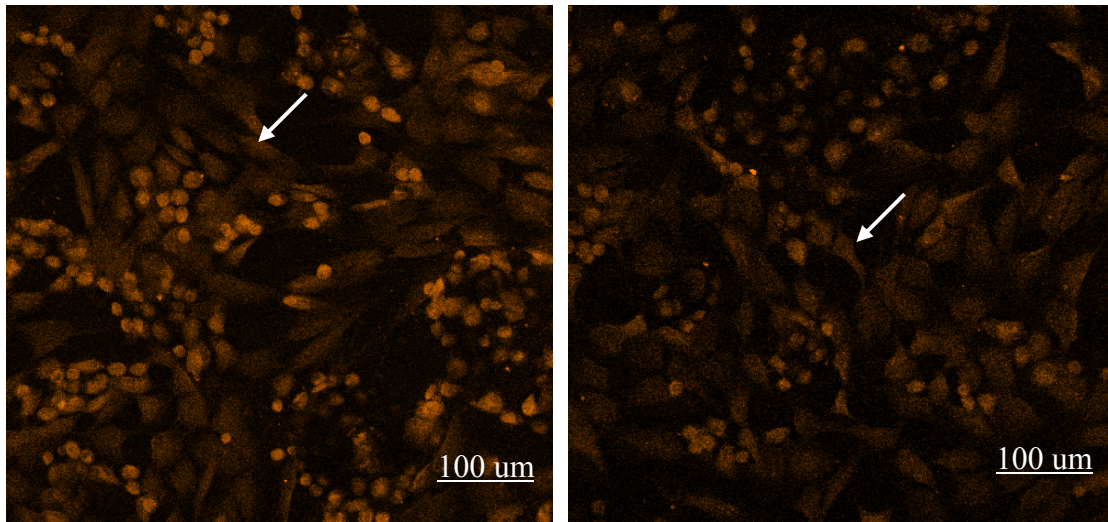
Figure 56 S-100 protein antibody immunochemical stain of one-week cultured chondrocytes (100×). (a) Control group (b) Cells treated with 0.32ug/ml betulin experimental group.
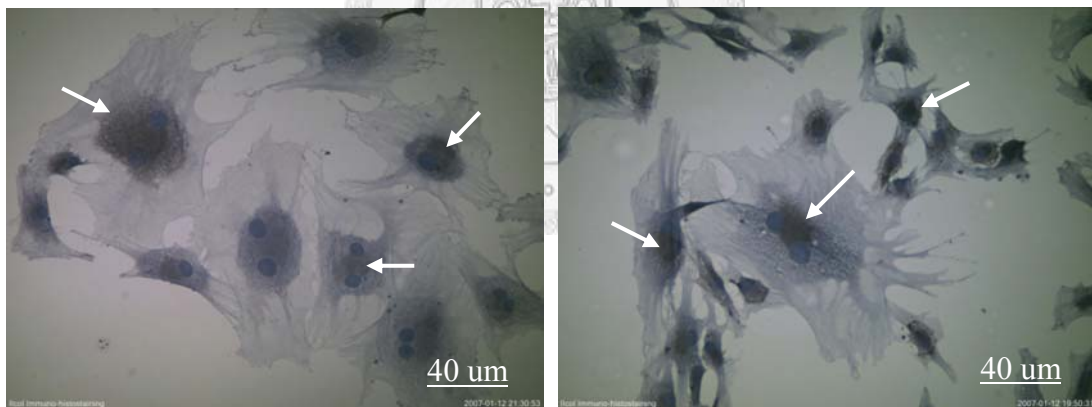
Figure 57 type II collagen antibody immunochemical stain of one-week cultured chondrocytes (200×). (a) Control group (b) Cells treated with 0.32ug/ml betulin experimental group.

4-2 Three-dimensional Scaffold Culture

4-2.1 Scanning electron microscopy

An SEM photograph of gelatin/C6S/C4S/HA modified tricopolymer scaffold is showed in Figure 58. It showed a highly porous structure which had an average 40um pore size ranging from 15um to 60um, and all of the pores in the tricopolymer scaffolds were interconnected.
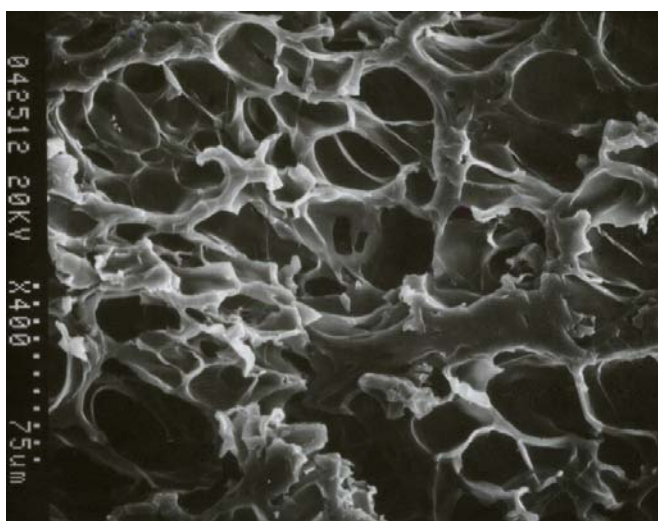
Figure 58 An SEM photograph of gelatin/C6S/C4S/HA modified tricopolymer scaffold (400×).

SEM photographs of cell-scaffold hybrids which were taken immediately after cell seeding are showed in Figure 59. It showed that the seeded cells deeply penetrated and evenly distributed in the scaffold. Also, SEM photographs of the control and experimental cell-scaffold hybrids group were taken at the end of 1, 2, and 4-week culture, and the results are showed in Figure 60, 61, and 62, respectively.
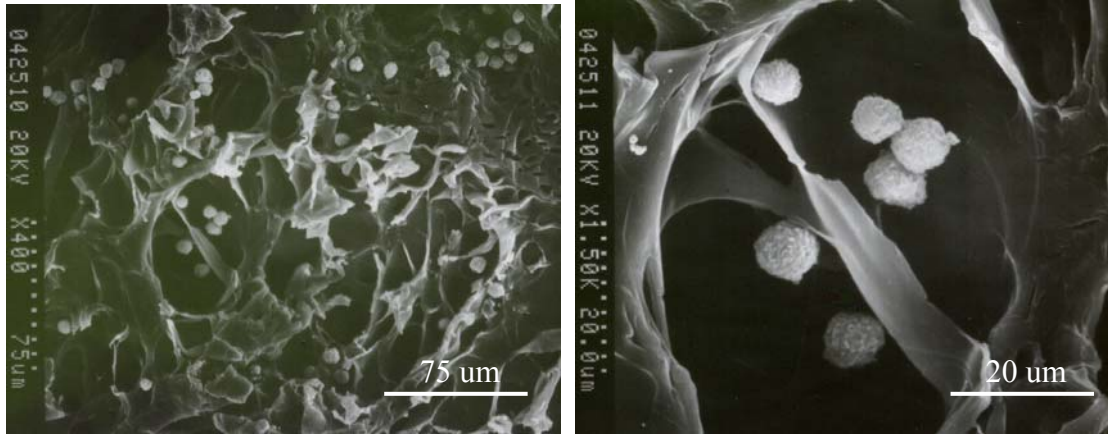
Figure 59 SEM photographs of cell-scaffold hybrids which were taken immediately after cell seeding. (a) 400× (b) 1500×
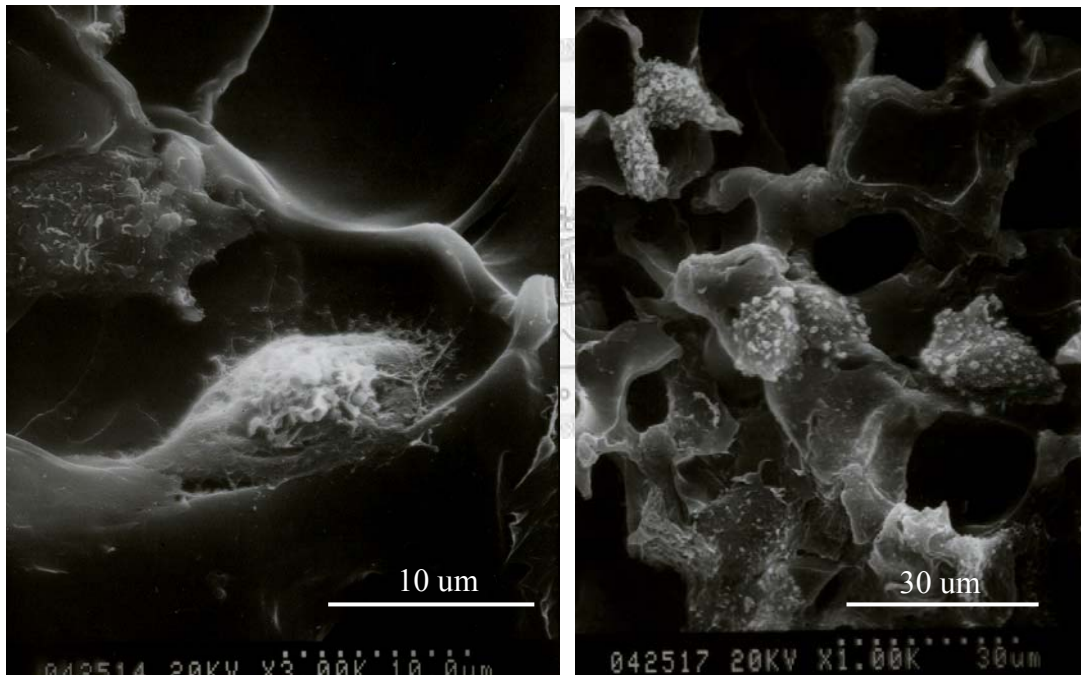
Figure 60 SEM photographs of cell-scaffold hybrids which were taken at the end of 1-week culture. (a) Control group (3000×) (b) Betulin-treated experimental group (1000×).
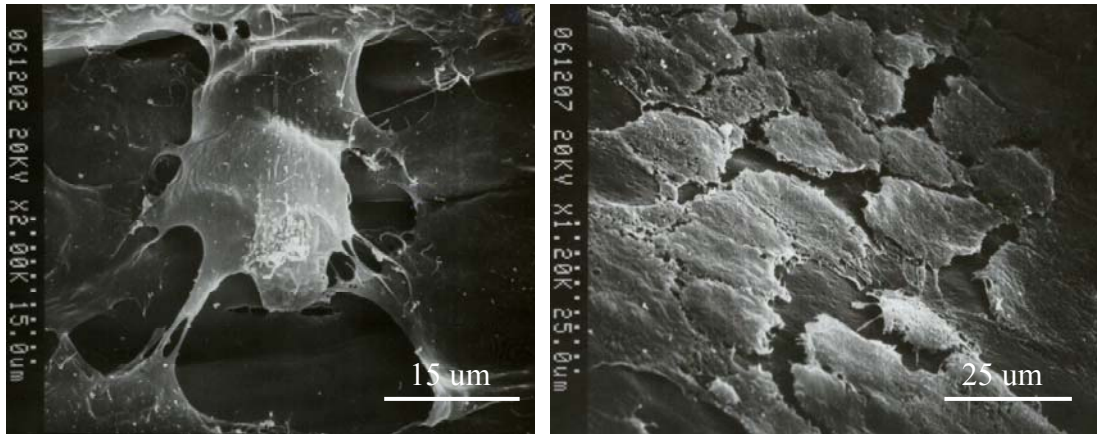
Figure 61 SEM photographs of cell-scaffold hybrids which were taken at the end of 2-week culture. (a) Control group (2000×) (b) Betulin-treated experimental group (1200×).
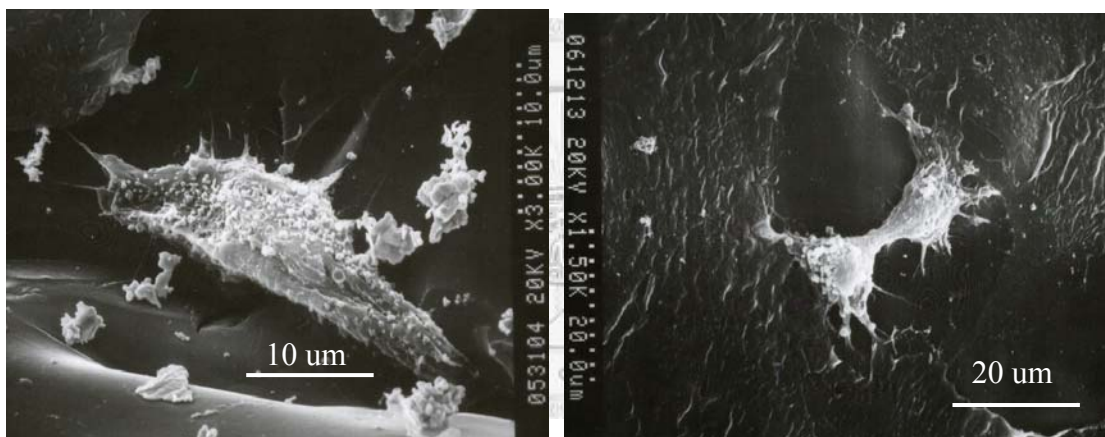
Figure 62 SEM photographs of cell-scaffold hybrids which were taken at the end of 4-week culture. (a) Control group (3000×) (b) Betulin-treated experimental group. The chondrocytes were just in the phase of cell division (1500×).

4-2.2 WST-1 Assay for Cell Proliferation

The OD_{450} of cell-scaffold hybrids control group and cell-scaffold hybrids experimental group which were treated with 0.32ug/ml betulin were obtained after 1-week, 2-week, and 4-week culture, and the scaffolds without cells seeded were used as the negative control group. The results were summarized in Figure 63, which showed that all of cell-scaffold hybrids treated with betulin had statistically significant and higher OD values than cell-scaffold hybrids control group at the end of each tested week. At the end of 1-week culture, the OD values of the experimental group and the control group are 1.129 ± 0.025 and 1.080 ± 0.019 respectively, and the p value was 0.006 lower than 0.05. At the end of 2-week culture, the OD values between the experimental group and the control group are 1.428 ± 0.145 and 1.280 ± 0.083 where the p value was 0.03 and lower than 0.05. Besides this, at the end of 4-week culture, the OD values of the experimental group and the control group are 1.936 ± 0.169 and 1.648 ± 0.033 ($p=0.009<0.05$).

The results also showed that the longer the cells were cultured in 3D environment, the higher the OD values obtained. For instances, the OD_{450} of 4-week experimental group was significantly higher than the 2-week one ($p = 1.79 \times 10^{-6}$), and the OD_{450} of 2-week experimental group was also higher than the 1-week one ($p = 0.0003$).
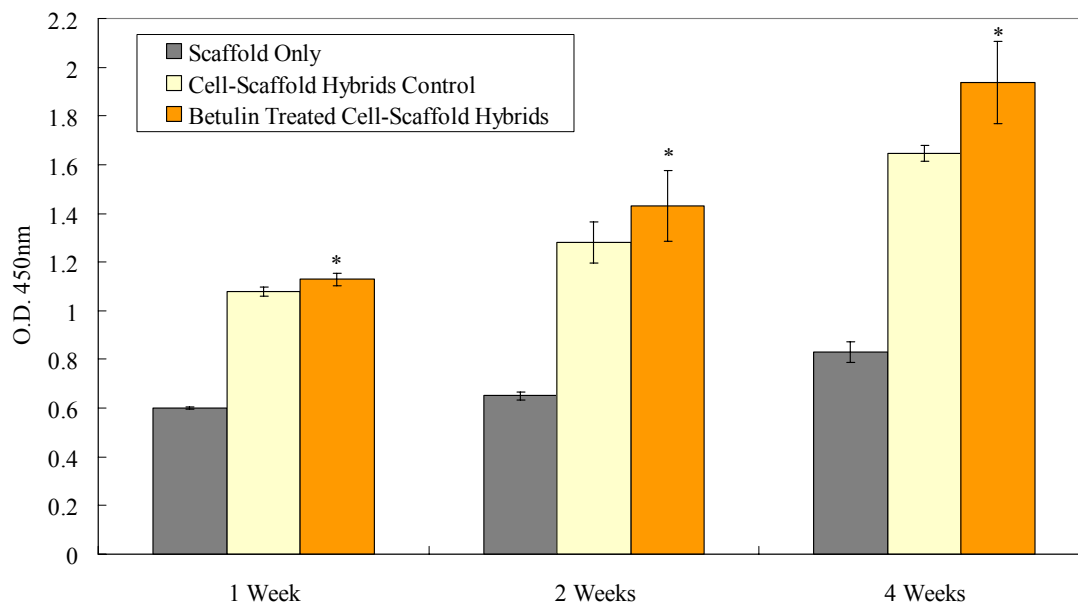
Figure 63 WST-1 assay of three-dimensional scaffold culture. In WST-1 assay, all of cell-scaffold hybrids experimental groups had statistically significant and higher OD values than cell-scaffold hybrids control groups.

4-2.3 Total DNA for Cell Proliferation Quantification

The total DNA amount of cell-scaffold hybrids control group and experimental group which were treated with 0.32ug/ml betulin were obtained after 1-week, 2-week, and 4-week culture. The results were summarized in Figure 64 and showed that all of cell-scaffold hybrids treated with betulin had higher DNA amount than cell-scaffold hybrids control group at the end of each tested week. At the end of 1-week culture, the DNA amount of the experimental group and the control group are 6.428 ± 0.428 and 5.082 ± 0.590 respectively, and the p value was 0.15. At the end of 2-week culture, the DNA amount between the experimental group and the control group are 6.718 ± 0.626 and 5.873 ± 0.025 where the p value was 0.15. Besides this, at the end of 4-week culture, the DNA amount of the experimental group and the control group are 12.153 ± 0.544 and 10.775 ± 0.110 ($p=0.13$).

The results also showed that the longer the cells were cultured in 3D environment, the higher the DNA amount obtained. For instances, the DNA amount of 4-week experimental group was significantly higher than the 2-week one ($p = 0.02<0.05$).
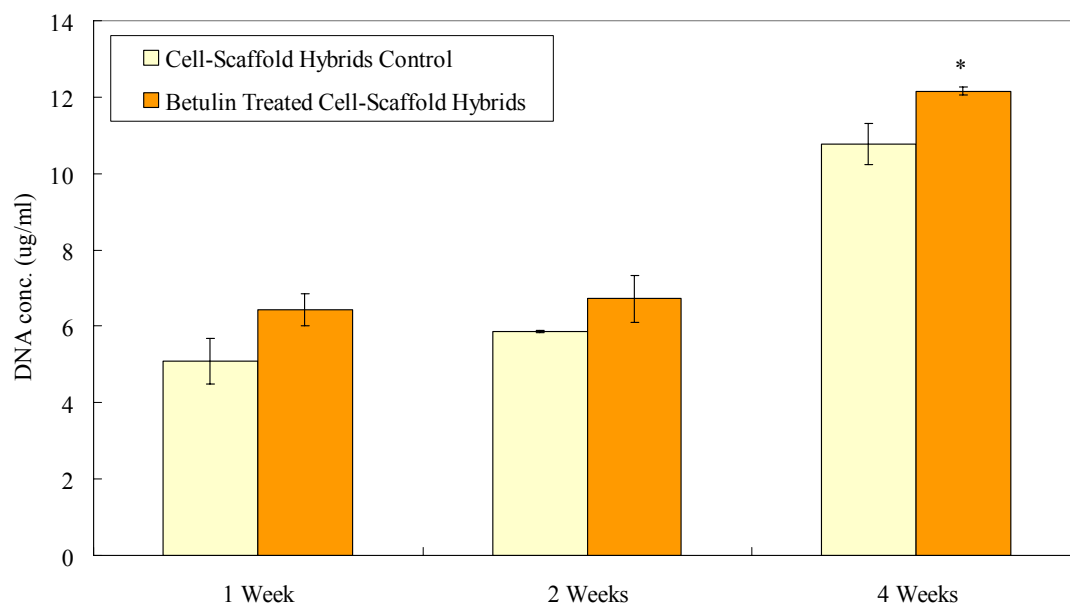
Figure 64 Total DNA assay of three-dimensional scaffold culture. In total DNA assay, all of cell-scaffold hybrids experimental groups had higher DNA amount than cell-scaffold hybrids control groups.
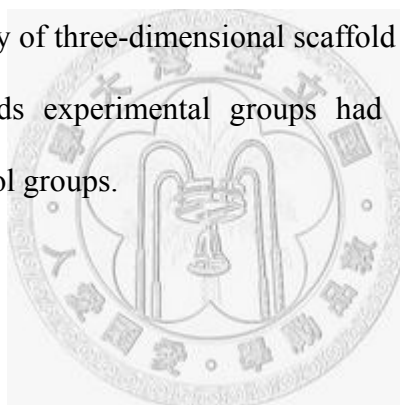
4-2.4 DMMB Assay for Sulfated Glycosaminoglycans Content

When conducting DMMB assay, a linear standard curve should be obtained from GAG standards: 0–100 mg/mL of chondroitin-6-sulfate (C-4384, Sigma), which were then used to estimate the GAG content in each experimental sample. The OD_{570} obtained from C6S standards are summarized in Figure 65. The linear regression trend line of C6S standards was: y = -198.2x + 198.83.

$$y = -198.2x + 198.83$$
$$R^2 = 0.9853$$
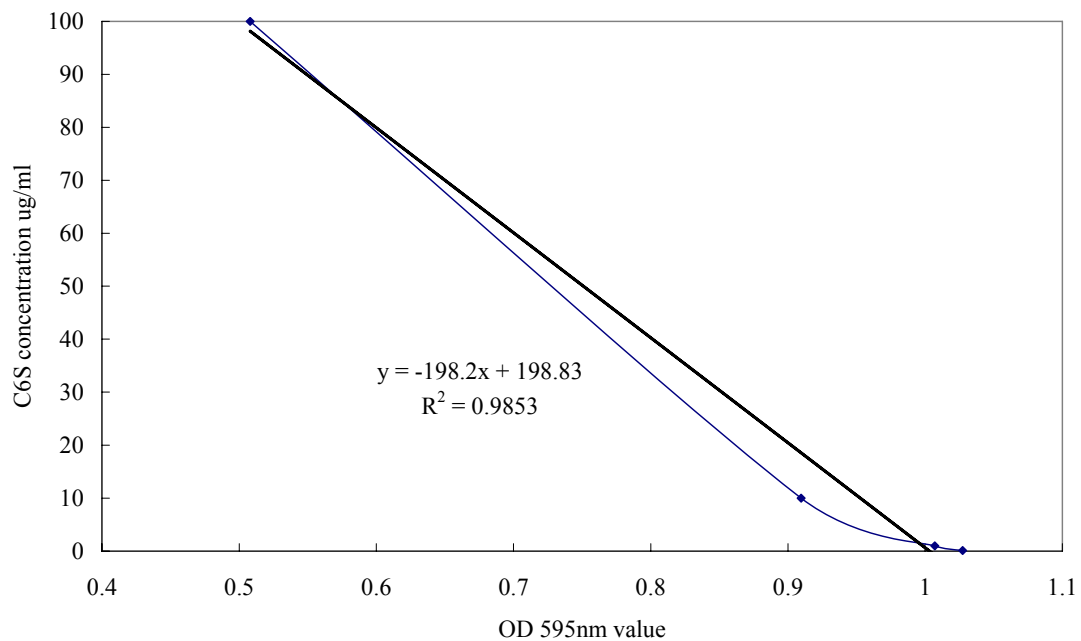
Figure 65 Linear standard curve of glycosaminoglycans standards. The absorbance at 570 nm was measured. The linear regression trend line of glycosaminoglycans standards was: y = -198.2x + 198.83.

The glycosaminoglycans content of cell-scaffold hybrids control groups and cell-scaffold hybrids experimental groups which were treated with 0.32ug/ml betulin was obtained after 1-week, 2-week, and 4-week culture and summarized in Figure 66, and the scaffolds without cells seeded were used as the negative control group. At the end of 1-week culture, betulin-treated experimental group didn't show a higher GAG content than control group (79.365 ±2.690 ug/ml vs. 84.518 ±4.092 ug/ml, $p = 0.017$). However, at the end of 2-week culture, betulin-treated experimental groups showed statistically significant higher GAG content than their relative control groups (94.924 ± 0.862 vs. 80.158 ±8.611, $P = 0.0177 < 0.05$). Similarly, at the end of 4-week culture, betulin-treated experimental groups showed higher but not statistically significant GAG content than their relative control groups.

The results also showed that when the cell-scaffold hybrids were treated with betulin, at the end of 2-week culture, the amount of GAGs got maxima. Since former research and the experimental result here have shown that the GAG originally entrapped in the scaffold substrate can not be retained by the scaffold and is lost into the culture medium during the in vitro culture period (data showed in Figure 67), the GAGs content increase of the experimental group means that the GAGs were newly secreted by chondrocytes themselves. Here, we didn't discover that the longer the cells were cultured in 3D environment, the higher the GAGs content existed.
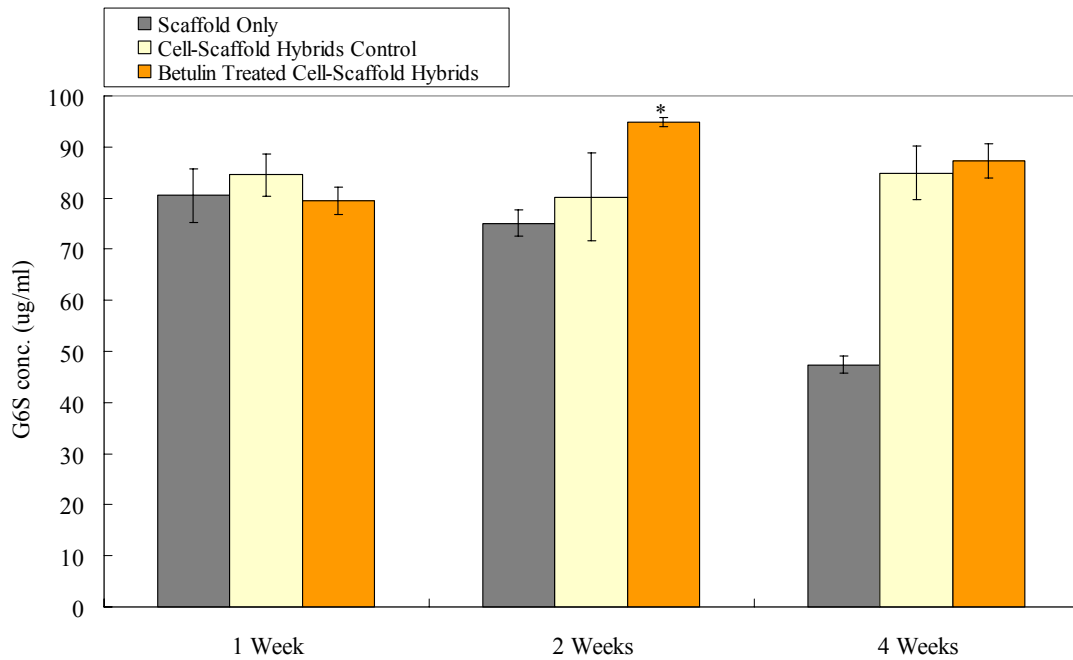
Figure 66 The GAG contents of cell-scaffold hybrids control groups and betulin-treated cell-scaffold hybrids experimental groups after cultured for 1, 2, and 4 weeks were shown.
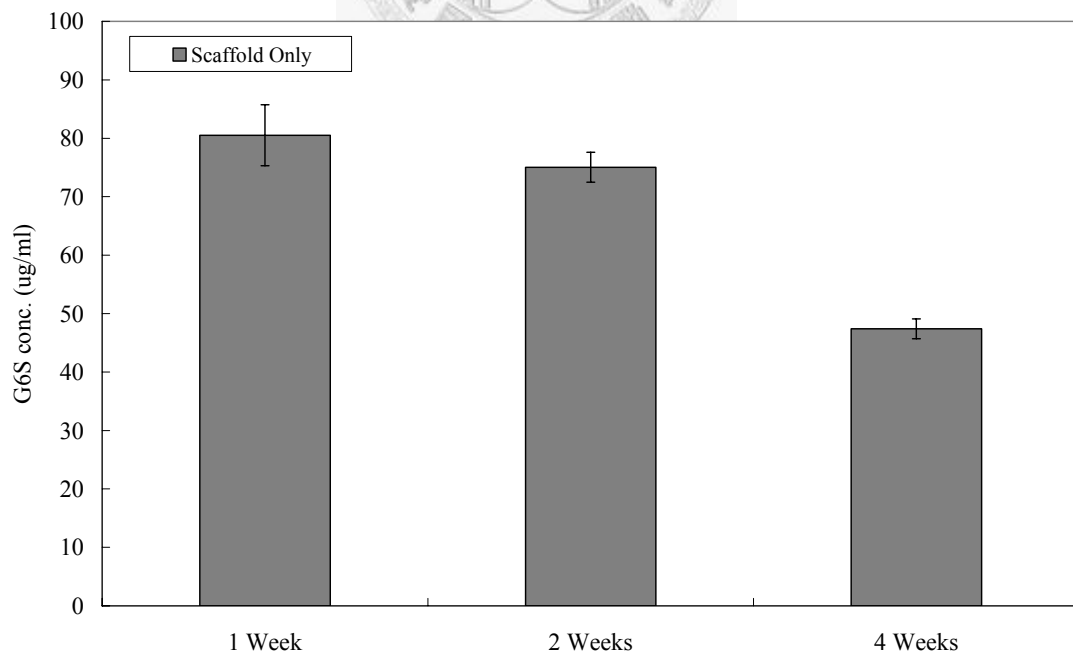
Figure 67 The GAG contents of the scaffolds without cells seeded negative control group after cultured for 1, 2, and 4 weeks were shown.

4-2.5 Real-time Reverse-Transcriptase Polymerase Chain Reaction for mRNA Expression Quantification

In real-time PCR, the $-\triangle$Ct values of each target gene were normalized by the house-keeping gene, GAPDH, and relative expressions of each target gene between the experimental groups and the control group are shown by the $-\triangle$CT and summarized as follows.

4-2.5.1 mRNA Expression of Collagens

The expression of type II collagen, type I collagen and type X collagen were shown in Figure 68, Figure 69 and Figure 70, respectively. Type II collagen, one of the major components in the extracellular matrix of articular cartilage, increased with the culture time when cell-scaffold hybrids were treated by betulin (Figure 68). Also, at the end of each tested week, betulin-treated experimental groups showed statistically significant higher type II collagen gene expression than their relative control groups. In contrast, in the control groups, the expression of type II collagen didn't show constant increase within culture time. For Type I collagen gene, although at the end of the first week betulin-treated experimental groups showed statistically significant higher type I collagen gene expression than the control groups (Figure 69). However, at the end of 2 and 4 weeks, the type I collagen gene expression of control groups increased dramatically, and betulin-treated experimental groups showed statistically significant lower type I collagen gene expression than their relative control groups. When chondrocytes cultured in the betulin-treated experimental group, type X collagen expression was kept in a very low level, and at the end of 1 and 2 weeks it was significantly lower then the control group (Figure 70).
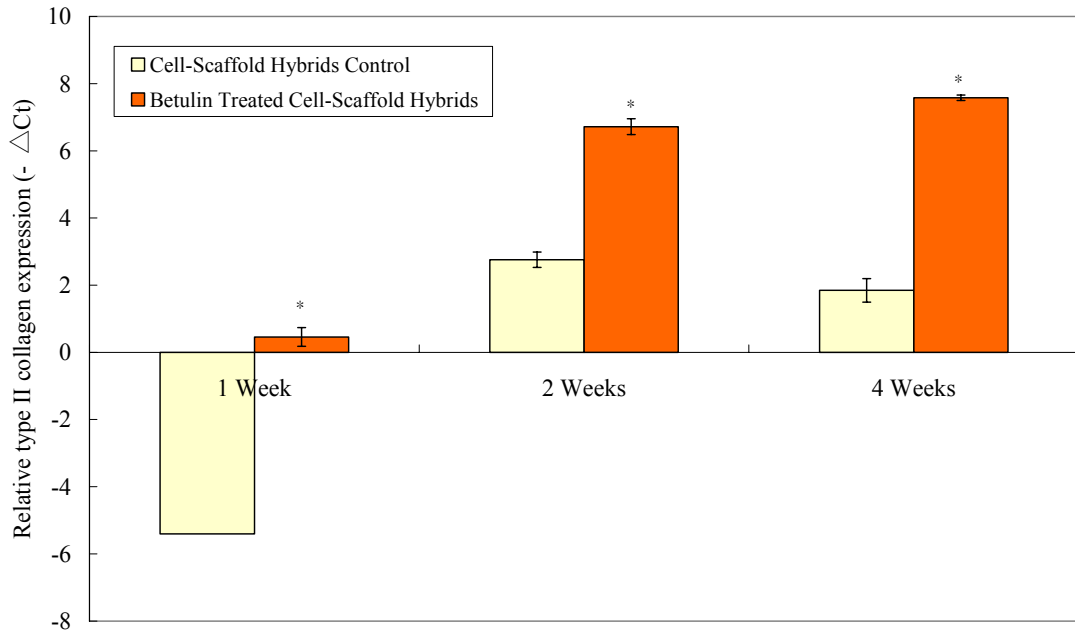
Figure 68 At the end of 1, 2, and 4-week, the values of $-\triangle Ct$ of relative type II collagen gene expression were obtained. In the bar chart, $-\triangle Ct$ was shown by mean with S.D. (* means p-value<0.01).
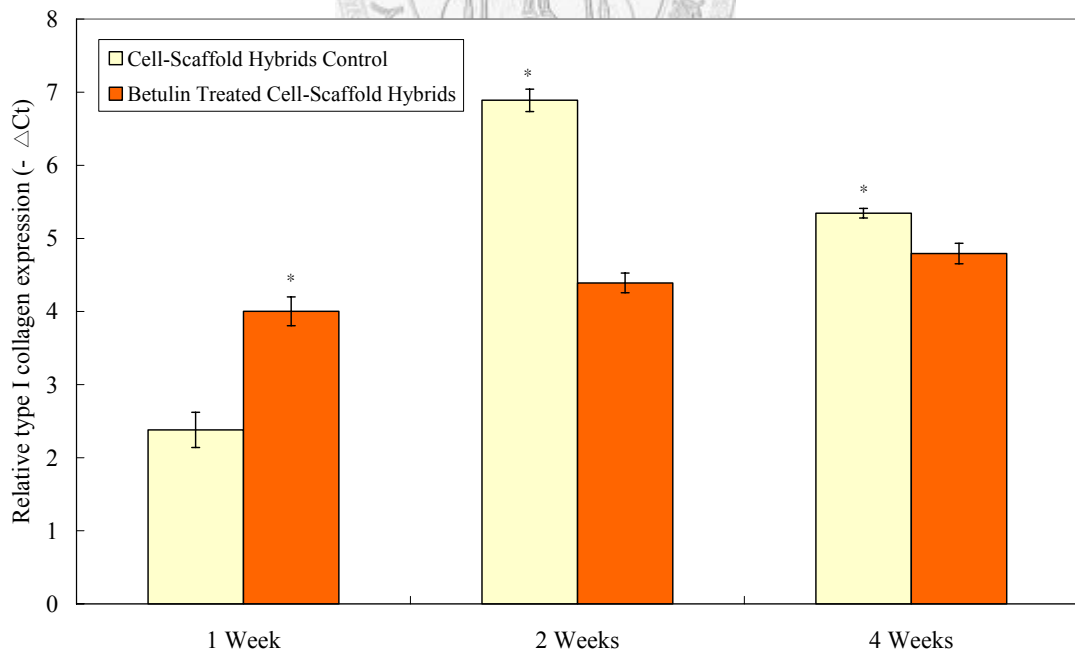
Figure 69 At the end of 1, 2, and 4-week, the values of $-\triangle Ct$ of relative type I collagen gene expression were obtained. In the bar chart, $-\triangle Ct$ was shown by mean with S.D. (* means p-value<0.01)
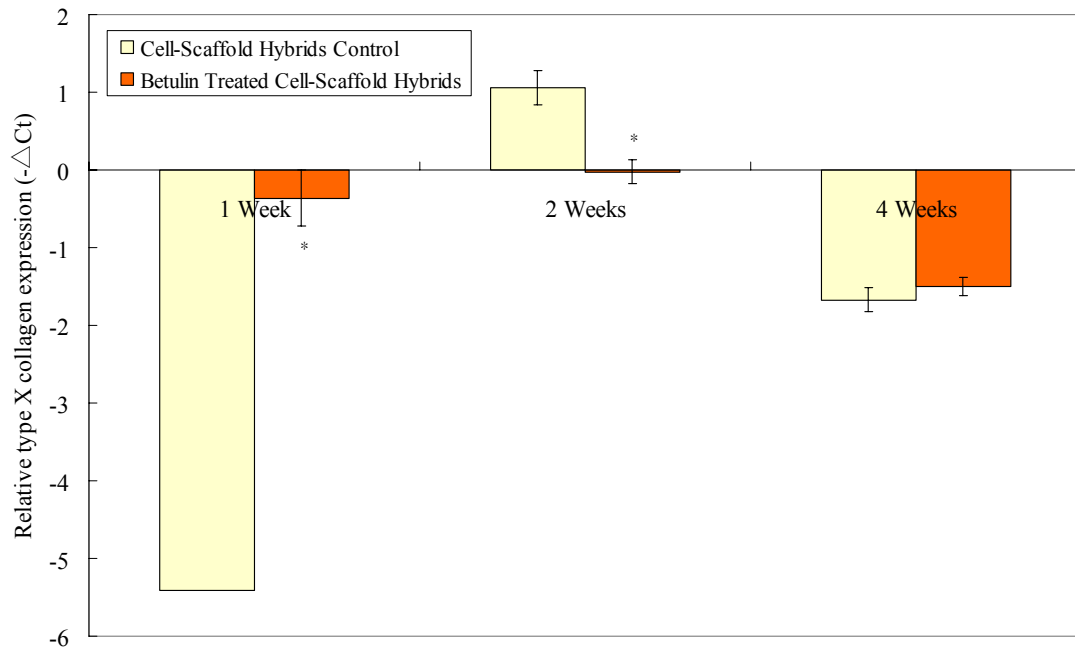
Figure 70 At the end of 1, 2, and 4-week, the values of $-\triangle Ct$ of relative type X collagen gene expression were obtained. In the bar chart, $-\triangle Ct$ was shown by mean with S.D. (* means p-value<0.01).
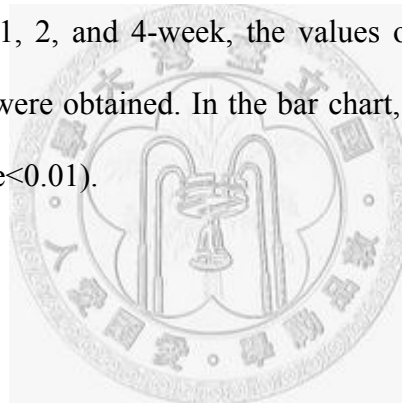
4-2.5.2 mRNA Expression of Proteoglycans

The expression of proteoglycans including aggrecan and decorin were shown in Figure 71 and Figure 72, respectively. In the betulin-treated experimental groups, at the end of each tested week, mRNA expression of aggrecan showed statistically significant higher than their relative control groups. Moreover, at the end of 2 weeks, betulin successfully increased the expression of aggrecan to the maximum. Similarly, mRNA expression of decorin also showed statistically significant higher than their relative control groups at the end of 1 week and 2 weeks.

Figure 71 At the end of 1, 2, and 4-week, the values of $-\triangle$Ct of relative aggrecan gene expression were obtained. In the bar chart, $-\triangle$Ct was shown by mean with S.D. (* means p-value<0.01).
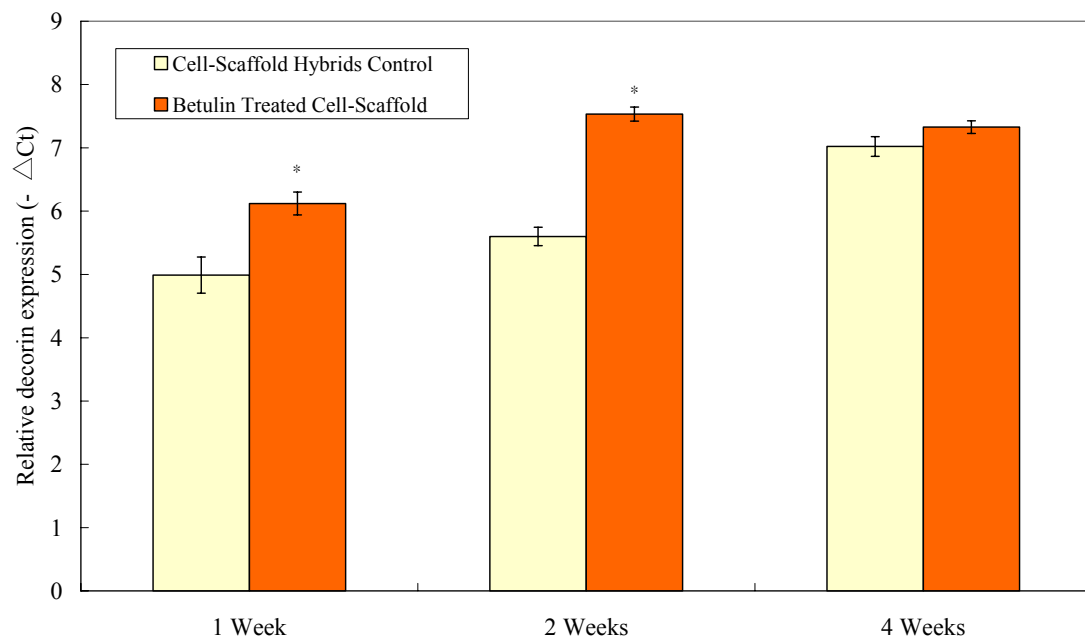
Figure 72 At the end of 1, 2, and 4-week, the values of $-\triangle Ct$ of relative decorin gene expression were obtained. In the bar chart, $-\triangle Ct$ was shown by mean with S.D. (* means p-value<0.01).
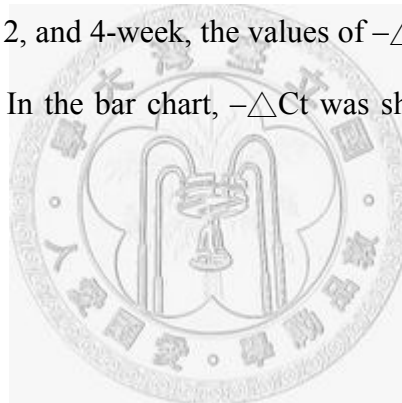
4-2.5.3 mRNA Expression of ECM Regulators

The mRNA expression of three major factors related to extra-cellular matrix degradation, TIMP-1, MMP-2 and MT1-MMP, were measured, and results were shown in Figure 73, Figure 74 and Figure 75, respectively. The mRNA expression of TIMP-1 increased with the culture time when cell-scaffold hybrids were treated by betulin (Figure 73). Although the mRNA expression of TIMP-1 had no statistical significance between the control group and the experimental group, at the end of 1 week and 2 weeks, the expression value of experimental groups were still higher than the control group.
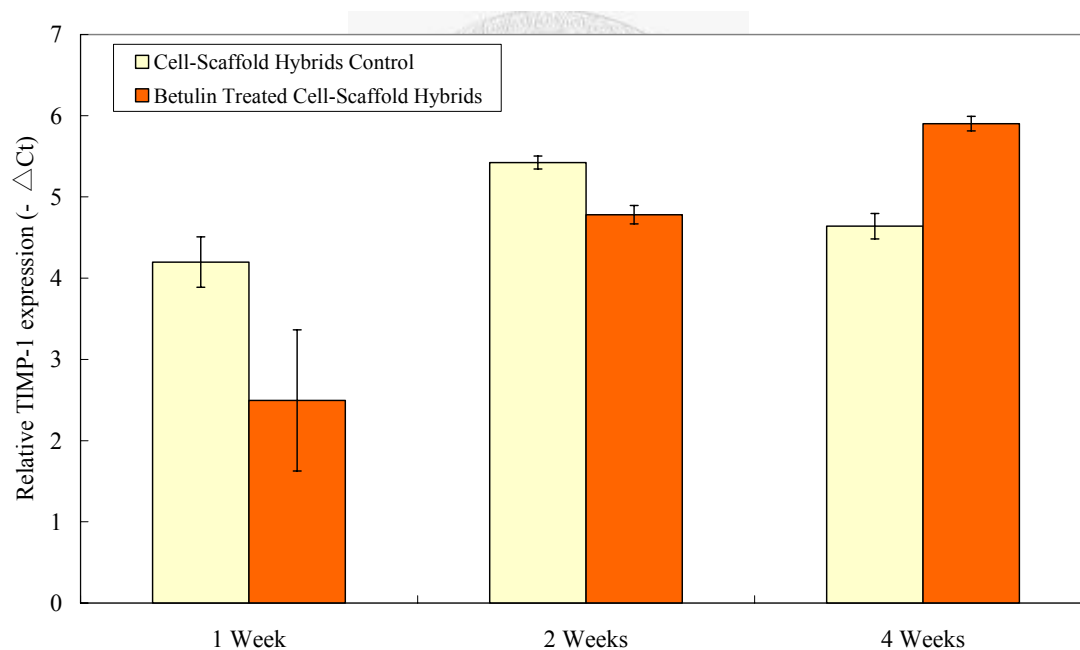
Figure 73 At the end of 1, 2, and 4-week, the values of $-\triangle Ct$ of relative TIMP-1 gene expression were obtained. In the bar chart, $-\triangle Ct$ was shown by mean with S.D. (* means p-value<0.01).

In MMP-2 mRNA expression, betulin-treated experimental group successfully kept the expression of MMP-2 in a significant low level although the expression amount was increase with the culture time (Figure 74).
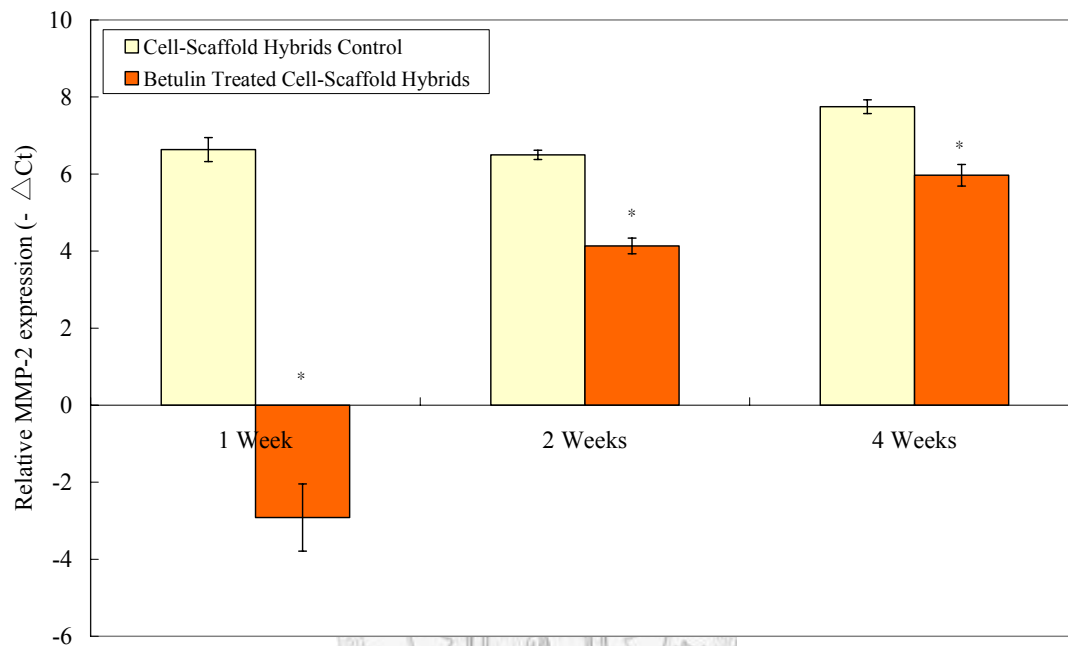
Figure 74 At the end of 1, 2, and 4-week, the values of $-\triangle Ct$ of relative MMP-2 gene expression were obtained. In the bar chart, $-\triangle Ct$ was shown by mean with S.D. (* means p-value<0.01).

Although at the end of the first week the mRNA expression of membrane-type 1 metalloproteinase (MT1-MMP) of betulin-treated experimental group was significantly higher that the control group. However, at the end of 2 weeks, mRNA expression of MT1-MMP betulin group showed statistically significant lower value their relative control groups (Figure 75).
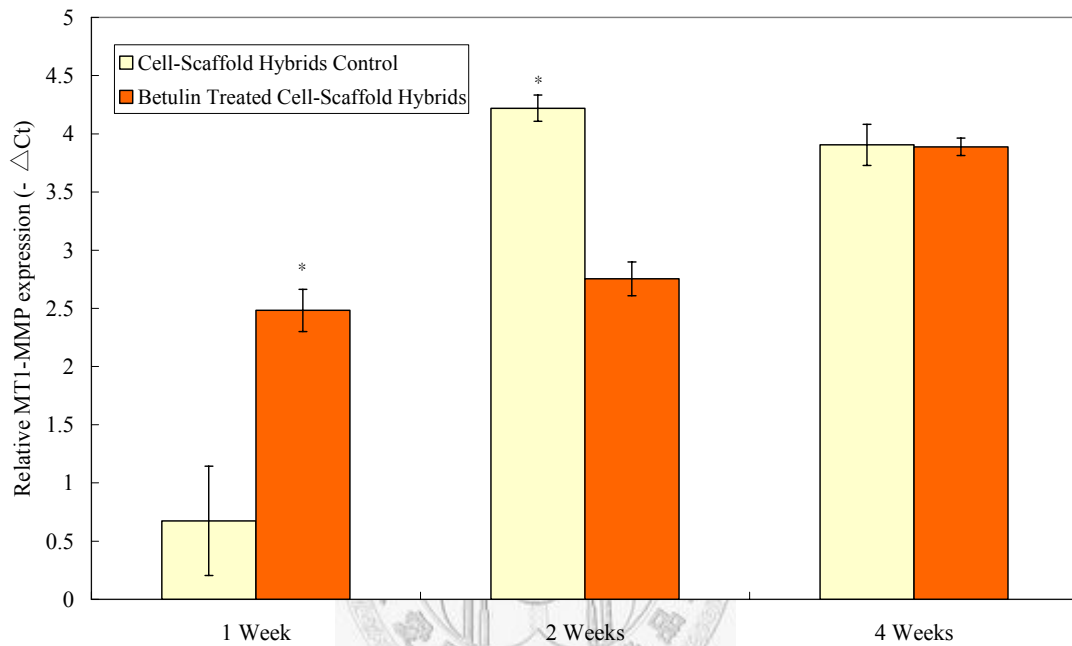
Figure 75 At the end of 1, 2, and 4-week, the values of $-\triangle Ct$ of relative MT1-MMP gene expression were obtained. In the bar chart, $-\triangle Ct$ was shown by mean with S.D. (* means p-value<0.01).

4-2.5.4 mRNA Expression of Growth and Differentiation Factors

In TGF-β1, there was no significant difference between the control and experimental group after 1-week culture, and at the end of 2 weeks the TGF-β1 mRNA expression of control group increased to a significant higher value than the betulin-treated experimental group. However, after 4-week culture the mRNA expression of betulin-treated experimental group increased to a significant higher value than the control group (Figure 76).
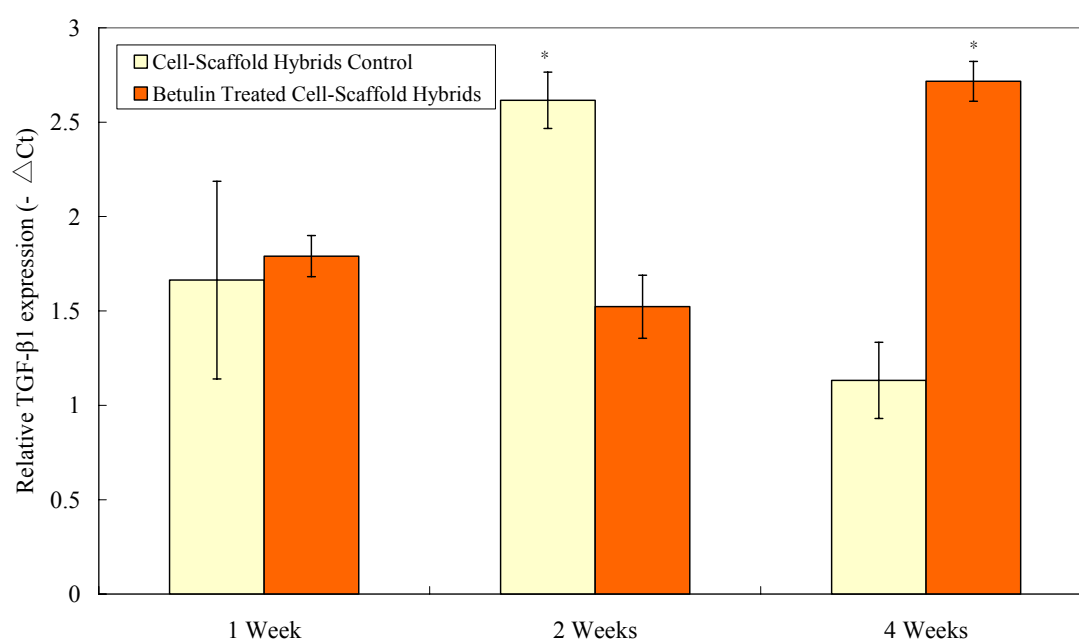
Figure 76 At the end of 1, 2, and 4-week, the values of $-\triangle Ct$ of relative TGF-β1 gene expression were obtained. In the bar chart, $-\triangle Ct$ was shown by mean with S.D. (* means p-value<0.01).

The results of BMP-7 mRNA expression showed that the longer the cells were cultured in betulin-treated 3D environment, the higher the mRNA expression amount obtained. At the end of 1 week and 2 weeks, mRNA expression of BMP-7 successfully increased to a significant higher value than their relative control groups.
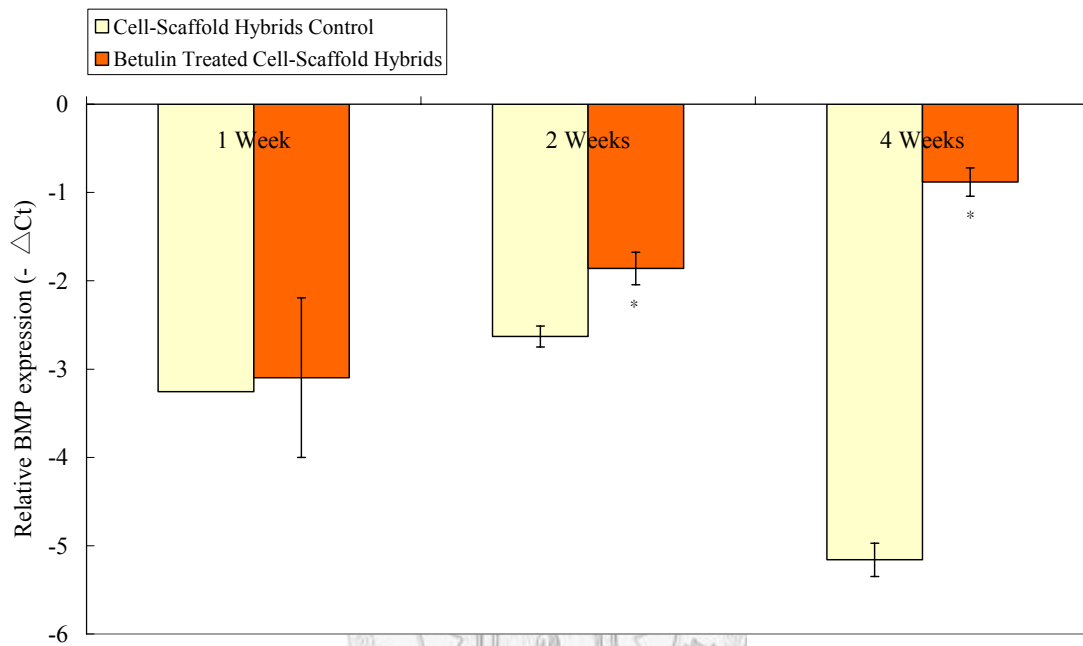
Figure 77 At the end of 1, 2, and 4-week, the values of $-\triangle Ct$ of relative BMP-7 gene expression were obtained. In the bar chart, $-\triangle Ct$ was shown by mean with S.D. (* means p-value<0.01).

Also, in the results of IGF-1 mRNA expression showed that the longer the cells were cultured in betulin-treated 3D environment, the higher the mRNA expression obtained. At the end of 1 week and 2 weeks, mRNA expression of IGF-1 successfully increased to a significant higher value than their relative control groups.
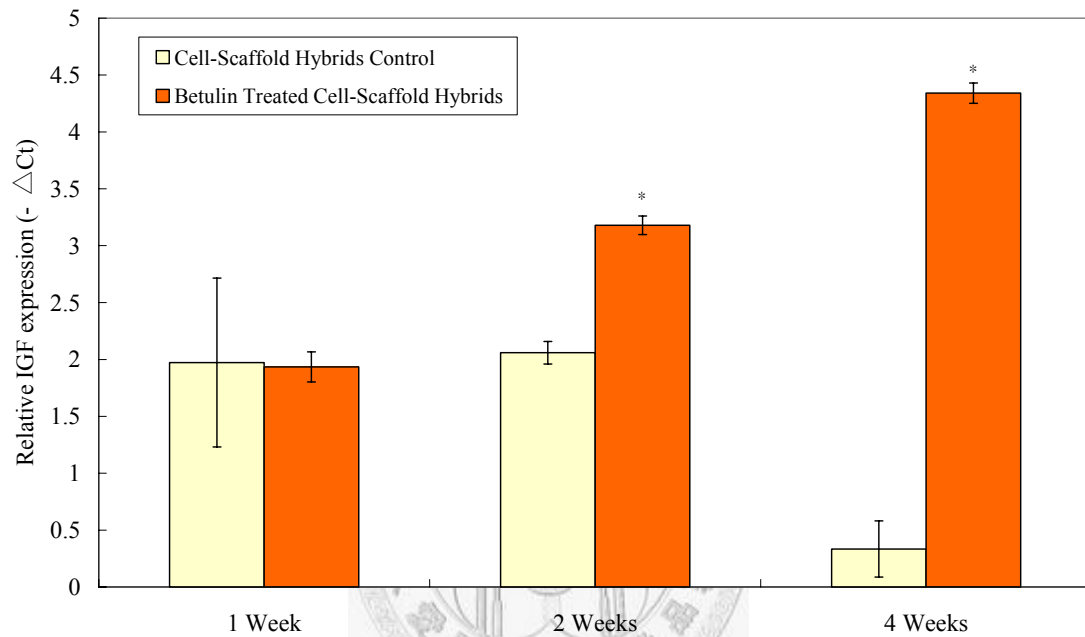
Figure 78 At the end of 1, 2, and 4-week, the values of $-\triangle Ct$ of relative IGF-1 gene expression were obtained. In the bar chart, $-\triangle Ct$ was shown by mean with S.D. (* means p-value<0.01).

4-2.5.5 mRNA Expression of Catabolic Cytokines

When chondrocytes cultured in the 3D environment, IL-1β expression was kept in a quite low level, and at the end of 1 and 2 weeks it was significantly lower then the control group (Figure 79).
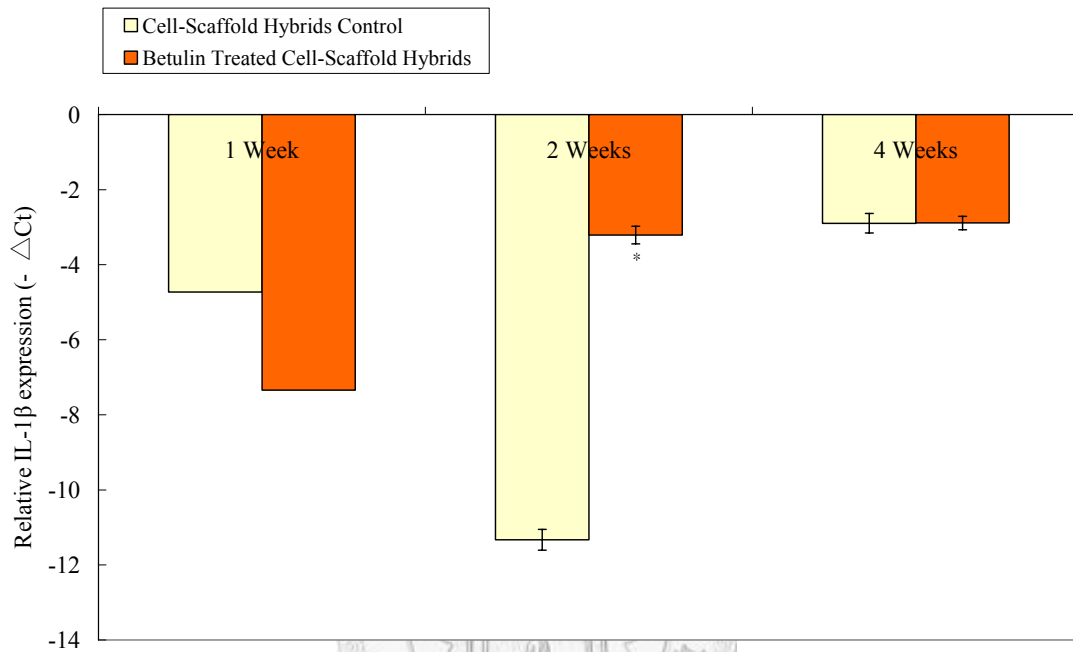
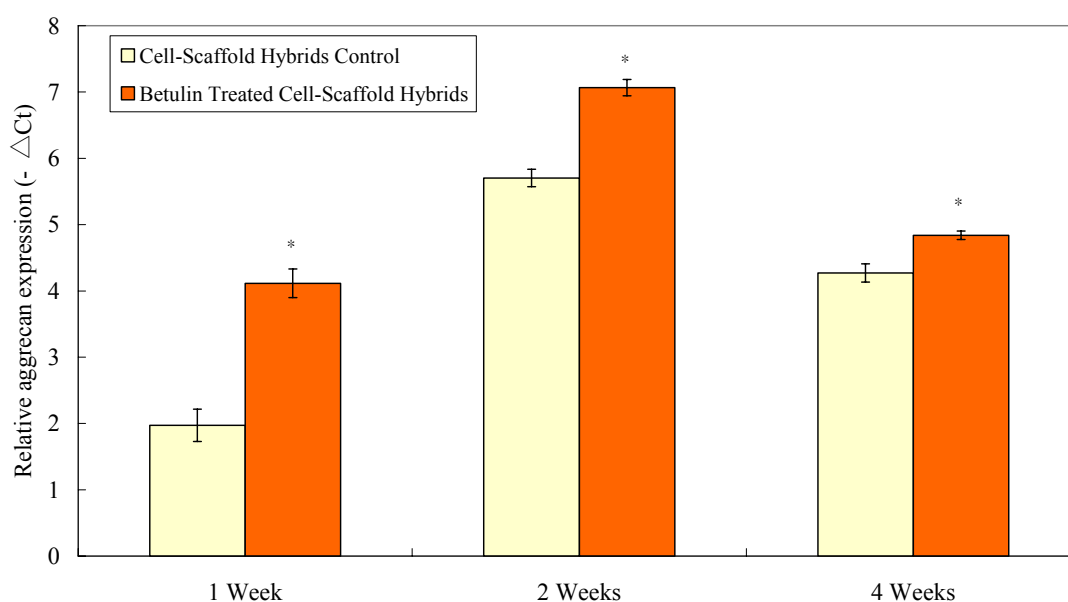**Figure 79** At the end of 1, 2, and 4-week, the values of $-\triangle Ct$ of relative IL-1β gene expression were obtained. In the bar chart, $-\triangle Ct$ was shown by mean with S.D. (* means p-value<0.01).

CHAPTER 5

# DISCUSSIONS

5-1 Two-dimensional Chondrocytes Culture

In aucubin treated experiment, our findings clearly showed that under the lowest concentration of aucubin treatment, the chondrocytes increased the expression of ECM-related mRNA, although the $O_2^{\bullet-}$ was not significantly scavenged under this concentration and the chondrocytes did not significantly increase in cell number. Because constantly expressing type II collagen is an important biomarker of articular cartilage, it showed that the in vitro cultured chondrocytes under this condition could maintain their phenotype. The expression of ECM-related mRNAs were further proved by histochemical and immunohistochemical staining.

The middle concentration of aucubin treated environment may be the worst environment to chondrocytes because it increased the expression of type I collagen which implied that the chondrocytes were on the way toward fibrosis. On the other hand, the decrease in MMP-2 mRNA expression seemed to be a positive phenomenon because the number of MMP-2 protein decreased in the ECM and hence prevented the degradation of gelatin-related macromolecules in the ECM. However, as we noted before, MMP-2 widely expresses in many noninflamed healthy connect tissue and to compare with the lack of increase in the expression of ECM-related mRNA, maybe the chondrocytes were in an unhealthy state.

Under the highest concentration of aucubin treatment, $O_2^{\bullet-}$ was significantly scavenged, but there were no significant increases in chondrocytes proliferation and the expression of ECM-related mRNAs, which may show that $O_2^{\bullet-}$ did not directly modulate the proliferation and the expression of ECM-related genes.

In betulin treated experiment, our findings clearly showed that under the lowest concentration of betulin treatment, $O_2^{\bullet -}$ was significantly scavenged and the number of chondrocytes was increased, which may show that by decreasing the amount of $O_2^{\bullet -}$, the replicative senescence of chondrocytes was slowed down. However, the mitochondrial respiratory activity, an indirect indicator of cell viability, decreased in this environment.

The middle concentration of betulin treated environment may be the best environment to chondrocytes because it not only significantly scavenged $O_2^{\bullet -}$, increased the number of chondrocytes, but also increased the expression of type II collagen. On the other hand, the MMP-2 mRNA expression also decreased in this environment. This result showed that the middle concentration of betulin is an effective protectant of chondrocytes against superoxide anion and maybe possessed chondrogenesis activity by increasing extracellular matrix mRNA.

Under the highest concentration of betulin treatment, despite there was no significant increase in the number of chondrocytes, $O_2^{\bullet -}$ was significantly scavenged and the expression of type II collagen and aggrecan mRNAs were increased. On the other hand, the MMP-2 mRNA expression also decreased in this environment. Comparing with the results of the lowest and middle concentration treatment of betulin, we can conclude that under an appropriate concentration range, betulin is an effective protectant of chondrocytes against superoxide anion and by focusing on the chemical structure of betulin, the antioxidant activity of betulin may rely on the resonance structure of chemicals.

Table 10 Summary of two-dimensional chondrocytes culture results

		Aucubin			Betulin		
		[L]	[M]	[H]	[L]	[M]	[H]
LDH		.	.	.	.	.	.
MTT		.	.	+	−	.	−
Total DNA		.	−	.	+	+	.
GAGs conc.		.	.	.	.	.	.
qPCR	type I / type II	. / +	+ / .	. / .	. / .	. / +	. / +
	Aggrecan / Decorin	+ / +	. / +	. / .	. / .	. / .	+ / .
	MMP-2 / TIMP-1	. / .	− / .	− / .	. / .	− / .	− / .
	SOX-9 / TGF-beta1	− / .	− / .	− / −	− / .	− / .	− / .
O$_2^-$ Scavenging		.	.	+	+	+	+

5-2 Three-dimensional Scaffold Culture

In three-dimensional scaffold culture environment, the results showed that no matter the cell-scaffold hybrids were cultured for 1, 2, or 4 weeks, the viability of chondrocytes significantly increased. Moreover, as long as the cell-scaffold hybrids were cultured, the cell number whereupon increased. Furthermore, the mRNA expression of type II collagen, aggrecan, BMP-7, and IGF-1 significantly increased after the cultivation of two weeks.

In two-week cultivation, ECM-related mRNAs expression was significantly increased, which was compatible with the result of DMMB assay, and the mRNA expression of type I collagen and type II collagen were significantly decreased, which suggested that the chondrocytes were neither on the way toward fibrosis nor hypertrophy. Moreover, although we did not know whether the mRNA expression of TIMP-2 was increased or decreased, the mRNA expression of MT1-MMP was significantly decreased. Because the activation of MMP-2 is tightly regulated by the expression of MT1-MMP, the mRNA expression of MMP-2 was decreased due to the decreased expression of MT1-MMP.

In four-week cultivation, the chondrocytes not only increased in their number but also increased their viability, which may infer that in the future application the *in vitro* three-dimensional cultivation of chondrocyte-scaffold hybrids should be maintained more than four weeks. The mRNA expression of type II collagen and aggrecan were significantly increased in this environment, and especially the mRNA expression of three kinds of growth factors were all increased, which suggested that the chondrocytes were well modulated under this environment. Also, the mRNA expression of MMP-2 was decreased here.

Table 11 Summary of three-dimensional scaffold culture results

		3D Tissue Engineering		
		1w	2w	4w
WST-1		+	+	+
Total DNA		.	.	+
GAGs conc.		.	+	.
qPCR	type I	.	−	−
	type II	+	+	+
	type X	−	−	.
	Aggrecan	+	+	+
	Decorin	+	+	.
	TIMP-1	.	.	.
	MMP-2	−	−	−
	MT1-MMP	.	−	.
	TGF-beta1	.	.	+
	BMP-7	.	+	+
	IGF-1	.	+	+
	IL-1beta	.	−	.
	SOX-9	.	.	.

CHAPTER 6

CONCLUSIONS

In two-dimensional chondrocytes culture, both aucubin and betulin could effectively promote the mRNA expression of ECM and inhibit the mRNA expression related with ECM degradation at appropriate concentration, and the ability of $O_2^{\bullet-}$ scavenging made aucubin and betulin as protectants of chondrocytes, which would stimulate chondrocyte proliferation and maintain the basic chondrocyte activities.

In three-dimensional scaffold culture environment, betulin can significantly stimulate chondrocyte proliferation and maintain the basic chondrocyte activities until four-week cultivation, which suggested that in the future application the *in vitro* three-dimensional cultivation of chondrocyte-scaffold hybrids should be maintained more than four weeks, and of course the addition of 0.32μg/ml of betulin into the cultured environment possessed positive effects toward chondrocytes and the whole cartilage-mimic tissue.

REFERENCES

1. F.W. Bora, Jr. and G. Miller, Joint physiology, cartilage metabolism, and the etiology of osteoarthritis. Hand Clin, 1987. **3**(3): p. 325-36.

2. K.E. Kuettner, Biochemistry of articular cartilage in health and disease. Clin Biochem, 1992. **25**(3): p. 155-63.

3. P. Bursac, C.V. McGrath, S.R. Eisenberg, and D. Stamenovic, A microstructural model of elastostatic properties of articular cartilage in confined compression. J Biomech Eng, 2000. **122**(4): p. 347-53.

4. H.A. Wieland, M. Michaelis, B.J. Kirschbaum, and K.A. Rudolphi, Osteoarthritis - an untreatable disease? Nat Rev Drug Discov, 2005. **4**(4): p. 331-44.

5. T. Walles, B. Giere, P. Macchiarini, and H. Mertsching, Expansion of chondrocytes in a three-dimensional matrix for tracheal tissue engineering. Ann Thorac Surg, 2004. **78**(2): p. 444-8; discussion 448-9.

6. W.M. Burch and K.S. McCarty, Jr., Hormonal stimulation of avian embryonic cartilage growth in vitro: Histologic and ultrastructural features. In Vitro, 1984. **20**(4): p. 329-38.

7. R.F. Loeser, Integrin-mediated attachment of articular chondrocytes to extracellular matrix proteins. Arthritis Rheum, 1993. **36**(8): p. 1103-10.

8. K. Sudo, M. Kanno, K. Miharada, S. Ogawa, T. Hiroyama, K. Saijo, and Y. Nakamura, Mesenchymal progenitors able to differentiate into osteogenic, chondrogenic, and/or adipogenic cells in vitro are present in most primary fibroblast-like cell populations. Stem Cells, 2007. **25**(7): p. 1610-7.

9. H. Claassen, C. Cellarius, K.E. Scholz-Ahrens, J. Schrezenmeir, C.C. Gluer, M. Schunke, and B. Kurz, Extracellular matrix changes in knee joint cartilage following bone-active drug treatment. Cell Tissue Res, 2006: p. 1-11.

10. J.A. Buckwalter, H.J. Mankin, and A.J. Grodzinsky, Articular cartilage and osteoarthritis. Instr Course Lect, 2005. **54**: p. 465-80.

11. J.A. Buckwalter and H.J. Mankin, Articular cartilage: Tissue design and chondrocyte-matrix interactions. Instr Course Lect, 1998. **47**: p. 477-86.

12. H.C. Blair, M. Zaidi, and P.H. Schlesinger, Mechanisms balancing skeletal matrix synthesis and degradation. Biochem J, 2002. **364**(Pt 2): p. 329-41.

13. H. Lipshitz, R. Etheredge, 3rd, and M.J. Glimcher, In vitro wear of articular cartilage. J Bone Joint Surg Am, 1975. **57**(4): p. 527-34.

14. F. Paulsen and B. Tillmann, Composition of the extracellular matrix in human cricoarytenoid joint articular cartilage. Arch Histol Cytol, 1999. **62**(2): p. 149-63.

15. R.J. Fernandes, M. Weis, M.A. Scott, R.E. Seegmiller, and D.R. Eyre, Collagen xi chain misassembly in cartilage of the chondrodysplasia (cho) mouse. Matrix Biol, 2007.

16. L. Rosenberg, Cartilage proteoglycans. Fed Proc, 1973. **32**(4): p. 1467-73.

17. J.A. Buckwalter and L.C. Rosenberg, Electron microscopic studies of cartilage proteoglycans. Electron Microsc Rev, 1988. **1**(1): p. 87-112.

18. J. Fischer, H. Lullmann, and R. Lullmann-Rauch, Drug-induced lysosomal storage of sulphated glycosaminoglycans. Gen Pharmacol, 1996. **27**(8): p. 1317-24.

19. M. Jensen, P. Birch Hansen, S. Murdan, S. Frokjaer, and A.T. Florence, Loading into and electro-stimulated release of peptides and proteins from chondroitin 4-sulphate hydrogels. Eur J Pharm Sci, 2002. **15**(2): p. 139-48.

20. S. Lohmander, C.A. Antonopoulos, and U. Friberg, Chemical and metabolic heterogeneity of chondroitin sulfate and keratin sulfate in guinea pig cartilage and nucleus pulposus. Biochim Biophys Acta, 1973. **304**(2): p. 430-48.

21. S.M. Bychkov, E.V. Vinogradova, I.N. Mikhailov, and V.N. Kharlamova, Electron microscopic study of isolated proteoglycans. Biull Eksp Biol Med, 1979. **87**(2): p. 132-4.

22. L. Wachsmuth, S. Soder, Z. Fan, F. Finger, and T. Aigner, Immunolocalization of matrix proteins in different human cartilage subtypes. Histol Histopathol, 2006. **21**(5): p. 477-85.

23. D.R. Eyre and H. Muir, The distribution of different molecular species of collagen in fibrous, elastic and hyaline cartilages of the pig. Biochem J, 1975. **151**(3): p. 595-602.

24. R.M. Williams, W.R. Zipfel, M.L. Tinsley, and C.E. Farnum, Solute transport in growth plate cartilage: In vitro and in vivo. Biophys J, 2007. **93**(3): p. 1039-50.

25. J.W. Calvert, K. Brenner, M. DaCosta-Iyer, G.R. Evans, and R.K. Daniel, Histological analysis of human diced cartilage grafts. Plast Reconstr Surg, 2006. **118**(1): p. 230-6.

26. C.A. Pezowicz, P.A. Robertson, and N.D. Broom, The structural basis of interlamellar cohesion in the intervertebral disc wall. J Anat, 2006. **208**(3): p. 317-30.

27. R. Putz and M. Muller-Gerbl, Anatomic characteristics of the pelvic girdle. Unfallchirurg, 1992. **95**(4): p. 164-7.

28. A. Gigante, M. Marinelli, C. Chillemi, and F. Greco, Fibrous cartilage in the rotator cuff: A pathogenetic mechanism of tendon tear? J Shoulder Elbow Surg, 2004. **13**(3): p. 328-32.

29. M. Egerbacher, R. Krestan, and P. Bock, Morphology, histochemistry, and differentiation of the cat's epiglottic cartilage: A supporting organ composed of elastic cartilage, fibrous cartilage, myxoid tissue, and fat tissue. Anat Rec, 1995. **242**(4): p. 471-82.

30. A. Naumann, J.E. Dennis, A. Awadallah, D.A. Carrino, J.M. Mansour, E. Kastenbauer, and A.I. Caplan, Immunochemical and mechanical characterization of cartilage subtypes in rabbit. J Histochem Cytochem, 2002. **50**(8): p. 1049-58.

31. S.M. Mithieux and A.S. Weiss, Elastin. Adv Protein Chem, 2005. **70**: p. 437-61.

32. D.R. Eyre, Collagens and cartilage matrix homeostasis. Clin Orthop Relat Res, 2004(427 Suppl): p. S118-22.

33. S.P. Scully, J.W. Lee, P.M.A. Ghert, and W. Qi, The role of the extracellular matrix in articular chondrocyte regulation. Clin Orthop Relat Res, 2001(391 Suppl): p. S72-89.

34. F.O. Sangiorgi, V. Benson-Chanda, W.J. de Wet, M.E. Sobel, and F. Ramirez, Analysis of cdna and genomic clones coding for the pro alpha 1 chain of calf type ii collagen. Nucleic Acids Res, 1985. **13**(8): p. 2815-26.

35. G. Zernia and D. Huster, Collagen dynamics in articular cartilage under osmotic pressure. NMR Biomed, 2006. **19**(8): p. 1010-9.

36. M. Aumailley, K. Mann, H. von der Mark, and R. Timpl, Cell attachment properties of collagen type vi and arg-gly-asp dependent binding to its alpha 2(vi) and alpha 3(vi) chains. Exp Cell Res, 1989. **181**(2): p. 463-74.

37. F.H. Silver and A.I. Glasgold, Cartilage wound healing. An overview. Otolaryngol Clin North Am, 1995. **28**(5): p. 847-64.

38. R.E. Topping, M.E. Bolander, and G. Balian, Type x collagen in fracture callus and the effects of experimental diabetes. Clin Orthop Relat Res, 1994(308): p. 220-8.

39. H.M. Kronenberg, Developmental regulation of the growth plate. Nature, 2003. **423**(6937): p. 332-6.

40. K.S. Mix, M.B. Sporn, C.E. Brinckerhoff, D. Eyre, and D.J. Schurman, Novel inhibitors of matrix metalloproteinase gene expression as potential therapies for arthritis. Clin Orthop Relat Res, 2004(427 Suppl): p. S129-37.

41. D.S. Bramono, J.C. Richmond, P.P. Weitzel, D.L. Kaplan, and G.H. Altman, Matrix metalloproteinases and their clinical applications in orthopaedics. Clin Orthop Relat Res, 2004(428): p. 272-85.

42. K. Naito, M. Takahashi, K. Kushida, M. Suzuki, T. Ohishi, M. Miura, T. Inoue, and A. Nagano, Measurement of matrix metalloproteinases (mmps) and

tissue inhibitor of metalloproteinases-1 (timp-1) in patients with knee osteoarthritis: Comparison with generalized osteoarthritis. Rheumatology (Oxford), 1999. **38**(6): p. 510-5.

43. T. Hayakawa, Multiple functions of tissue inhibitors of metalloproteinases (timps): A new aspect involving osteoclastic bone resorption. J Bone Miner Metab, 2002. **20**(1): p. 1-13.

44. L.B. Creemers, I.D. Jansen, A.J. Docherty, J.J. Reynolds, W. Beertsen, and V. Everts, Gelatinase a (mmp-2) and cysteine proteinases are essential for the degradation of collagen in soft connective tissue. Matrix Biol, 1998. **17**(1): p. 35-46.

45. C. Feliciani, P. Vitullo, G. D'Orazi, R. Palmirotta, P. Amerio, S.M. Pour, G. Coscione, P.L. Amerio, and A. Modesti, The 72-kda and the 92-kda gelatinases, but not their inhibitors timp-1 and timp-2, are expressed in early psoriatic lesions. Exp Dermatol, 1997. **6**(6): p. 321-7.

46. Y. Henrotin, B. Kurz, and T. Aigner, Oxygen and reactive oxygen species in cartilage degradation: Friends or foes? Osteoarthritis Cartilage, 2005. **13**(8): p. 643-54.

47. C.T. Brighton and R.B. Heppenstall, Oxygen tension in zones of the epiphyseal plate, the metaphysis and diaphysis. An in vitro and in vivo study in rats and rabbits. J Bone Joint Surg Am, 1971. **53**(4): p. 719-28.

48. M. Safran and W.G. Kaelin, Jr., Hif hydroxylation and the mammalian oxygen-sensing pathway. J Clin Invest, 2003. **111**(6): p. 779-83.

49. R. Rajpurohit, C.J. Koch, Z. Tao, C.M. Teixeira, and I.M. Shapiro, Adaptation of chondrocytes to low oxygen tension: Relationship between hypoxia and cellular metabolism. J Cell Physiol, 1996. **168**(2): p. 424-32.

50. P. Otte, Basic cell metabolism of articular cartilage. Manometric studies. Z Rheumatol, 1991. **50**(5): p. 304-12.

51. C. Domm, M. Schunke, K. Christesen, and B. Kurz, Redifferentiation of dedifferentiated bovine articular chondrocytes in alginate culture under low oxygen tension. Osteoarthritis Cartilage, 2002. **10**(1): p. 13-22.

52. U. Hansen, M. Schunke, C. Domm, N. Ioannidis, J. Hassenpflug, T. Gehrke, and B. Kurz, Combination of reduced oxygen tension and intermittent hydrostatic pressure: A useful tool in articular cartilage tissue engineering. J Biomech, 2001. **34**(7): p. 941-9.

53. B. Kurz, C. Domm, M. Jin, R. Sellckau, and M. Schunke, Tissue engineering of articular cartilage under the influence of collagen i/iii membranes and low oxygen tension. Tissue Eng, 2004. **10**(7-8): p. 1277-86.

54. S. Saini and T.M. Wick, Effect of low oxygen tension on tissue-engineered

cartilage construct development in the concentric cylinder bioreactor. Tissue Eng, 2004. **10**(5-6): p. 825-32.

55.   K. Scherer, M. Schunke, R. Sellckau, J. Hassenpflug, and B. Kurz, The influence of oxygen and hydrostatic pressure on articular chondrocytes and adherent bone marrow cells in vitro. Biorheology, 2004. **41**(3-4): p. 323-33.

56.   Z. Nevo, A. Beit-Or, and Y. Eilam, Slowing down aging of cultured embryonal chick chondrocytes by maintenance under lowered oxygen tension. Mech Ageing Dev, 1988. **45**(2): p. 157-65.

57.   G. Martin, R. Andriamanalijaona, S. Grassel, R. Dreier, M. Mathy-Hartert, P. Bogdanowicz, K. Boumediene, Y. Henrotin, P. Bruckner, and J.P. Pujol, Effect of hypoxia and reoxygenation on gene expression and response to interleukin-1 in cultured articular chondrocytes. Arthritis Rheum, 2004. **50**(11): p. 3549-60.

58.   H.A. Shenkin, Acute subdural hematoma. Review of 39 consecutive cases with high incidence of cortical artery rupture. J Neurosurg, 1982. **57**(2): p. 254-7.

59.   S.B. Trippel, S.C. Ghivizzani, and A.J. Nixon, Gene-based approaches for the repair of articular cartilage. Gene Ther, 2004. **11**(4): p. 351-9.

60.   J. Raghunath, H.J. Salacinski, K.M. Sales, P.E. Butler, and A.M. Seifalian, Advancing cartilage tissue engineering: The application of stem cell technology. Curr Opin Biotechnol, 2005. **16**(5): p. 503-9.

61.   E. de Bri, K. Jonsson, F.P. Reinholt, and O. Svensson, Focal destruction and remodeling in guinea pig arthrosis. Acta Orthop Scand, 1996. **67**(5): p. 498-504.

62.   F. Shapiro, S. Koide, and M.J. Glimcher, Cell origin and differentiation in the repair of full-thickness defects of articular cartilage. J Bone Joint Surg Am, 1993. **75**(4): p. 532-53.

63.   A.O. Adebajo, Osteoarthritis. Baillieres Clin Rheumatol, 1995. **9**(1): p. 65-74.

64.   T. Aigner, S.I. Vornehm, G. Zeiler, J. Dudhia, K. von der Mark, and M.T. Bayliss, Suppression of cartilage matrix gene expression in upper zone chondrocytes of osteoarthritic cartilage. Arthritis Rheum, 1997. **40**(3): p. 562-9.

65.   J.A. Martin and J.A. Buckwalter, Aging, articular cartilage chondrocyte senescence and osteoarthritis. Biogerontology, 2002. **3**(5): p. 257-64.

66.   K. Yudoh, T. Nguyen, H. Nakamura, K. Hongo-Masuko, T. Kato, and K. Nishioka, Potential involvement of oxidative stress in cartilage senescence and development of osteoarthritis: Oxidative stress induces chondrocyte telomere instability and downregulation of chondrocyte function. Arthritis Res Ther,

2005. **7**(2): p. R380-91.

67. Y.E. Henrotin, P. Bruckner, and J.P. Pujol, The role of reactive oxygen species in homeostasis and degradation of cartilage. Osteoarthritis Cartilage, 2003. **11**(10): p. 747-55.

68. H. Muir, The chondrocyte, architect of cartilage. Biomechanics, structure, function and molecular biology of cartilage matrix macromolecules. Bioessays, 1995. **17**(12): p. 1039-48.

69. K.H. Falchuk, E.J. Goetzl, and J.P. Kulka, Respiratory gases of synovial fluids. An approach to synovial tissue circulatory-metabolic imbalance in rheumatoid arthritis. Am J Med, 1970. **49**(2): p. 223-31.

70. T. Aigner, J. Rose, J. Martin, and J. Buckwalter, Aging theories of primary osteoarthritis: From epidemiology to molecular biology. Rejuvenation Res, 2004. **7**(2): p. 134-45.

71. H.M. Frost, Cybernetic aspects of bone modeling and remodeling, with special reference to osteoporosis and whole-bone strength. Am J Hum Biol, 2001. **13**(2): p. 235-48.

72. A. Schmidt, Harada, S. & Rodan, G.A., Principles of bone biology 2002: p. 1455-1466.

73. H.A. Awad, M.Q. Wickham, H.A. Leddy, J.M. Gimble, and F. Guilak, Chondrogenic differentiation of adipose-derived adult stem cells in agarose, alginate, and gelatin scaffolds. Biomaterials, 2004. **25**(16): p. 3211-22.

74. P. Bianco and P.G. Robey, Stem cells in tissue engineering. Nature, 2001. **414**(6859): p. 118-21.

75. C.R. Nuttelman, M.C. Tripodi, and K.S. Anseth, In vitro osteogenic differentiation of human mesenchymal stem cells photoencapsulated in peg hydrogels. J Biomed Mater Res A, 2004. **68**(4): p. 773-82.

76. M. Risbud, Tissue engineering: Implications in the treatment of organ and tissue defects. Biogerontology, 2001. **2**(2): p. 117-25.

77. M.R. Homicz, B.L. Schumacher, R.L. Sah, and D. Watson, Effects of serial expansion of septal chondrocytes on tissue-engineered neocartilage composition. Otolaryngol Head Neck Surg, 2002. **127**(5): p. 398-408.

78. B. Dozin, M. Malpeli, L. Camardella, R. Cancedda, and A. Pietrangelo, Response of young, aged and osteoarthritic human articular chondrocytes to inflammatory cytokines: Molecular and cellular aspects. Matrix Biol, 2002. **21**(5): p. 449-59.

79. V. Sottile, C. Halleux, F. Bassilana, H. Keller, and K. Seuwen, Stem cell characteristics of human trabecular bone-derived cells. Bone, 2002. **30**(5): p. 699-704.

80. O.K. Lee, T.K. Kuo, W.M. Chen, K.D. Lee, S.L. Hsieh, and T.H. Chen, Isolation of multipotent mesenchymal stem cells from umbilical cord blood. Blood, 2004. **103**(5): p. 1669-75.

81. M. Miura, S. Gronthos, M. Zhao, B. Lu, L.W. Fisher, P.G. Robey, and S. Shi, Shed: Stem cells from human exfoliated deciduous teeth. Proc Natl Acad Sci U S A, 2003. **100**(10): p. 5807-12.

82. P.H. Krebsbach and P.G. Robey, Dental and skeletal stem cells: Potential cellular therapeutics for craniofacial regeneration. J Dent Educ, 2002. **66**(6): p. 766-73.

83. M. Sittinger, D.W. Hutmacher, and M.V. Risbud, Current strategies for cell delivery in cartilage and bone regeneration. Curr Opin Biotechnol, 2004. **15**(5): p. 411-8.

84. M.V. Risbud and M. Sittinger, Tissue engineering: Advances in in vitro cartilage generation. Trends Biotechnol, 2002. **20**(8): p. 351-6.

85. V.F. Sechriest, Y.J. Miao, C. Niyibizi, A. Westerhausen-Larson, H.W. Matthew, C.H. Evans, F.H. Fu, and J.K. Suh, Gag-augmented polysaccharide hydrogel: A novel biocompatible and biodegradable material to support chondrogenesis. J Biomed Mater Res, 2000. **49**(4): p. 534-41.

86. L.A. Solchaga, V.M. Goldberg, and A.I. Caplan, Cartilage regeneration using principles of tissue engineering. Clin Orthop Relat Res, 2001(391 Suppl): p. S161-70.

87. M. Filip, I. Paduraru, L. Jerca, F. Filip, and A. Saramet, Oxygen biochemistry. I. Reactive species of reduced oxygen and endogenous sources. Rev Med Chir Soc Med Nat Iasi, 1992. **96**(3-4): p. 289-92.

88. L. Castro and B.A. Freeman, Reactive oxygen species in human health and disease. Nutrition, 2001. **17**(2): p. 161, 163-5.

89. N.J. Holbrook and S. Ikeyama, Age-related decline in cellular response to oxidative stress: Links to growth factor signaling pathways with common defects. Biochem Pharmacol, 2002. **64**(5-6): p. 999-1005.

90. Y. Liu, G. Fiskum, and D. Schubert, Generation of reactive oxygen species by the mitochondrial electron transport chain. J Neurochem, 2002. **80**(5): p. 780-7.

91. J.F. Turrens, Mitochondrial formation of reactive oxygen species. J Physiol, 2003. **552**(Pt 2): p. 335-44.

92. S.I. Liochev and I. Fridovich, Superoxide and iron: Partners in crime. IUBMB Life, 1999. **48**(2): p. 157-61.

93. J.S. Beckman and W.H. Koppenol, Nitric oxide, superoxide, and peroxynitrite: The good, the bad, and ugly. Am J Physiol, 1996. **271**(5 Pt 1): p. C1424-37.

94. H.E. Seifried, D.E. Anderson, E.I. Fisher, and J.A. Milner, A review of the interaction among dietary antioxidants and reactive oxygen species. J Nutr Biochem, 2007.

95. T. Finkel, Reactive oxygen species and signal transduction. IUBMB Life, 2001. **52**(1-2): p. 3-6.

96. Y.Y. Lo, J.A. Conquer, S. Grinstein, and T.F. Cruz, Interleukin-1 beta induction of c-fos and collagenase expression in articular chondrocytes: Involvement of reactive oxygen species. J Cell Biochem, 1998. **69**(1): p. 19-29.

97. R.M. Clancy, P.F. Gomez, and S.B. Abramson, Nitric oxide sustains nuclear factor kappab activation in cytokine-stimulated chondrocytes. Osteoarthritis Cartilage, 2004. **12**(7): p. 552-8.

98. J.M. Mates, C. Perez-Gomez, and I. Nunez de Castro, Antioxidant enzymes and human diseases. Clin Biochem, 1999. **32**(8): p. 595-603.

99. Z.Q. Liu and H.Y. Shan, Cholesterol, not polyunsaturated fatty acids, is target molecule in oxidation induced by reactive oxygen species in membrane of human erythrocytes. Cell Biochem Biophys, 2006. **45**(2): p. 185-93.

100. J.M. McCord and I. Fridovich, Superoxide dismutase: The first twenty years (1968-1988). Free Radic Biol Med, 1988. **5**(5-6): p. 363-9.

101. K. Oracz, M. Bouteau Hel, J.M. Farrant, K. Cooper, M. Belghazi, C. Job, D. Job, F. Corbineau, and C. Bailly, Ros production and protein oxidation as a novel mechanism for seed dormancy alleviation. Plant J, 2007. **50**(3): p. 452-65.

102. T.S. Hiran, P.J. Moulton, and J.T. Hancock, Detection of superoxide and nadph oxidase in porcine articular chondrocytes. Free Radic Biol Med, 1997. **23**(5): p. 736-43.

103. P.J. Moulton, T.S. Hiran, M.B. Goldring, and J.T. Hancock, Detection of protein and mrna of various components of the nadph oxidase complex in an immortalized human chondrocyte line. Br J Rheumatol, 1997. **36**(5): p. 522-9.

104. C.I. Suh, N.D. Stull, X.J. Li, W. Tian, M.O. Price, S. Grinstein, M.B. Yaffe, S. Atkinson, and M.C. Dinauer, The phosphoinositide-binding protein p40phox activates the nadph oxidase during fcgammaiia receptor-induced phagocytosis. J Exp Med, 2006. **203**(8): p. 1915-25.

105. O. Vajragupta, C. Boonyarat, Y. Murakami, M. Tohda, K. Musatmoto, A.J. Olson, and H. Watanabe, A novel neuroprotective agent with antioxidant and nitric oxide synthase inhibitory action. Free Radic Res, 2006. **40**(7): p. 685-95.

106. N. Basso and J.N. Heersche, Effects of hind limb unloading and reloading on nitric oxide synthase expression and apoptosis of osteocytes and chondrocytes.

Bone, 2006. **39**(4): p. 807-14.

107. K. Yamazaki, K. Fukuda, M. Matsukawa, F. Hara, T. Matsushita, N. Yamamoto, K. Yoshida, H. Munakata, and C. Hamanishi, Cyclic tensile stretch loaded on bovine chondrocytes causes depolymerization of hyaluronan: Involvement of reactive oxygen species. Arthritis Rheum, 2003. **48**(11): p. 3151-8.

108. N. Jallali, H. Ridha, C. Thrasivoulou, P. Butler, and T. Cowen, Modulation of intracellular reactive oxygen species level in chondrocytes by igf-1, fgf, and tgf-beta1. Connect Tissue Res, 2007. **48**(3): p. 149-58.

109. J.M. Mates, Effects of antioxidant enzymes in the molecular control of reactive oxygen species toxicology. Toxicology, 2000. **153**(1-3): p. 83-104.

110. M.D. Carlo, Jr. and R.F. Loeser, Increased oxidative stress with aging reduces chondrocyte survival: Correlation with intracellular glutathione levels. Arthritis Rheum, 2003. **48**(12): p. 3419-30.

111. H.Z. Chae, S.W. Kang, and S.G. Rhee, Isoforms of mammalian peroxiredoxin that reduce peroxides in presence of thioredoxin. Methods Enzymol, 1999. **300**: p. 219-26.

112. G.N. Landis and J. Tower, Superoxide dismutase evolution and life span regulation. Mech Ageing Dev, 2005. **126**(3): p. 365-79.

113. S.T. Deahl, 2nd, L.W. Oberley, T.D. Oberley, and J.H. Elwell, Immunohistochemical identification of superoxide dismutases, catalase, and glutathione-s-transferases in rat femora. J Bone Miner Res, 1992. **7**(2): p. 187-98.

114. F. Ursini and A. Bindoli, The role of selenium peroxidases in the protection against oxidative damage of membranes. Chem Phys Lipids, 1987. **44**(2-4): p. 255-76.

115. T. Finkel and N.J. Holbrook, Oxidants, oxidative stress and the biology of ageing. Nature, 2000. **408**(6809): p. 239-47.

116. M.L. Tiku, G.T. Allison, K. Naik, and S.K. Karry, Malondialdehyde oxidation of cartilage collagen by chondrocytes. Osteoarthritis Cartilage, 2003. **11**(3): p. 159-66.

117. R.A. Greenwald and W.W. Moy, Inhibition of collagen gelation by action of the superoxide radical. Arthritis Rheum, 1979. **22**(3): p. 251-9.

118. J.C. Monboisse, P. Braquet, A. Randoux, and J.P. Borel, Non-enzymatic degradation of acid-soluble calf skin collagen by superoxide ion: Protective effect of flavonoids. Biochem Pharmacol, 1983. **32**(1): p. 53-8.

119. J.C. Monboisse and J.P. Borel, Oxidative damage to collagen. Exs, 1992. **62**: p. 323-7.

120. H. Saari, Y.T. Konttinen, C. Friman, and T. Sorsa, Differential effects of reactive oxygen species on native synovial fluid and purified human umbilical cord hyaluronate. Inflammation, 1993. **17**(4): p. 403-15.

121. F.A. van de Loo, O.J. Arntz, F.H. van Enckevort, P.L. van Lent, and W.B. van den Berg, Reduced cartilage proteoglycan loss during zymosan-induced gonarthritis in nos2-deficient mice and in anti-interleukin-1-treated wild-type mice with unabated joint inflammation. Arthritis Rheum, 1998. **41**(4): p. 634-46.

122. R.K. Studer, R. Bergman, T. Stubbs, and K. Decker, Chondrocyte response to growth factors is modulated by p38 mitogen-activated protein kinase inhibition. Arthritis Res Ther, 2004. **6**(1): p. R56-R64.

123. M.S. Hickery and M.T. Bayliss, Interleukin-1 induced nitric oxide inhibits sulphation of glycosaminoglycan chains in human articular chondrocytes. Biochim Biophys Acta, 1998. **1425**(2): p. 282-90.

124. G.A. Murrell, D. Jang, and R.J. Williams, Nitric oxide activates metalloprotease enzymes in articular cartilage. Biochem Biophys Res Commun, 1995. **206**(1): p. 15-21.

125. H. Burkhardt, M. Schwingel, H. Menninger, H.W. Macartney, and H. Tschesche, Oxygen radicals as effectors of cartilage destruction. Direct degradative effect on matrix components and indirect action via activation of latent collagenase from polymorphonuclear leukocytes. Arthritis Rheum, 1986. **29**(3): p. 379-87.

126. F. Shabani, J. McNeil, and L. Tippett, The oxidative inactivation of tissue inhibitor of metalloproteinase-1 (timp-1) by hypochlorous acid (hoci) is suppressed by anti-rheumatic drugs. Free Radic Res, 1998. **28**(2): p. 115-23.

127. J.H. Suh, H. Wang, R.M. Liu, J. Liu, and T.M. Hagen, (r)-alpha-lipoic acid reverses the age-related loss in gsh redox status in post-mitotic tissues: Evidence for increased cysteine requirement for gsh synthesis. Arch Biochem Biophys, 2004. **423**(1): p. 126-35.

128. J.A. Martin and J.A. Buckwalter, Telomere erosion and senescence in human articular cartilage chondrocytes. J Gerontol A Biol Sci Med Sci, 2001. **56**(4): p. B172-9.

129. L. Liu, J.R. Trimarchi, P. Navarro, M.A. Blasco, and D.L. Keefe, Oxidative stress contributes to arsenic-induced telomere attrition, chromosome instability, and apoptosis. J Biol Chem, 2003. **278**(34): p. 31998-2004.

130. M.L. Tiku, R. Shah, and G.T. Allison, Evidence linking chondrocyte lipid peroxidation to cartilage matrix protein degradation. Possible role in cartilage aging and the pathogenesis of osteoarthritis. J Biol Chem, 2000. **275**(26): p.

20069-76.

131. M. Kirsch, H.G. Korth, R. Sustmann, and H. de Groot, The pathobiochemistry of nitrogen dioxide. Biol Chem, 2002. **383**(3-4): p. 389-99.

132. V. Yermilov, J. Rubio, and H. Ohshima, Formation of 8-nitroguanine in DNA treated with peroxynitrite in vitro and its rapid removal from DNA by depurination. FEBS Lett, 1995. **376**(3): p. 207-10.

133. G. Kopsidas, S.A. Kovalenko, J.M. Kelso, and A.W. Linnane, An age-associated correlation between cellular bioenergy decline and mtdna rearrangements in human skeletal muscle. Mutat Res, 1998. **421**(1): p. 27-36.

134. G.C. Kujoth, A. Hiona, T.D. Pugh, S. Someya, K. Panzer, S.E. Wohlgemuth, T. Hofer, A.Y. Seo, R. Sullivan, W.A. Jobling, J.D. Morrow, H. Van Remmen, J.M. Sedivy, T. Yamasoba, M. Tanokura, R. Weindruch, C. Leeuwenburgh, and T.A. Prolla, Mitochondrial DNA mutations, oxidative stress, and apoptosis in mammalian aging. Science, 2005. **309**(5733): p. 481-4.

135. G.M. Coopper, The cell. A molecular approach. Second edition. ASM Associates (Washington), 2000.

136. D.D.D.L. K. Kühn, S. Hashimoto and M. Lotz, Cell death in cartilage. Osteoarthritis Cartilage., 2004.

137. C.T. Chen, N. Burton-Wurster, C. Borden, K. Hueffer, S.E. Bloom, and G. Lust, Chondrocyte necrosis and apoptosis in impact damaged articular cartilage. J Orthop Res, 2001. **19**(4): p. 703-11.

138. T. Aigner, M. Hemmel, D. Neureiter, P.M. Gebhard, G. Zeiler, T. Kirchner, and L. McKenna, Apoptotic cell death is not a widespread phenomenon in normal aging and osteoarthritis human articular knee cartilage: A study of proliferation, programmed cell death (apoptosis), and viability of chondrocytes in normal and osteoarthritic human knee cartilage. Arthritis Rheum, 2001. **44**(6): p. 1304-12.

139. F.J. Blanco, R. Guitian, E. Vazquez-Martul, F.J. de Toro, and F. Galdo, Osteoarthritis chondrocytes die by apoptosis. A possible pathway for osteoarthritis pathology. Arthritis Rheum, 1998. **41**(2): p. 284-9.

140. F.J. Blanco, R.L. Ochs, H. Schwarz, and M. Lotz, Chondrocyte apoptosis induced by nitric oxide. Am J Pathol, 1995. **146**(1): p. 75-85.

141. M. Del Carlo, Jr. and R.F. Loeser, Nitric oxide-mediated chondrocyte cell death requires the generation of additional reactive oxygen species. Arthritis Rheum, 2002. **46**(2): p. 394-403.

142. B. Kurz, A. Lemke, M. Kehn, C. Domm, P. Patwari, E.H. Frank, A.J. Grodzinsky, and M. Schunke, Influence of tissue maturation and antioxidants on the apoptotic response of articular cartilage after injurious compression.

Arthritis Rheum, 2004. **50**(1): p. 123-30.

143. T.D. Spector and A.J. MacGregor, Risk factors for osteoarthritis: Genetics. Osteoarthritis Cartilage, 2004. **12 Suppl A**: p. S39-44.

144. M.J. Wu, J.H. Yen, L. Wang, and C.Y. Weng, Antioxidant activity of porcelainberry (ampelopsis brevipedunculata (maxim.) trautv.). Am J Chin Med, 2004. **32**(5): p. 681-93.

145. M. Galvez, C. Martin-Cordero, P.J. Houghton, and M.J. Ayuso, Antioxidant activity of plantago bellardii all. Phytother Res, 2005. **19**(12): p. 1074-6.

146. N. Mitchell and N. Shepard, The resurfacing of adult rabbit articular cartilage by multiple perforations through the subchondral bone. J Bone Joint Surg Am, 1976. **58**(2): p. 230-3.

147. M.J. Glade, Y.S. Kanwar, and T.J. Hefley, Enzymatic isolation of chondrocytes from immature rabbit articular cartilage and maintenance of phenotypic expression in culture. J Bone Miner Res, 1991. **6**(3): p. 217-26.

148. D.N. Hu, P.Y. Yang, M.C. Ku, C.H. Chu, A.Y. Lim, and M.H. Hwang, Isolation and cultivation of human articular chondrocytes. Kaohsiung J Med Sci, 2002. **18**(3): p. 113-20.

149. E. Harper, Collagenases. Annu Rev Biochem, 1980. **49**: p. 1063-78.

150. R. Lecybyl, T. Trzeciak, and J. Kruczynski, The possibility of isolation, culture and storage of articular cartilage cells. Chir Narzadow Ruchu Ortop Pol, 2000. **65**(6): p. 633-8.

151. G.M. Lee, C.A. Poole, S.S. Kelley, J. Chang, and B. Caterson, Isolated chondrons: A viable alternative for studies of chondrocyte metabolism in vitro. Osteoarthritis Cartilage, 1997. **5**(4): p. 261-74.

152. V. Jouis, J. Bocquet, J.P. Pujol, M. Brisset, and G. Loyau, Effect of ascorbic acid on secreted proteoglycans from rabbit articular chondrocytes. FEBS Lett, 1985. **186**(2): p. 233-40.

153. F.M. Watt, Effect of seeding density on stability of the differentiated phenotype of pig articular chondrocytes in culture. J Cell Sci, 1988. **89 (Pt 3)**: p. 373-8.

154. S.K. Hidvegi NC, Izadi D, Ong J, Kellam P, Eastwood D, Butler PE. , A low temperature method of isolating normal human articular chondrocytes. Osteoarthritis and Cartilage, 2006. **14**: p. 89-93.

155. F.Y. Yu, S.B. Lu, X.M. Cui, B. Zhao, W.J. Xu, M. Yuan, M.X. Sun, W.T. Zhang, and J.X. Huang, Biological characterization of rabbit's articular chondrocytes by confluent culture in vitro. Zhonghua Wai Ke Za Zhi, 2006. **44**(12): p. 848-51.

156. J.N. Ho, Y.H. Lee, Y.D. Lee, W.J. Jun, H.K. Kim, B.S. Hong, D.H. Shin, and

H.Y. Cho, Inhibitory effect of aucubin isolated from eucommia ulmoides against uvb-induced matrix metalloproteinase-1 production in human skin fibroblasts. Biosci Biotechnol Biochem, 2005. **69**(11): p. 2227-31.

157. A. Szuster-Ciesielska and M. Kandefer-Szerszen, Protective effects of betulin and betulinic acid against ethanol-induced cytotoxicity in hepg2 cells. Pharmacol Rep, 2005. **57**(5): p. 588-95.

158. G. Fotakis and J.A. Timbrell, In vitro cytotoxicity assays: Comparison of ldh, neutral red, mtt and protein assay in hepatoma cell lines following exposure to cadmium chloride. Toxicol Lett, 2006. **160**(2): p. 171-7.

159. D. Lobner, Comparison of the ldh and mtt assays for quantifying cell death: Validity for neuronal apoptosis? J Neurosci Methods, 2000. **96**(2): p. 147-52.

160. A.P. Shpakova, K.S. Pavlova, and T.I. Bulycheva, Mtt-colorimetric method for detection the cytotoxic activity of human natural killer cells. Klin Lab Diagn, 2000(2): p. 20-3.

161. L. Peng, B. Wang, and P. Ren, Reduction of mtt by flavonoids in the absence of cells. Colloids Surf B Biointerfaces, 2005. **45**(2): p. 108-11.

162. Y. Liu, D.A. Peterson, H. Kimura, and D. Schubert, Mechanism of cellular 3-(4,5-dimethylthiazol-2-yl)-2,5-diphenyltetrazolium bromide (mtt) reduction. J Neurochem, 1997. **69**(2): p. 581-93.

163. T. Bernas and J. Dobrucki, Mitochondrial and nonmitochondrial reduction of mtt: Interaction of mtt with tmre, jc-1, and nao mitochondrial fluorescent probes. Cytometry, 2002. **47**(4): p. 236-42.

164. M.V. Berridge and A.S. Tan, The protein kinase c inhibitor, calphostin c, inhibits succinate-dependent mitochondrial reduction of mtt by a mechanism that does not involve protein kinase c. Biochem Biophys Res Commun, 1992. **185**(3): p. 806-11.

165. S.R. Kim, M.J. Park, M.K. Lee, S.H. Sung, E.J. Park, J. Kim, S.Y. Kim, T.H. Oh, G.J. Markelonis, and Y.C. Kim, Flavonoids of inula britannica protect cultured cortical cells from necrotic cell death induced by glutamate. Free Radic Biol Med, 2002. **32**(7): p. 596-604.

166. H.Y. Lin, S.H. Juan, S.C. Shen, F.L. Hsu, and Y.C. Chen, Inhibition of lipopolysaccharide-induced nitric oxide production by flavonoids in raw264.7 macrophages involves heme oxygenase-1. Biochem Pharmacol, 2003. **66**(9): p. 1821-32.

167. C. Wongsawad, P. Wongsawad, J.Y. Chai, T. Paratasilpin, and S. Anuntalabhochai, Dna quantities and qualities from various stages of some trematodes using optical and hat-rapd methods. Southeast Asian J Trop Med Public Health, 2006. **37 Suppl 3**: p. 62-8.

168. N. Mattheus, A.K. Ekramoddoullah, and S.P. Lee, Isolation of high-quality rna from white spruce tissue using a three-stage purification method and subsequent cloning of a transcript from the pr-10 gene family. Phytochem Anal, 2003. **14**(4): p. 209-15.

169. B. Brosius, D. Riesner, and W. Hillen, Interaction of nucleic acids with lipid membranes. J Biomol Struct Dyn, 1984. **1**(6): p. 1535-41.

170. J.L. Palmer, A.L. Bertone, and H. McClain, Assessment of glycosaminoglycan concentration in equine synovial fluid as a marker of joint disease. Can J Vet Res, 1995. **59**(3): p. 205-12.

171. K.S. Kim, S.T. Yoon, J.S. Park, J. Li, M.S. Park, and W.C. Hutton, Inhibition of proteoglycan and type ii collagen synthesis of disc nucleus cells by nicotine. J Neurosurg, 2003. **99**(3 Suppl): p. 291-7.

172. D.C. Grant, S.D. Forrester, D.L. Panciera, and J.B. Meldrum, Measurement of urinary glycosaminoglycans in dogs. Am J Vet Res, 2006. **67**(1): p. 51-5.

173. G. Muller and M. Hanschke, Quantitative and qualitative analyses of proteoglycans in cartilage extracts by precipitation with 1,9-dimethylmethylene blue. Connect Tissue Res, 1996. **33**(4): p. 243-8.

174. A.S. Bell and L.C. Ranford-Cartwright, Real-time quantitative pcr in parasitology. Trends Parasitol, 2002. **18**(8): p. 337-42.

175. A. Matsuu, S. Ono, H. Ikadai, T. Uchide, S. Imamura, M. Onuma, S. Okano, and S. Higuchi, Development of a sybr green real-time polymerase chain reaction assay for quantitative detection of babesia gibsoni (asian genotype) DNA. J Vet Diagn Invest, 2005. **17**(6): p. 569-73.

176. Z. Yang, E.L. Woodahl, X.Y. Wang, T. Bui, D.D. Shen, and R.J. Ho, Semi-quantitative rt-pcr method to estimate full-length mrna levels of the multidrug resistance gene. Biotechniques, 2002. **33**(1): p. 196, 198, 200 passim.

177. E.B. Khomyakova, E.V. Dreval, M. Tran-Dang, M.C. Potier, and F.P. Soussaline, Innovative instrumentation for microarray scanning and analysis: Application for characterization of oligonucleotide duplexes behavior. Cell Mol Biol (Noisy-le-grand), 2004. **50**(3): p. 217-24.

178. C.H. Chang, H.C. Liu, C.C. Lin, C.H. Chou, and F.H. Lin, Gelatin-chondroitin-hyaluronan tri-copolymer scaffold for cartilage tissue engineering. Biomaterials, 2003. **24**(26): p. 4853-8.